NATIONAL CENTER FOR EARTHQUAKE ENGINEERING RESEARCH
State University of New York at Buffalo

PB95-138483

Sliding Mode Control for Seismic-Excited Linear and Nonlinear Civil Engineering Structures

by

J.N. Yang, J.C. Wu, A.K. Agrawal and Z. Li
University of California/Irvine
Department of Civil Engineering
Irvine, California 92717

Technical Report NCEER-94-0017

June 21, 1994

REPRODUCED BY:
U.S. Department of Commerce
National Technical Information Service
Springfield, Virginia 22161

This research was conducted at the University of California, Irvine and was partially supported by the National Science Foundation under Grant No. BCS 90-25010 and the New York State Science and Technology Foundation under Grant No. NEC-91029.

NOTICE

This report was prepared by the University of California, Irvine as a result of research sponsored by the National Center for Earthquake Engineering Research (NCEER) through grants from the National Science Foundation, the New York State Science and Technology Foundation, and other sponsors. Neither NCEER, associates of NCEER, its sponsors, the University of California, Irvine, nor any person acting on their behalf:

a. makes any warranty, express or implied, with respect to the use of any information, apparatus, method, or process disclosed in this report or that such use may not infringe upon privately owned rights; or

b. assumes any liabilities of whatsoever kind with respect to the use of, or the damage resulting from the use of, any information, apparatus, method or process disclosed in this report.

Any opinions, findings, and conclusions or recommendations expressed in this publication are those of the author(s) and do not necessarily reflect the views of the National Science Foundation, the New York State Science and Technology Foundation, or other sponsors.

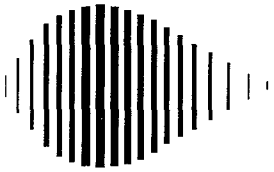

Sliding Mode Control for Seismic-Excited Linear and Nonlinear Civil Engineering Structures

by

J.N. Yang[1], J.C. Wu[2], A.K. Agrawal[2] and Z. Li[3]

June 21, 1994

Technical Report NCEER-94-0017

NCEER Task Number 93-5123
and
NSF Grant Number 91-20128

NSF Master Contract Number BCS 90-25010
and
NYSSTF Grant Number NEC-91029

1 Professor, Department of Civil and Environmental Engineering, University of California, Irvine
2 Graduate Student, Department of Civil and Environmental Engineering, University of California, Irvine
3 Post Doctoral Associate, Department of Civil and Environmental Engineering, University of California, Irvine

NATIONAL CENTER FOR EARTHQUAKE ENGINEERING RESEARCH
State University of New York at Buffalo
Red Jacket Quadrangle, Buffalo, NY 14261

PREFACE

The National Center for Earthquake Engineering Research (NCEER) was established to expand and disseminate knowledge about earthquakes, improve earthquake-resistant design, and implement seismic hazard mitigation procedures to minimize loss of lives and property. The emphasis is on structures in the eastern and central United States and lifelines throughout the country that are found in zones of low, moderate, and high seismicity.

NCEER's research and implementation plan in years six through ten (1991-1996) comprises four interlocked elements, as shown in the figure below. Element I, Basic Research, is carried out to support projects in the Applied Research area. Element II, Applied Research, is the major focus of work for years six through ten. Element III, Demonstration Projects, have been planned to support Applied Research projects, and will be either case studies or regional studies. Element IV, Implementation, will result from activity in the four Applied Research projects, and from Demonstration Projects.

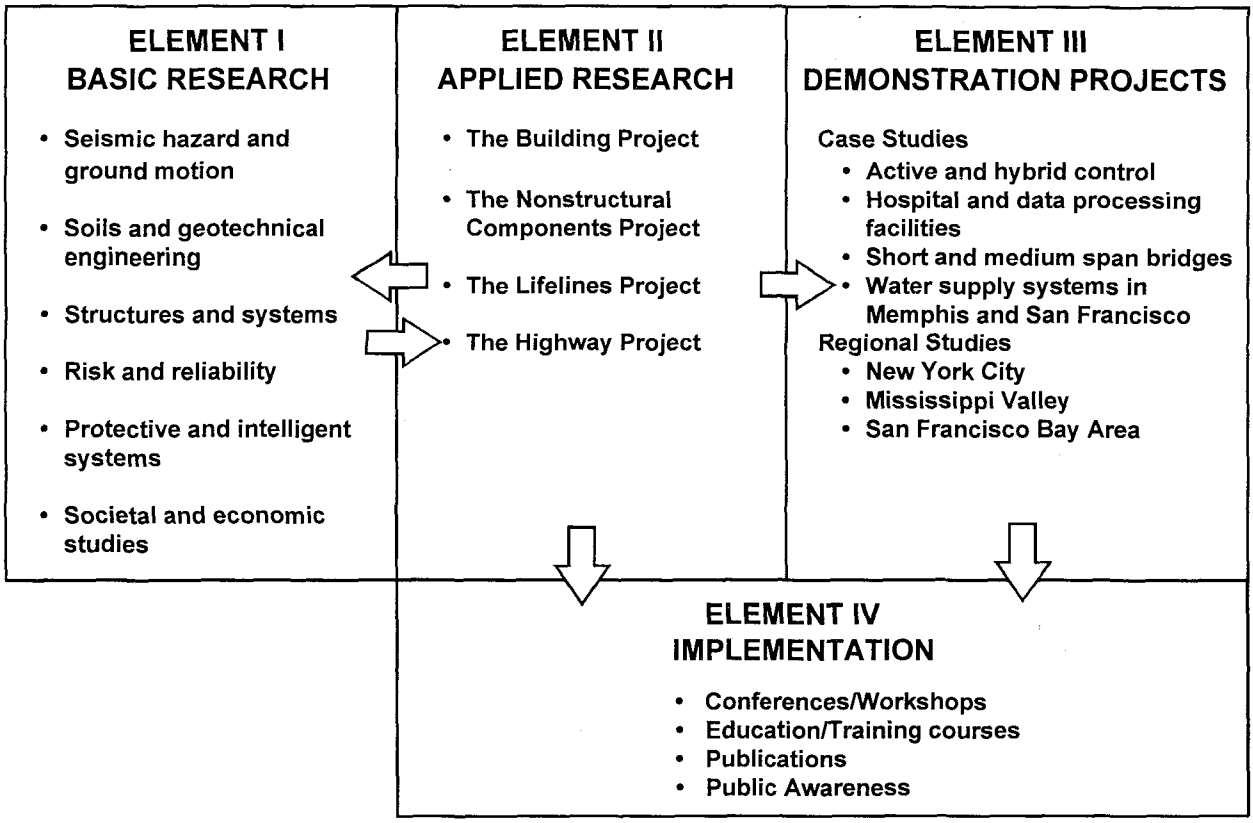

Research in the **Building Project** focuses on the evaluation and retrofit of buildings in regions of moderate seismicity. Emphasis is on lightly reinforced concrete buildings, steel semi-rigid frames, and masonry walls or infills. The research involves small- and medium-scale shake table tests and full-scale component tests at several institutions. In a parallel effort, analytical models and computer programs are being developed to aid in the prediction of the response of these buildings to various types of ground motion.

Two of the short-term products of the **Building Project** will be a monograph on the evaluation of lightly reinforced concrete buildings and a state-of-the-art report on unreinforced masonry.

The **protective and intelligent systems program** constitutes one of the important areas of research in the **Building Project**. Current tasks include the following:

1. Evaluate the performance of full-scale active bracing and active mass dampers already in place in terms of performance, power requirements, maintenance, reliability and cost.
2. Compare passive and active control strategies in terms of structural type, degree of effectiveness, cost and long-term reliability.
3. Perform fundamental studies of hybrid control.
4. Develop and test hybrid control systems.

A method of active control based on the theory of sliding mode control for building applications is studied in this report. Robustness, direct output feedback, and control saturation are addressed through extensive numerical simulation. Potential applications of this control methodology to linear structures, fixed-base buildings with large ductility, base-isolated buildings using lead-core bearings, and nonlinear structures are presented. Experimental verification of the control scheme has been carried out at the University at Buffalo using a three-story 1/4-scale linear structural model, showing excellent results using a discontinuous controller with small sliding margin. These experimental results will be presented in a subsequent NCEER report.

ABSTRACT

Control methods based on the theory of variable structure system (VSS) or sliding mode control (SMC) are presented for applications to seismic-excited linear, nonlinear and hysteretic civil engineering structures. These control methods are robust with respect to parametric uncertainties of the structures. The controllers have no adverse effect should the actuator be saturated due to unexpected extreme earthquakes. Emphasis is placed on continuous sliding mode control methods, which do not have possible chattering effects. Static output feedback controllers using only the measured information from a limited number of sensors installed at strategic locations are also presented for practical implementations. Furthermore, controllers are proposed for applications to parametric control, including the use of active variable stiffness (AVS) systems and active variable dampers (AVD). Under suitable conditions, a complete compensation of the structural response can be achieved, i.e., the structural response can be reduced to zero. Among the contributions of this report are the establishment of saturated controllers, controllers for static output feedback, parametric control, etc. The robustness of the control methods, the application of the static output feedback controllers, the control effectiveness in case of actuator saturation and the applicability to parametric control are all demonstrated by numerical simulation results. Applications of the control methods to linear buildings, fixed-base buildings with large ductility, base-isolated buildings using lead-core rubber bearings and elastic nonlinear structures are presented. Numerical simulation results indicate that the performance of the control methods is remarkable. Practical implementations of the control methods are discussed. Shaking table experimental verifications for the control methods presented for linear and nonlinear structures have been made and the results were presented elsewhere.

ACKNOWLEDGEMENTS

This research is partially supported by the National Science Foundation Grant No. BCS-91-20128 and the National Center for Earthquake Engineering Research Grant No. 935123. Valuable discussion with Dr. David K. K. Young of YKK Systems, Mountain View, CA is gratefully acknowledged.

TABLE OF CONTENTS

LIST OF FIGURES

LIST OF TABLES

SECTION 1
INTRODUCTION

Intensive research efforts have been made recently, both theoretically and experimentally, in active and hybrid control of civil engineering structures against strong winds and earthquakes [e.g., Soong 1990, Soong et al 1991, Spencer et al 1991, 1993, Inaudi & Kelly 1993, Lai & Soong 1992, Reinhorn, Soong et al 1992, Reinhorn et al 1993a, 1993b, Schmitendorf et al 1994, Calise et al 1993, Yang et al 1991, 1992a, etc.]. In addition to actuator-based control systems, such as active bracing systems (ABS), active mass dampers (AMD), active tendons, etc., active variable stiffness (AVS) systems [e.g., Kobori & Kamagata 1992a,b, Yang et al 1994e] and active variable dampers [e.g., Kawashima et al 1992a, 1992b, Feng & Shinozuka 1990, Yang et al 1993b] have also been proposed for applications to seismic-excited buildings and bridges. These types of control systems belong to the category of parametric control, since control appears in the parameter of the equation of motion. Most of the control methods investigated for civil engineering applications use either the full state feedback or the observer-based controllers [e.g., Schmitendorf et al 1994]. More recently, the method of variable structure system (VSS) or sliding mode control (SMC) [e.g., Slotine & Li 1991, Utkin 1992, Young 1993] was explored in a preliminary manner for control of linear buildings [Yang et al 1993a,c,d] and bridges [Yang et al 1993b, 1994a].

Aseismic hybrid protective systems, consisting of a combination of active control devices and passive base isolation systems, have been shown to be quite effective. Since the dynamic behavior of most base isolation systems, such as lead-core rubber bearings or frictional-type sliding bearings, is either highly nonlinear or inelastic, hybrid protective systems involve control of nonlinear or hysteretic structural systems. Likewise, under strong earthquakes, yielding may occur even if the fixed-base building is equipped with active control systems. As a result, control of nonlinear or hysteretic civil engineering structures has attracted considerable attention recently. Various control methods have been investigated for applications to nonlinear and

hysteretic structural systems, including pulse control [e.g., Reinhorn et al 1987], polynomial control [Spencer et al 1992, Suhardjo, et al 1992], acceleration control [Nagarajaiah et al 1993, Reinhorn et al 1993b,c, Riley et al 1993], instantaneous optimal control [Feng & Shinozuka 1991, Yang et al 1992b], dynamic linearization [Yang et al 1994c, Reinhorn, et al 1993c, Riley et al 1993], nonlinear control [Yang et al, 1992a 1994b], discontinuous sliding mode control [Yang et al 1993d, 1994d], etc. To date, investigations are needed to explore promising control methods for applications to seismic-excited nonlinear and hysteretic civil engineering structures.

For practical implementations of active/hybrid control systems in large civil engineering structures, it may not be possible to install all sensors to measure the full state vector. An observer, however, requires on-line computations thus increasing the system time delay. As a result, static output feedback control using only the measured information from a limited number of sensors installed at strategic locations is highly desirable. For seismic hazard mitigation, the earthquake ground acceleration, including both the magnitude and frequency content, involves the biggest uncertainty among others. It is conceivable that a controller with a limited capacity, such as an actuator, may be saturated under unexpected strong earthquakes. An actuator saturation may result in a serious consequence to the controlled structure, such as instability. Therefore, it is desirable to have controllers whose performance will not be affected significantly by the saturation. Likewise, systematic studies for parametric control of civil engineering structures have not been conducted.

Sections 2 through 5 present control methods for linear civil engineering structures based on the theory of variable structure system (VSS) or sliding mode control (SMC) [e.g., Utkin 1992, Young 1993, Zhou and Fisher 1992]. Both continuous and discontinuous sliding mode controllers are presented. However, emphasis is placed on continuous controllers which do not have possible chattering effect. In the case of discontinuous controllers, a boundary layer is introduced to remove the possible chattering effect. Saturated controllers are also presented, so that the control performance is not subject to an adverse effect should the actuator be saturated due to unexpected strong earthquakes. When each degree-of-freedom (or story unit) is implemented with a controller, a complete compensation for the structural response can be achieved, i.e., the response state vector can be reduced to zero. Furthermore, the Lyapunov-type controllers are presented for applications to parametric control of civil engineering

structures, including the use of active variable stiffness (AVS) systems and active variable dampers (AVD). Finally, static output feedback controllers using only the measured information from a limited number of sensors installed at strategic locations are presented. Static output feedback controllers can be implemented readily for practical applications. Simulation results are obtained to demonstrate the robustness, performance and other desirable features of the control methods for linear structures.

In Sections 6 through 9, sliding mode control methods are presented for applications to control of nonlinear and hysteretic civil engineering structures subjected to strong earthquakes. Although both continuous and discontinuous controllers are presented, emphasis is placed on continuous sliding mode controllers which do not have possible chattering effects and the control forces are continuous. Static output feedback controllers using only a few sensors as well as saturated controllers are presented. Simulation results are obtained for control of (i) a Duffing structural model, (ii) a base-isolated building using lead-core rubber bearings, and (iii) a fixed-base building with large ductility. Numerical simulation results indicate that the control designs presented are robust with respect to system uncertainties and their performance is quite remarkable.

SECTION 2
SLIDING MODE CONTROL OF LINEAR STRUCTURES

2.1 EQUATION OF MOTION

Consider an n degree-of-freedom linear building structure subjected to a one-dimensional earthquake ground acceleration $\ddot{X}_0(t)$ as shown in Fig. 2-1. The vector equation of motion is given by

$$M\ddot{X}(t) + C\dot{X}(t) + KX(t) = HU(t) + \eta\ddot{X}_0(t) \tag{2.1}$$

in which $X(t) = [x_1,x_2,\ldots,x_n]' =$ an n vector with $x_j(t)$ being the drift of a designated story unit; $U(t) =$ a r vector consisting of r control forces; and η is an n vector denoting the influence of the earthquake excitation. M, C and K are (nxn) mass, damping and stiffness matrices, respectively, and H is a (nxr) matrix denoting the location of r controllers. In the state space, Eq. (2.1) becomes

$$\dot{Z}(t) = AZ(t) + BU(t) + E(t) \tag{2.2}$$

where Z(t) is a 2n state vector, A is a (2nx2n) system matrix, B is a (2nxr) matrix and, E(t) is a 2n excitation vector, respectively, given by

$$Z(t) = \begin{bmatrix} X(t) \\ \dot{X}(t) \end{bmatrix};\ E(t) = \begin{bmatrix} 0 \\ M^{-1}\eta \end{bmatrix}\ddot{X}_0(t);\ B = \begin{bmatrix} 0 \\ M^{-1}H \end{bmatrix};\ A = \begin{bmatrix} 0 & I \\ -M^{-1}K & -M^{-1}C \end{bmatrix} \tag{2.3}$$

2.2 DESIGN OF SLIDING SURFACE

The theory of variable structure system (VSS) or sliding mode control (SMC) is to design controllers to drive the response trajectory into the sliding surface (or switching surface) and maintain it there, whereas the motion on the sliding surface is stable as shown schematically in Fig. 2-2. In the design of the sliding surface, the external excitation E(t) is neglected; however, it is taken into account in the design of controllers. For simplicity, let S=0 be a r-dimensional sliding surface consisting of a linear combination of the state variables

$$S = PZ = 0 \tag{2.4}$$

in which S is a r-vector consisting of r sliding variables, $S_1,S_2,\ldots,S_r$, with r being the total

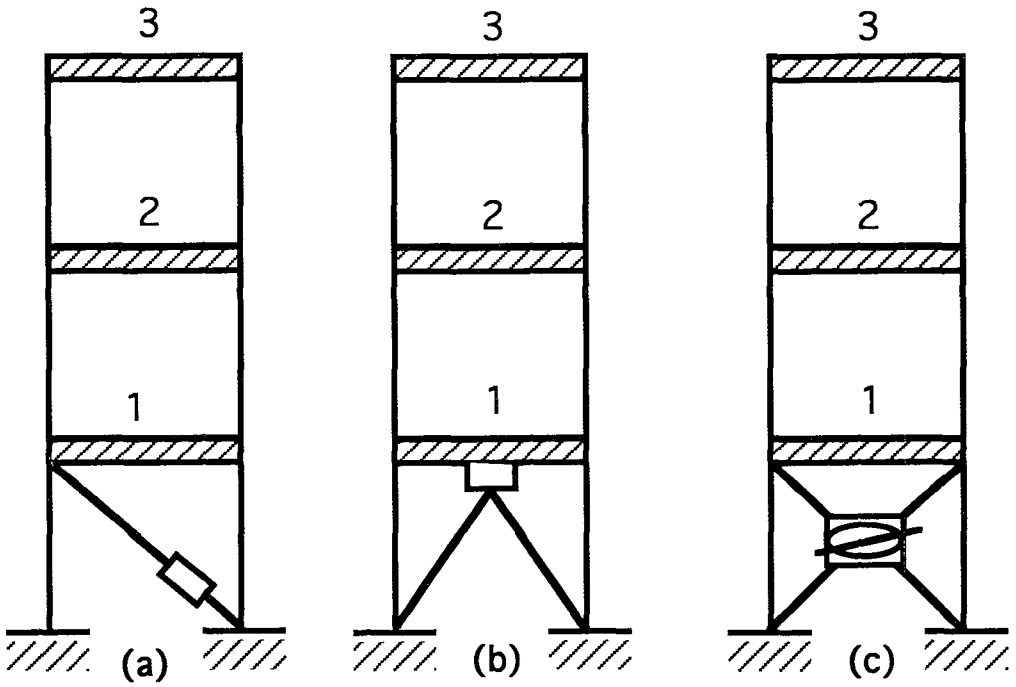

Fig. 2-1 : Building Model; (a) With Active Bracing System; (b) With Active Variable Stiffness; (c) With Active Variable Damper

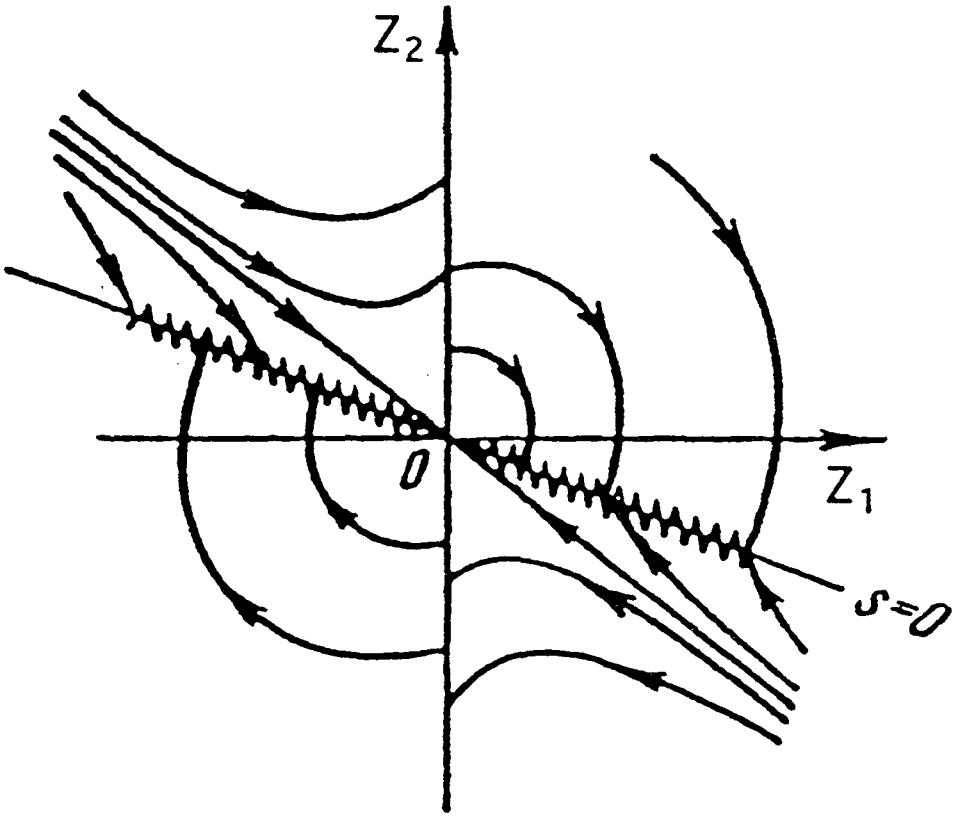

Fig. 2-2 : Phase Plane for Sliding Mode Control

number of controllers, i.e.,

$$S = [S_1, S_2, \ldots, S_r]' \tag{2.5}$$

where a prime denotes the transpose of a vector or matrix. In Eq. (2.4), P is a (rx2n) matrix to be determined such that the motion on the sliding surface is stable. For the response trajectory to stay on the sliding surface, once it reaches there, one has $\dot{S}=0$. It follows from Eqs. (2.4) and (2.2) that

$$\dot{S} = (\partial S/\partial Z)\dot{Z} = P(AZ + BU) = 0 \tag{2.6}$$

in which the argument t for Z(t) and U(t) has been dropped for simplicity. The solution of Eq. (2.6) for U yields the so-called equivalent control U_{eq} on the sliding surface; with the result

$$U_{eq} = U = -(PB)^{-1}PAZ \tag{2.7}$$

in which PB is nonsingular. Substitution of Eq. (2.7) into Eq. (2.2), with the external excitation E(t) being neglected, leads to the following

$$\dot{Z} = [A - B(PB)^{-1}PA]Z \tag{2.8}$$

Hence, the equations of motion on the sliding surface are defined by r equations given in Eq. (2.4) and (2n-r) equations out of 2n equations given by Eq. (2.8). The usual procedure is to solve r state variables from Eq. (2.4) in terms of the remaining 2n-r state variables and substitute these relations into (2n-r) equations in Eq. (2.8). Then, the P matrix is determined such that the motion on the sliding surface is stable.

One systematic approach for the determination of the P matrix is to convert the state equation of motion, Eq. (2.2), into the so-called regular form by the following transformation [Utkin 1992]. Let

$$Y = DZ \quad or \quad Z = D^{-1}Y \tag{2.9}$$

in which D is a transformation matrix

$$D = \begin{bmatrix} I_{2n-r} & -B_1B_2^{-1} \\ 0 & I_r \end{bmatrix} \; ; \; D^{-1} = \begin{bmatrix} I_{2n-r} & B_1B_2^{-1} \\ 0 & I_r \end{bmatrix} \tag{2.10}$$

where I_{2n-r} and I_r are (2n-r) x (2n-r) and (rxr) identity matrices, respectively, and B_1 and B_2 are (2n-r)xr and rxr submatrices obtained from the partition of the B matrix, Eq. (2.2), as follows

$$B = \begin{bmatrix} B_1 \\ B_2 \end{bmatrix} \tag{2.11}$$

Note that the (rxr) B_2 matrix should be nonsingular. If the B_2 matrix is singular in the original state equation, then the state equation should be rearranged such that B_2 is nonsingular.

With the transformation matrix D, the state equation, Eq. (2.2), and the sliding surface, Eq. (2.4), become

$$\dot{Y} = \bar{A}Y + \bar{B}U \tag{2.12}$$

$$S = \bar{P}Y = 0 \tag{2.13}$$

in which

$$\bar{A} = DAD^{-1} \;\; ; \;\; \bar{P} = PD^{-1} \;\; ; \;\; \bar{B} = \begin{bmatrix} 0 \\ B_2 \end{bmatrix} \tag{2.14}$$

Equation (2.12) is referred to as the regular form in which $\bar{B}$ is given by Eq. (2.14). As observed from Eq. (2.12), only the last r equations involve the equivalent control force U. Thus, the equations of motion on the sliding surface is defined by r equations in Eq. (2.13) and 2n-r equations in the upper part of Eq. (2.12).

Let Y, $\bar{A}$ and $\bar{P}$ be partitioned as follows

$$Y = \begin{bmatrix} Y_1 \\ Y_2 \end{bmatrix} \;\; ; \;\; \bar{A} = \begin{bmatrix} \bar{A}_{11} & \bar{A}_{12} \\ \bar{A}_{21} & \bar{A}_{22} \end{bmatrix} \;\; ; \;\; \bar{P} = \begin{bmatrix} \bar{P}_1 \vdots \bar{P}_2 \end{bmatrix} \tag{2.15}$$

in which Y_1 and Y_2 are 2n-r and r vectors, respectively, and $\bar{A}_{11}$, $\bar{A}_{22}$, $\bar{P}_1$ and $\bar{P}_2$ are, respectively, (2n-r)x(2n-r), rxr, rx(2n-r) and rxr matrices. Substituting Eq. (2.15) into Eqs. (2.12) and (2.13), one obtains the equations of motion on the sliding surface

$$\dot{Y}_1 = \bar{A}_{11} Y_1 + \bar{A}_{12} Y_2 \tag{2.16}$$

$$S = \bar{P}_1 Y_1 + \bar{P}_2 Y_2 = 0 \tag{2.17}$$

For simplicity, $\bar{P}_2$ is chosen to be an identity matrix, i.e.,

$$\bar{P}_2 = I_r \tag{2.18}$$

and hence Eq. (2.17) becomes

$$Y_2 = -\bar{P}_1 Y_1 \tag{2.19}$$

Substitution of Eq. (2.19) into Eq. (2.16) leads to (2n-r) equations of motion on the sliding surface

$$\dot{Y}_1 = (\bar{A}_{11} - \bar{A}_{12}\bar{P}_1) Y_1 \tag{2.20}$$

The $\bar{P}_1$ matrix can be determined from Eq. (2.20) such that the motion $Y = [Y_1', Y_2']'$ on the sliding surface is stable. After determining $\bar{P}_1$, the unknown matrix P is obtained from Eq. (2.14). While several approaches can be used for the determination of the $\bar{P}$ matrix, only two methods will be used herein. In the case of a full state feedback, either the method of LQR or pole assignment will be used. In the case of static output feedbacks using a limited number of sensors, the method of pole assignment will be used. The use of the pole assignment method for the determination of the $\bar{P}_1$ matrix in Eq. (2.20) is well-known, whereas the method of LQR is described briefly in the following.

The design of the sliding surface $S = PZ = 0$ is obtained by minimizing the integral of the quadratic function of the state vector

$$J = \int_o^\infty Z'(t) Q Z(t) dt \tag{2.21}$$

in which Q is a (2nx2n) positive definite weighting matrix. In terms of the transformed state vector Y, Eq. (2.9), the performance index J becomes

$$J = \int_0^\infty [Y_1', Y_2']' \; T \begin{bmatrix} Y_1 \\ Y_2 \end{bmatrix} dt \tag{2.22}$$

in which

$$T = (D^{-1})' Q D^{-1} \quad ; \quad T = \begin{bmatrix} T_{11} & T_{12} \\ T_{21} & T_{22} \end{bmatrix} \tag{2.23}$$

where T_{11} and T_{22} are (2n-r)x(2n-r) and (rxr) matrices, respectively.

Minimizing the performance index J given by Eq. (2.22) subjected to the constraint of the equations of motion, Eq. (2.16), one obtains [see detailed derivation in Yang et al, 1994b]

$$Y_2 = -0.5 T_{22}^{-1} (\bar{A}_{12}' \hat{P} + 2 T_{21}) Y_1 \tag{2.24}$$

in which $\hat{P}$ is a (2n-r)x(2n-r) Riccati matrix satisfying the following matrix Riccati equation

$$\hat{A}' \hat{P} + \hat{P} \hat{A} - 0.5 \hat{P} \bar{A}_{12} T_{22}^{-1} \bar{A}_{12}' \hat{P} = -2 (T_{11} - T_{12} T_{22}^{-1} T_{12}') \tag{2.25}$$

where

$$\hat{A} = \bar{A}_{11} - \bar{A}_{12} T_{22}^{-1} T_{21} \tag{2.26}$$

A comparison between Eqs. (2.19) and (2.24) indicates that

$$\bar{P}_1 = 0.5 T_{22}^{-1} (\bar{A}_{12}' \hat{P} + 2 T_{21}) \tag{2.27}$$

Finally, the original sliding surface $S = PZ = 0$ is obtained from Eq. (2.14) as

$$P = \bar{P} D = [\bar{P}_1 \vdots I_r] D \tag{2.28}$$

in which $\bar{P}_1$ is obtained from Eq. (2.27).

2.3 DESIGN OF CONTROLLERS USING LYAPUNOV DIRECT METHOD

The controllers are designed to drive the state trajectory into the sliding surface $S=0$. To achieve this goal, a Lyapunov function V is considered.

$$V = 0.5 S'S = 0.5 Z' P' P Z \tag{2.29}$$

The sufficient condition for the sliding mode $S=0$ to occur as $t \to \infty$ is

$$\dot{V} = S' \dot{S} \leq 0 \tag{2.30}$$

Taking derivative and using the state equation of motion, Eq. (2.2), one obtains

$$\dot{V} = \lambda (U - G) = \sum_{i=1}^{r} \lambda_i (u_i - G_i) = \sum_{i=1}^{r} \dot{V}_i \tag{2.31}$$

in which λ' and G are r-vectors with the ith elements λ_i and G_i, respectively, and $u_i = u_i(t)$ is the ith control force, where

$$\lambda = S' P B \;\; ; \;\; G = -(PB)^{-1} P(AZ + E) \;\; ; \;\; \dot{V}_i = \lambda_i (u_i - G_i) \tag{2.32}$$

For $\dot{V} \leq 0$, a possible <u>continuous</u> controller is given by

$$u_i(t) = G_i - \delta_i \lambda_i \tag{2.33}$$

in which $\delta_i \geq 0$ is referred to as the sliding margin. In the vector form, Eq. (2.33) can be expressed as

$$U = G - \bar{\delta}\lambda' \tag{2.34}$$

in which $\bar{\delta}$ is a (rxr) diagonal matrix with diagonal elements $\delta_1,\delta_2,\ldots,\delta_r$. Substitution of Eq. (2.34) into Eq. (2.31) yields $\dot{V} \leq 0$, i.e.,

$$\dot{V} = -\lambda\bar{\delta}\lambda' \leq 0 \tag{2.35}$$

In addition to the continuous controller given by Eq. (2.34), two possible discontinuous controllers are given in the following

$$u_i(t) = \begin{cases} G_i - \delta_i H(|\lambda| - \epsilon_0) ; & \text{if } \lambda_i > 0 \\ G_i + \delta_i H(|\lambda| - \epsilon_0) ; & \text{if } \lambda_i < 0 \end{cases} \tag{2.36}$$

and

$$u_i(t) = \begin{cases} G_i - \delta_i H(|\lambda| - \epsilon_0) ; & \text{if } \lambda_i > 0 \text{ , } G_i < 0 \\ G_i + \delta_i H(|\lambda| - \epsilon_0) ; & \text{if } \lambda_i < 0 \text{ , } G_i > 0 \\ 0 \ ; & \text{otherwise} \end{cases} \tag{2.37}$$

in which $H(|\lambda|-\epsilon_0)$ is the unit step function, i.e. $H(|\lambda|-\epsilon_0)=0$ for $|\lambda| < \epsilon_0$ and $H(|\lambda|-\epsilon_0)=1$ for $|\lambda| \geq \epsilon_0$. In the expression above, $|\lambda|$ is any norm of the λ row vector and ϵ_0 is the thickness of the boundary layer of the chattering surface $\lambda=0$ (or sliding surface $S=0$). The idea of using the unit step function $H(|\lambda|-\epsilon_0)$ is to introduce a boundary layer in the vicinity of $\lambda=0$ in which the sliding margins are zero, thus removing the undesirable chattering effect. Since $\lambda=S'PB$ and PB is nonsingular, $\lambda=0$ implies $S=0$. The size of the boundary layer ϵ_0 can be designed appropriately to achieve the purpose [Utkin 1992]. Note that the unit of δ_i for the continuous controller in Eq. (2.33) is different from that of δ_i for the discontinuous controllers in Eqs.(2.36) and (2.37).

It is observed form Eqs. (2.34)-(2.37) that both the feedback loop, PAZ, and the feedforward compensation, PE, are taken into account in the design of the controllers. The constant sliding margin $\delta_i(i=1,2,\ldots,r)$ is used to guarantee the condition $\dot{V} \leq 0$.

2.4 COMPLETE COMPENSATION

When each degree-of-freedom of the structure is implemented with a controller, i.e., r=n, e.g., each story unit is equipped with an ABS system, the external earthquake excitation

can be compensated completely, such that the response state vector approaches zero. In this case, the P matrix is (nx2n) and the B_2 matrix is (nxn). The proof is given in the following. Let the P matrix be partitioned as $P=[P_1,P_2]$ such that the sliding surface is given by

$$S = PZ = P_1 X + P_2 \dot{X} = 0 \tag{2.38}$$

and hence

$$B(PB)^{-1}P = \begin{bmatrix} 0 & 0 \\ P_2^{-1}P_1 & I_n \end{bmatrix} \tag{2.39}$$

Substituting the controllers in Eqs. (2.34) and (2.36), respectively, into the state equation of motion, Eq. (2.2), and using Eqs. (2.38)-(2.39), one obtains the vector equations of motion for the controlled structure for each controller as follows

$$\ddot{X}(t) = -[P_2^{-1}P_1 + B_2\bar{\delta}B_2'P_2'P_2]\dot{X}(t) - B_2\bar{\delta}B_2'P_2'P_1X(t) \tag{2.40}$$

and

$$\ddot{X}(t) = -P_2^{-1}P_1\dot{X}(t) - B_2\delta H(|\lambda| - \epsilon_0)sgn(\lambda') \tag{2.41}$$

in which λ' and δ are n-vectors with the ith elements, λ_i and δ_i, respectively. As observed from Eqs. (2.40) and (2.41), the earthquake excitation $\ddot{X}_0(t)$ is completely compensated and the controlled response depends on the sliding margins δ and $\bar{\delta}$. Since, however, the sliding surface is stable, Eqs. (2.40) and (2.41) are overdamped systems and hence the response approaches to zero rapidly.

2.5 SATURATED CONTROLLERS

We assume that the structure is stable without control. This assumption is reasonable for civil engineering structures which are designed to be stable without any control systems. Let $\dot{V}_{in}$ correspond to $\dot{V}_i$, Eqs. (2.31) and (2.32), when no control action is taken by the ith controller, i.e., $u_i(t)=0$ and

$$\dot{V}_{in} = -\lambda_i G_i \tag{2.42}$$

Then, at every time instant, t, the control action will be taken either to reduce the derivative of the Lyapunov function $\dot{V}_i \leq \dot{V}_{in}$ or to maintain $\dot{V}_i \leq 0$. Based on this premise, the following saturated controller corresponding to the continuous controller, Eq. (2.33), is presented.

$$u_i(t) = \begin{cases} \alpha_i^* G_i - \delta_i \lambda_i \; ; & \text{if } | \alpha_i^* G_i - \delta_i \lambda_i | \le \bar{u}_{imax} \\ \bar{u}_{imax} sgn(\alpha_i^* G_i - \delta_i \lambda_i) \; ; & \text{otherwise} \end{cases} \tag{2.43}$$

in which $0 \le \alpha_i^* \le 1$ and $\pm \bar{u}_{imax}$ (i=1,2,...,r) are the upper and lower bounds of the control force. Both α^* and $\bar{u}_{imax}$ are specified by the designer.

The saturated controller corresponding to discontinuous controllers given by Eqs. (2.36) and (2.37) are given as follows

$$u_i^*(t) = \begin{cases} \alpha_i^* G_i - \delta_i H(|\lambda| - \epsilon_0) \; ; & \text{if } \lambda_i > 0 \\ \alpha_i^* G_i + \delta_i H(|\lambda| - \epsilon_0) \; ; & \text{if } \lambda_i < 0 \end{cases} \tag{2.44}$$

$$u_i(t) = \begin{cases} u_i^*(t) \; ; & \text{if } |u_i^*(t)| < \bar{u}_{imax} \\ \bar{u}_{imax} sgn[u_i^*(t)] \; ; & \text{if } |u_i^*(t)| > \bar{u}_{imax} \end{cases} \tag{2.45}$$

and

$$u_i^*(t) = \begin{cases} \alpha_i G_i - \delta_i H(|\lambda| - \epsilon_0) \; ; & \text{if } \lambda_i > 0 \; , \; G_i < 0 \\ \alpha_i G_i + \delta_i H(|\lambda| - \epsilon_0) \; ; & \text{if } \lambda_i < 0 \; , \; G_i > 0 \\ 0 \; ; & \text{otherwise} \end{cases} \tag{2.46}$$

$$u_i(t) = \begin{cases} u_i^*(t) \; ; & \text{if } |u_i^*(t)| < \bar{u}_{imax} \\ \bar{u}_{imax} sgn[u_i^*(t)] \; ; & \text{if } |u_i^*(t)| > \bar{u}_{imax} \end{cases} \tag{2.47}$$

in which $\alpha_i > 0$ (i=1,2,...,r) are specified by the designer.

The theoretical justification for the controllers above is that at every time instant, either the event $\dot{V} \le 0$ occurs or the event $\dot{V}_i \le \dot{V}_{in}$ occurs. From the condition that $\dot{V}_i \le \dot{V}_{in}$ and the fact that the structure is stable without control, it can be shown that V is bounded, and hence the state vector Z is bounded, i.e., $|Z| < \infty$. Design parameters α_i^*, α_i and $\bar{u}_{imax}$ (for i=1,2,...,r) can be used to make a trade-off between the control effort and the structural response. Controllers presented above are referred to as the saturated controllers, since the control effort $u_i(t)$ is saturated (or bounded) at $\bar{u}_{imax}$. Special controllers that utilize either the full capacity or constant control force of the actuator corresponding to Eqs. (2.45) and (2.47) are bang-bang controllers,

$$u_i(t) = \begin{cases} -\bar{u}_{imax} H(|\lambda| - \epsilon_0) \; ; & \text{if } \lambda_i > 0 \\ \bar{u}_{imax} H(|\lambda| - \epsilon_0) \; ; & \text{if } \lambda_i < 0 \end{cases} \tag{2.48}$$

and

$$u_i(t) = \begin{cases} -\bar{u}_{imax} H(|\lambda| - \epsilon_0) \; ; & \text{if } \lambda_i > 0 \text{ , } G_i < 0 \\ \bar{u}_{imax} H(|\lambda| - \epsilon_0) \; ; & \text{if } \lambda_i < 0 \text{ , } G_i > 0 \\ 0 \; ; & \text{otherwise} \end{cases} \tag{2.49}$$

The saturated controllers presented above have a nice feature in the sense that if the actual capacity of the actuator used for the control system is exceeded by the demand, a saturation will occur but the controllers still perform well using the maximum capacity. When saturation occurs for other types of controllers, a severe degradation of the control performance may result and the system may even become unstable.

2.6 ROBUSTNESS OF CONTROLLERS

The theory of variable structure system or sliding mode control was developed for control of uncertain nonlinear systems [e.g., Utkin 1992] and the robustness of such a theory is well documented. The robustness of the controllers presented above with respect to parametric uncertainties of the structure will be demonstrated by simulation results in Section 5.

SECTION 3
PARAMETRIC CONTROL OF LINEAR STRUCTURE

The control methods presented above are applicable to actuator-based control systems in which the controller is capable of producing positive and negative control forces. One type of the control system, referred to as the active variable stiffness (AVS) system, has been shown to be quite effective for buildings against strong earthquakes [Kobori & Kamagata 1992a,b]. The AVS system consists of stand-by bracings attached to selected story units of the building, and the locking and unlocking devices. During the earthquake ground motion, some of the bracings may be locked at a particular time instant t to increase the stiffness of the corresponding story unit. Locking and unlocking of different bracings at each time instant are regulated by a control algorithm in order to reduce the building response against earthquakes. Consequently, the stiffness of each story unit, in which the AVS system is installed, varies as a function of time.

Another type of control system is referred to as the variable damper. Variable dampers are viscous dampers in which the damping coefficient can be regulated actively by adjusting the opening of the orifice of the oil flow. As a result, the damping coefficient of the structure is actively controlled. This type of control system has been developed successfully for applications to bridge structures against earthquakes [e.g., Kawashima et al 1992a, 1992b, Feng & Shinozuka 1990, Yang et al 1993b]. Control methods for the two types of control systems described above, which are essentially parametric control, will be presented in the following.

For the AVS systems and variable dampers, the coefficient matrix of the control vector, B, is a function of the state variables and the procedures for determining the sliding surface are described in Utkin (1992). With the control systems above and following the procedures in Utkin (1992), we find that the design of the sliding surface (or switching surface) is identical to that presented previously where either the damping force from variable dampers or the stiffness force from AVS systems are considered as the control force. However, the design of controllers is different because of the limitations of the capacity of the AVS system and variable dampers. In the following, the structure is designed to be stable whether any or all of AVS systems are locked, and whatever (positive) damping coefficients variable dampers may take.

3.1 CONTROLLER DESIGN FOR VARIABLE DAMPER SYSTEMS

Suppose r variable dampers are installed in r selected story units. The equations of motion are given in Eqs. (2.1) and (2.2) except that the components of the control vector $U(t)=[u_1(t),u_2(t),\ldots,u_r(t)]'$ should be expressed in terms of the state variables $Z(t)=[z_1(t), z_2(t),\ldots,z_{2n}(t)]'$ as follows

$$u_i(t) = \xi_i(t)\, z_{n+k,i}(t) \tag{3.1}$$

in which $z_{n+k,i}(t)=z_{n+k}(t) = \dot{x}_k$ is the interstory velocity of the kth story unit in which the ith variable damper (or ith variable damper group) is installed. In Eq. (3.1), the damping coefficient $\xi_i(t)$, although can be actively regulated, is bounded by a minimum value ξ_{imin} and a maximum value ξ_{imax}, i.e.,

$$\xi_{imin} \le \xi_i \le \xi_{imax} \tag{3.2}$$

in which $\xi_{imin} \ge 0$, since the variable damper always produces positive damping.

Substituting Eq. (3.1) into Eq. (2.31), one obtains

$$\dot{V} = \sum_{i=1}^{r} \lambda_i \; [\xi_i(t)\, z_{n+k,i}(t) - G_i] \tag{3.3}$$

in which λ_i and G_i are the ith components of λ and G, respectively, given by Eq. (2.32).

One possible controller is to minimize $\dot{V}$ in Eq. (3.3) as follows

$$\xi_i(t) = \begin{cases} \xi_{imin}, & \text{if } \lambda_i\, z_{n+k,i} > 0 \\ \xi_{imax}, & \text{if } \lambda_i\, z_{n+k,i} < 0 \end{cases} \tag{3.4}$$

The controller proposed above is a two-state variable damper in which the damper switches between the maximum and minimum dampings. This type of damper is the simplest and most reliable. Other types of controllers have also been presented in Yang et al (1993b, 1994a).

3.2 CONTROLLER DESIGN FOR ACTIVE VARIABLE STIFFNESS SYSTEM

For the AVS control system, suppose r active bracing systems are installed in r selected story units. The equations of motion given by Eqs. (2.1) and (2.2) hold except that the ith component $u_i(t)$ of the control vector is given by

$$u_i(t) = g_i \, \bar{k}_{i,k} \, z_{k,i}(t) \tag{3.5}$$

where $z_{k,i}(t) = z_k(t)$ is the drift of the kth story unit in which the ith bracing system is installed, and $\bar{k}_{i,k}$ is the stiffness of the ith bracing system installed in the kth story unit. The on-off control g_i takes the values $g_i=1$ if the ith bracing is locked and $g_i=0$ if the ith bracing is unlocked. Substitution of Eq. (3.5) into Eq. (2.31) leads to the following

$$\dot{V} = \sum_{i=1}^{r} \lambda_i \, [g_i \, \bar{k}_{i,k} \, z_{k,i}(t) - G_i] \tag{3.6}$$

To minimize $\dot{V}$, one possible controller is as follows

$$g_i = \begin{cases} 1 \; ; & \text{if } \lambda_i z_{k,i} < 0 \\ 0 \; ; & \text{if } \lambda_i z_{k,i} > 0 \end{cases} \tag{3.7}$$

Other types of controllers have been presented in Yang et al (1994e).

SECTION 4

STATIC (DIRECT) OUTPUT FEEDBACK OF LINEAR STRUCTURES

The control methods presented in the previous section require full state feedback, either through measurements or an observer. For practical implementations of active/hybrid control systems in large civil engineering structures, it may not be practical to install sensors to measure the full state vector. On the other hand, an observer may require a significant amount of on-line computational efforts, resulting in a system time delay. In this section, static output feedback controllers using only the measured information from a limited number of sensors installed at strategic locations are presented. However, one limitation is imposed; namely, wherever a controller is installed, a measurement of the corresponding velocity state variable is required. In other words, collocated velocity sensors are required as a minimum. Furthermore, both the sliding surface and the controller are designed using only the observation (output) vector.

4.1 DESIGN OF SLIDING SURFACE

Let Z_m be a m-dimensional observation (output) vector consisting of m measured state variables with $m \geq r$, where r is the number of controllers,

$$Z_m = C_m Z \;\; ; \;\; C_m = \begin{bmatrix} \tilde{C} & 0 \\ 0 & I_r \end{bmatrix} \tag{4.1}$$

in which C_m is a (mx2n) observation matrix and I_r is a (rxr) identity matrix indicating the collocated velocity sensors. The sliding surface is given by

$$S = P_m Z_m = P_m C_m Z = PZ = 0 \tag{4.2}$$

in which P_m is a (rxm) matrix and $P = P_m C_m$. It should be noted that the order of the equations of motion, Eq. (2.1), has been rearranged such that the equations associated with the collocated velocity sensors are placed in the lower part, see Eq. (4.1). Hence, the order of the state variables in Z has been rearranged. This can be done, however, in the computer program easily.

Using the same transformation given by Eqs. (2.9) and (2.10), one obtains the regular form and the equations of motion on the sliding surface

$$\dot{Y}_1 = \bar{A}_{11} Y_1 + \bar{A}_{12} Y_2 \tag{4.3}$$

$$S = P_m C_m D^{-1} Y = \bar{P} Y = 0 \tag{4.4}$$

in which P_m and $\bar{P}$ are partitioned as follows

$$P_m = [P_{m1}, P_{m2}] \tag{4.5}$$

$$\bar{P} = [P_{m1}\tilde{C}\ ,\ P_{m1}\tilde{C}B_1B_2^{-1} + P_{m2}] \tag{4.6}$$

where $\tilde{C}$ is given by Eq. (4.1). Similar to Eq. (2.18), the second matrix of $\bar{P}$ in Eq. (4.6) is chosen to be I_r for convenience, i.e.,

$$P_{m1}\tilde{C}B_1B_2^{-1} + P_{m2} = I_r \tag{4.7}$$

Substituting Eq. (4.7) into Eq. (4.6) and then into Eq. (4.4), one obtains

$$Y_2 = -P_{m1}\tilde{C}Y_1 \tag{4.8}$$

With the equation of motion given by Eq. (4.3) and the output observation $y=\tilde{C}Y_1$, the gain matrix P_{m1} in Eq. (4.8) can be determined easily using the method of pole assignment. Obviously, the gain matrix P_{m1} depends on the preassigned locations of the closed-loop poles of the sliding surface. Once P_{m1} is determined, P_{m2} can be obtained from Eq. (4.7). Thus, P_m in Eq. (4.5) and P in Eq. (4.2) are completely determined.

4.2 DESIGN OF CONTROLLERS

The same Lyapunov function V and its time derivative given by Eqs. (2.29) to (2.32) are considered. For the continuous controller, we choose

$$U(t) = -(PB)^{-1}P[A(NC_m)Z + E] - \bar{\delta}\lambda' \tag{4.9}$$

in which N is a (2nxm) matrix to be determined such that $\dot{V} \leq 0$. Substituting Eq. (4.9) into Eq. (2.31), one obtains

$$\dot{V} = Z'[P'PA(I_{2n} - NC_m) - P'PB\bar{\delta}B'P'P]Z \tag{4.10}$$

Thus, N is chosen such that the matrix Λ given below is negative semidefinite,

$$\Lambda = P'PA(I_{2n} - NC_m) - P'PB\bar{\delta}B'P'P \tag{4.11}$$

in which the second matrix $-P'PB\bar{\delta}B'P'P$ is negative semidefinite.

Let $\bar{Z}_m$ be a 2n-dimensional modified observation (output) vector consisting of m

measured (output) state variables (i.e., Z_m) and zero elements for those state variables that are not measured. Then, $\bar{Z}_m$ can be expressed as

$$\bar{Z}_m = \bar{C}_m Z \tag{4.12}$$

in which $\bar{C}_m$ is the expanded version of the observation matrix C_m, Eq. (4.1). In other words, C_m is a submatrix of $\bar{C}_m$ and other elements of $\bar{C}_m$ are zero. The (2nx2n) matrix NC_m in Eq. (4.9) can be chosen to be $\bar{C}_m$. Because of the requirement of collocated velocity sensors, i.e., I_r in Eq. (4.1), and the fact that the structure without control is stable, the real parts of all eigenvalues of the matrix Λ in Eq. (4.11) are non-positive for $\bar{\delta}=0$, when NC_m is chosen to be $\bar{C}_m$, i.e., $NC_m=\bar{C}_m$. This special controller is identical to the continuous controller given by Eq. (2.34) in which Z is replaced by $\bar{Z}_m$, i.e., .

$$U = G - \bar{\delta}\lambda' \tag{4.13}$$

where

$$\lambda = \bar{Z}_m' P' P B \quad ; \quad G = -(PB)^{-1} P[A\bar{Z}_m + E] \tag{4.14}$$

Note that the sliding surface can be shown to be $S=P_mZ_m=P_mC_mZ=PZ=P\bar{Z}_m=0$. Such a relation has been used in Eq. (4.14).

For the discontinuous controller, we choose

$$u_i(t) = \begin{cases} -\left\{(PB)^{-1}P[A(NC_m)Z+E]\right\}_i - \delta_i H(|\lambda|-\epsilon_0) \; ; \; if \; \lambda_i > 0 \\ -\left\{(PB)^{-1}P[A(NC_m)Z+E]\right\}_i + \delta_i H(|\lambda|-\epsilon_0) \; ; \; if \; \lambda_i < 0 \end{cases} \tag{4.15}$$

in which $\{\}_i$ is the ith component of the vector in the bracket and N is a (2nxm) matrix to be determined such that $\dot{V} \le 0$. Substituting Eq. (4.15) into Eq. (2.31), one obtains

$$\dot{V} = Z'[P'PA(I_{2n} - NC_m)]Z - \left(\sum_{i=1}^{r} |\lambda_i \delta_i|\right) H(|\lambda| - \epsilon_0) \tag{4.16}$$

Thus, N is chosen such that the matrix Λ_1 is negative semidefinite

$$\Lambda_1 = P'PA(I_{2n} - NC_m) \tag{4.17}$$

Again, with the choice of $NC_m=\bar{C}_m$, the real parts of all eigenvalues of Λ_1 are nonpositive, because of the requirement of collocated velocity sensors and the fact that the uncontrolled structure is stable. This special controller is identical to the controller given by Eq.

(2.36) with Z replaced by $\bar{Z}_m$ and $S=P\bar{Z}_m$, i.e.,

$$u_i(t) = \begin{cases} G_i - \delta_i H(|\lambda| - \epsilon_0) \; ; \; if \; \lambda_i > 0 \\ G_i + \delta_i H(|\lambda| - \epsilon_0) \; ; \; if \; \lambda_i < 0 \end{cases} \tag{4.18}$$

where

$$\lambda = \bar{Z}_m P'PB \; ; \; G = -(PB)^{-1}P[A\bar{Z}_m + E] \tag{4.19}$$

In a similar manner, the three-condition controllers given by Eqs. (2.37) and (2.47) and the bang-bang controllers in Eqs. (2.48) and (2.49) can be used for static output feedback in which the state vector Z should be replaced by $\bar{Z}_m$. For the three-condition discontinuous controllers above, it is not necessary that $\dot{V} \leq 0$ for all time t unless the sliding margin is large. However, the control action is always taken to reduce $\dot{V}$ such that $\dot{V}_i \leq \dot{V}_{in}$ and hence the response state vector Z can be shown to be bounded. Finally, the saturated controllers given by Eqs. (2.45) and (2.43) can be used for the static output feedback with Z being replaced by $\bar{Z}_m$; however, the stability condition should be checked by numerical simulations for each design. Because of the requirement of collocated velocity sensors, the controlled structures are usually stable.

SECTION 5

SIMULATION RESULTS OF LINEAR STRUCTURES

To demonstrate the applications of the sliding mode control methods presented and to compare their performances with that of Linear Quadratic Regulator (LQR), simulation results are obtained in this section. Two numerical examples are considered: (1) a three-story scaled building model equipped with: (i) ABS, (ii) active variable stiffness (AVS) system, and (iii) active variable damper (AVD) system, respectively; and (2) a six-story full-scale building equipped with ABS. For illustrative purpose, $\epsilon_0=0$ will be used in all the following examples for discontinuous controllers.

Example 1: A Three-Story Scaled Building Model

A three-story scaled building model studied by Kobori & Kamagata (1992a), in which every story unit is identically constructed, is considered as shown in Fig. 2-1. The mass, stiffness and damping coefficient of each story unit are $m_i=1$ metric ton, $k_i=980$kN/m, and $c_i=1.407$kN·s/m, respectively, for i=1,2, and 3. A controller, such as ABS, AVS, or AVD, is installed in the first story unit as shown in Fig. 2-1. Thus, there is only one sliding surface. For full-state feedback, the LQR method is used for the design of the sliding surface with a diagonal weighting matrix Q, Eq. (2.21), as follows: $Q_{ii}= (10^5,10^4,10^3,1,1,1)$. This results in a sliding surface as follows: $S_1=223.6x_1-17.32x_2+6.01x_3+3.68\dot{x}_1+2.68\dot{x}_2+1.01\dot{x}_3=0$. The El Centro earthquake (NS component) scaled to a maximum acceleration of 0.112g is used as the input excitation, see Fig. 5-1.

Case 1: Active Bracing System (ABS) with Full-State Feedback

Suppose an ABS is installed in the first story unit as shown in Fig. 2-1(a) and the sliding surface is obtained previously. Using the continuous controller given by Eq. (2.34) with $\delta_1=50$kN·kg·cm/s, the maximum interstory drifts, x_i, the maximum absolute floor accelerations, $\ddot{x}_{ai}$, and the maximum required control force U (in terms of % of the total building weight) within 30 seconds of the earthquake episode, are shown in columns (6) and (7) of Table 5-I, denoted by CSMC (continuous sliding mode control). The maximum response quantities for the structure without control are shown in columns (2) and (3). For comparison purposes, the

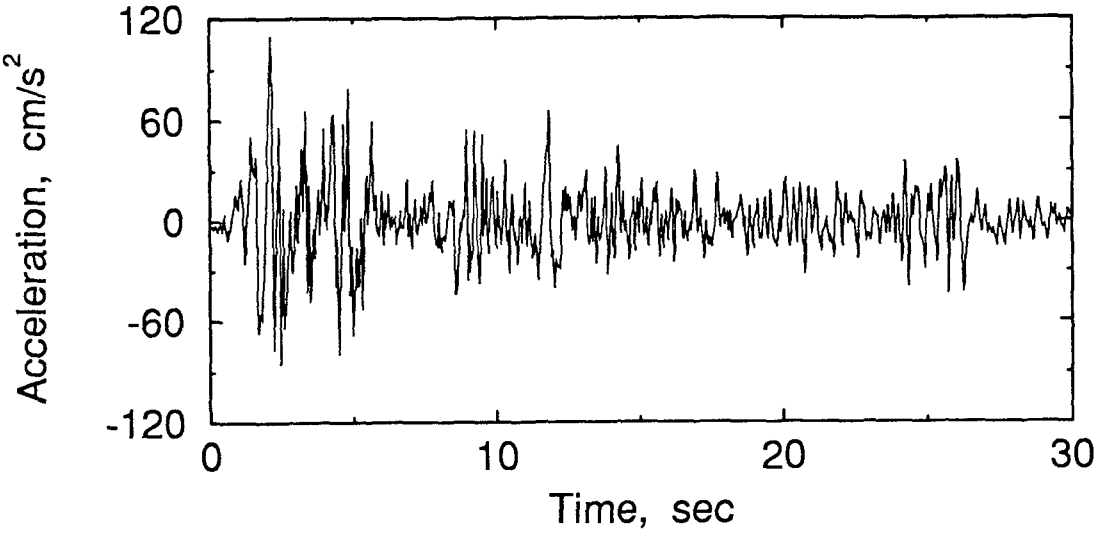

Fig. 5-1 : El Centro Earthquake (NS Component) Scaled to 0.112 g

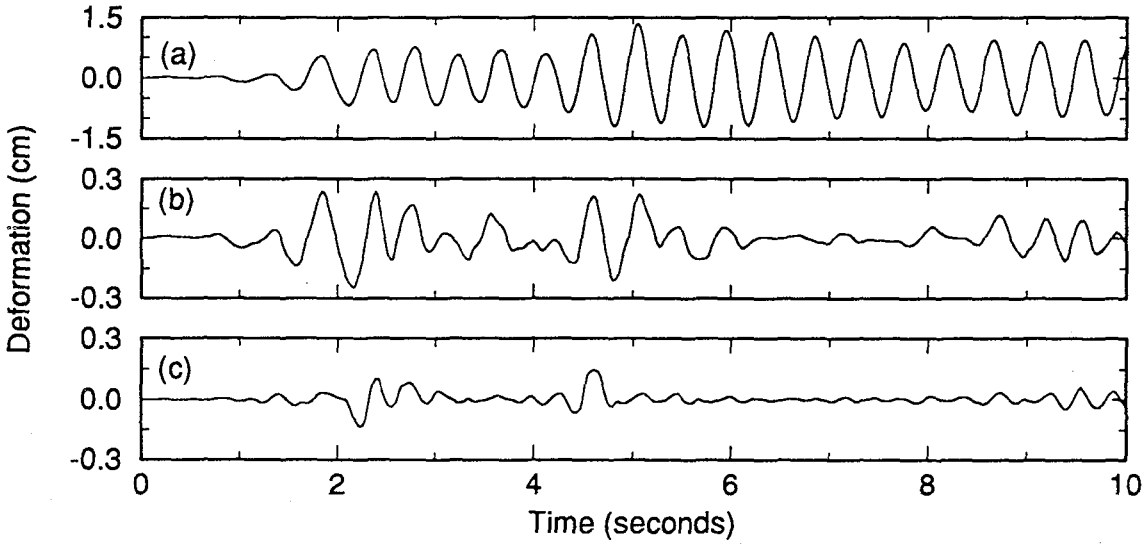

Fig. 5-2 : Deformation of The First Story Unit : (a) No Control; (b) with LQR; And (c) with CSMC

corresponding response quantities using the classical LQR method are displayed in columns (4) and (5) of Table 5-I. In using the method of LQR, the weighting matrix Q is identical to that used for CSMC, whereas the element (only one element) of the R matrix is adjusted so that the maximum control force is 12.3% of the total building weight. Using the discontinuous controllers given by Eqs. (2.36) and (2.37) with δ_1=50N, the corresponding response quantities are shown in columns (8)-(11) of Table 5-I designated as SMC I and SMC II, respectively.

Suppose the control force is bounded by 2500N, then the saturated controllers given by Eqs. (2.43), (2.45) and (2.47) with $\alpha_1^*=\alpha_1=1.0$ and $\bar{u}_{max}$=8.5% (2500N) are used. The corresponding maximum response quantities are presented in columns (14) to (19), whereas the results using the LQR control method are shown in columns (12) and (13) for comparison. Again, for the LQR method, the one element of the R matrix is adjusted so that the maximum control force is 8.5% (2500N). Time histories for the drift, $x_1(t)$, of the first story unit using the classical LQR control method and the continuous sliding mode control method are presented, respectively, in Figs. 5-2(b) and 5-2(c). The response without control is shown in Fig. 5-2(a) for comparison. Finally, a further reduction of the control force to a maximum of $\bar{u}_{max}$ = 5.1% (1500N) is considered. The results are shown in columns (20)-(27) of Table 5-I. One significant advantage of the sliding mode control (SMC) method is that there is no adverse effect due to actuator saturation. It is observed from Table 5-I that the performance of sliding mode control is better than that of the LQR method, in particular for the cases where the maximum control forces are bounded to be either U=8.5% or U=5.1%.

Case 2: Robustness with Respect to Parametric Uncertainties

It has been shown in the literature that sliding mode control is robust with respect to system parametric uncertainties. The robustness of the control design will be demonstrated through the following numerical simulations. ±30% variations of the stiffnesses for all the story units from their true values are considered. The designs of the sliding surface and the controller are based on ±30% deviations from their actual values. All the design parameters are identical to that used in Table 5-I. The results for the maximum response quantities are presented in Table 5-II. Note that columns (4)-(5), (10)-(11) and (16)-(17) of Table 5-II, corresponding to

Table 5-I : Maximum Response Quantities of a 3-Story Scaled Building Equipped with One ABS (Full State Feedback)

STORY NO (1)	No Control		LQR U=3603N U=12.3%		CSMC U=3603N U=12.3%		SMC I U=3525N U=12.0%		SMC II U=3950N U=13.4%	
	x_i cm (2)	$\ddot{x}_{ai}$ cm/s^2 (3)	x_i cm (4)	$\ddot{x}_{ai}$ cm/s^2 (5)	x_i cm (6)	$\ddot{x}_{ai}$ cm/s^2 (7)	x_i cm (8)	$\ddot{x}_{ai}$ cm/s^2 (9)	x_i cm (10)	$\ddot{x}_{ai}$ cm/s^2 (11)
1	1.33	312	0.09	147	0.09	135	0.09	127	0.09	318
2	1.02	473	0.32	169	0.31	162	0.31	162	0.31	162
3	0.59	580	0.21	203	0.20	199	0.20	199	0.20	199

STORY NO (1)	No Control		LQR U=2500N U=8.5%		CSMC U=2500N U=8.5%		SMC I U=2500N U=8.5%		SMC II U=2500N U=8.5%	
	x_i cm (2)	$\ddot{x}_{ai}$ cm/s^2 (3)	x_i cm (12)	$\ddot{x}_{ai}$ cm/s^2 (13)	x_i cm (14)	$\ddot{x}_{ai}$ cm/s^2 (15)	x_i cm (16)	$\ddot{x}_{ai}$ cm/s^2 (17)	x_i cm (18)	$\ddot{x}_{ai}$ cm/s^2 (19)
1	1.33	312	0.25	117	0.15	153	0.17	147	0.17	203
2	1.02	473	0.33	154	0.25	158	0.24	163	0.29	129
3	0.59	580	0.23	224	0.19	186	0.18	179	0.18	173

STORY NO (1)	No Control		LQR U=1500N U=5.1%		CSMC U=1500N U=5.1%		SMC I U=1500N U=5.1%		SMC II U=1500N U=5.1%	
	x_i cm (2)	$\ddot{x}_{ai}$ cm/s^2 (3)	x_i cm (20)	$\ddot{x}_{ai}$ cm/s^2 (21)	x_i cm (22)	$\ddot{x}_{ai}$ cm/s^2 (23)	x_i cm (24)	$\ddot{x}_{ai}$ cm/s^2 (25)	x_i cm (26)	$\ddot{x}_{ai}$ cm/s^2 (27)
1	1.33	312	0.50	157	0.29	177	0.38	158	0.36	174
2	1.02	473	0.42	212	0.33	224	0.33	225	0.33	217
3	0.59	580	0.26	258	0.20	201	0.23	224	0.26	254

Table 5-II : Maximum Response Quantities of a 3-Story Scaled Building with Uncertainties in Stiffness (Full-State Feedback)

CSMC								
STORY NO (1)	No Control		0% K U=3603N U= 12.3%		+30% K U=3662N U=12.5%		-30% K U=3590N U=12.3%	
	x_i cm (2)	$\ddot{x}_{ai}$ cm/s^2 (3)	x_i cm (4)	$\ddot{x}_{ai}$ cm/s^2 (5)	x_i cm (6)	$\ddot{x}_{ai}$ cm/s^2 (7)	x_i cm (8)	$\ddot{x}_{ai}$ cm/s^2 (9)
1	1.33	312	0.09	135	0.08	129	0.09	143
2	1.02	473	0.31	162	0.31	163	0.31	165
3	0.59	580	0.20	199	0.20	201	0.20	198
SMC I								
STORY NO (1)	No Control		0% K U=3525N U=12.0%		+30% K U=3655N U=12.4%		-30% K U=3584N U=12.2%	
	x_i cm (2)	$\ddot{x}_{ai}$ cm/s^2 (3)	x_i cm (10)	$\ddot{x}_{ai}$ cm/s^2 (11)	x_i cm (12)	$\ddot{x}_{ai}$ cm/s^2 (13)	x_i cm (14)	$\ddot{x}_{ai}$ cm/s^2 (15)
1	1.33	312	0.09	127	0.08	129	0.10	143
2	1.02	473	0.31	162	0.31	163	0.31	165
3	0.59	580	0.20	199	0.21	202	0.20	198
SMC II								
STORY NO (1)	No Control		0% K U=3950N U=13.4%		+30% K U=3621N U=12.3%		-30% K U=4096N U=13.9%	
	x_i cm (2)	$\ddot{x}_{ai}$ cm/s^2 (3)	x_i cm (16)	$\ddot{x}_{ai}$ cm/s^2 (17)	x_i cm (18)	$\ddot{x}_{ai}$ cm/s^2 (19)	x_i cm (20)	$\ddot{x}_{ai}$ cm/s^2 (21)
1	1.33	312	0.09	318	0.08	310	0.09	319
2	1.02	473	0.31	162	0.32	163	0.30	161
3	0.59	580	0.20	199	0.20	198	0.20	195

no uncertainty (0% variation), are identical to those presented in columns (6)-(11) of Table 5-I. Table 5-II demonstrates clearly that with uncertainties of $\pm 30\%$ for the stiffness of all story units, the control performance does not have any degradation. Extensive numerical results indicate that the sliding mode control methods are more robust with respect to uncertainties in dampings and masses. These results are consistent with the conclusion in [Yang et al, 1991] that the uncertainty in the stiffness estimation is more detrimental than uncertainties in the estimations of dampings and masses. It should be cautioned, however, that the robustness of the control methods presented above depends on the design parameters chosen. In general, the control design is more robust if (i) the gain margin δ_i is bigger, and (ii) the close-loop eigenvalues for the sliding surface are shifted to the left hand side as much as practical. In other words, the real parts of the close-loop eigenvalues for the sliding surface should be as large (negative) as practical.

Case 3: Static (Direct) Output Feedback and Robustness

The method of static (direct) output feedback presented in Section 4 will be demonstrated herein. Suppose only the responses of the first story unit, $x_1(t)$ and $\dot{x}_1(t)$, are measured in addition to the ground acceleration $\ddot{x}_0(t)$. With static output feedbacks of x_1 and $\dot{x}_1$, the sliding surface is chosen to be $S_1 = 1000x_1 + \dot{x}_1 = 0$. The output feedback (continuous) controller presented in Eqs. (4.13) and (4.14) with the sliding margin $\delta_1 = 50$ N·kg·cm/s is used. With this special controller, the maximum response quantities and the maximum control force are presented in columns (16) and (17) of Table 5-III, denoted by DOF(direct output feedback). These results are displayed in the upper part of Table 5-III, denoted by CSMC (continuous sliding mode control). For comparison, the corresponding results based on the full state feedback given in columns (6) and (7) of Table 5-I are shown in columns (4) and (5) of Table 5-III, denoted by FSF (full state feedback). A comparison between columns (4) and (5) with columns (16) and (17) indicates that the performance of the static output feedback controller is comparable with that of the full state feedback controller. However, the required maximum control force is bigger for the static output feedback controllers as expected.

To compare the static output feedback results with the results of the full-state feedback, on the basis of the same maximum control force U, the saturated controllers given by Eq. (2.43)

Table 5-III : Maximum Response Quantities of a 3-Story Building Equipped with An ABS Using Static Output Feedback

CSMC : $S=1000x_1+\dot{x}_1=0$; δ_1=50 N·kg·cm/s

ST NO (1)	No Control		FSF U=3603N U=12.3%		DOF U=3800N U=12.9%		FSF U=2500N U=8.5%		DOF U=2500N U=8.5%		FSF U=1500N U=5.1%		DOF U=1500N U=5.1%		DOF U=5439N U=18.5%	
	x_i cm (2)	$\ddot{x}_{ai}$ cm/s^2 (3)	x_i cm (4)	$\ddot{x}_{ai}$ cm/s^2 (5)	x_i cm (6)	$\ddot{x}_{ai}$ cm/s^2 (7)	x_i cm (8)	$\ddot{x}_{ai}$ cm/s^2 (9)	x_i cm (10)	$\ddot{x}_{ai}$ cm/s^2 (11)	x_i cm (12)	$\ddot{x}_{ai}$ cm/s^2 (13)	x_i cm (14)	$\ddot{x}_{ai}$ cm/s^2 (15)	x_i cm (16)	$\ddot{x}_{ai}$ cm/s^2 (17)
1	1.33	312	0.09	135	0.17	210	0.15	153	0.21	179	0.29	177	0.28	182	0.04	108
2	1.02	473	0.31	162	0.45	212	0.25	158	0.35	227	0.33	224	0.35	243	0.50	234
3	0.59	580	0.20	199	0.28	278	0.19	186	0.22	215	0.20	201	0.23	226	0.30	291

CSMC : $S=100x_1+\dot{x}_1=0$; δ_1=50 N·kg·cm/s

ST NO (1)	No Control		FSF U=3603N U=12.3%		DOF U=3800N U=12.9%		FSF U=2500N U=8.5%		DOF U=2500N U=8.5%		FSF U=1500N U=5.1%		DOF U=1500N U=5.1%		DOF U=4461N U=15.2%	
	x_i cm (2)	$\ddot{x}_{ai}$ cm/s^2 (3)	x_i cm (4)	$\ddot{x}_{ai}$ cm/s^2 (5)	x_i cm (6)	$\ddot{x}_{ai}$ cm/s^2 (7)	x_i cm (8)	$\ddot{x}_{ai}$ cm/s^2 (9)	x_i cm (10)	$\ddot{x}_{ai}$ cm/s^2 (11)	x_i cm (12)	$\ddot{x}_{ai}$ cm/s^2 (13)	x_i cm (14)	$\ddot{x}_{ai}$ cm/s^2 (15)	x_i cm (16)	$\ddot{x}_{ai}$ cm/s^2 (17)
1	1.33	312	0.09	135	0.30	103	0.15	153	0.39	138	0.29	177	0.56	201	0.30	107
2	1.02	473	0.31	162	0.24	132	0.25	158	0.29	179	0.33	224	0.38	215	0.24	125
3	0.59	580	0.20	199	0.16	158	0.19	186	0.18	177	0.20	201	0.31	301	0.16	162

SMC II : $S=1000x_1+\dot{x}_1=0$; δ_1=50 N

ST NO (1)	No Control		FSF U=3950N U=13.4%		DOF U=3800N U=12.9%		FSF U=2500N U=8.5%		DOF U=2500N U=8.5%		FSF U=1500N U=5.1%		DOF U=1500N U=5.1%	
	x_i cm (2)	$\ddot{x}_{ai}$ cm/s^2 (3)	x_i cm (4)	$\ddot{x}_{ai}$ cm/s^2 (5)	x_i cm (6)	$\ddot{x}_{ai}$ cm/s^2 (7)	x_i cm (8)	$\ddot{x}_{ai}$ cm/s^2 (9)	x_i cm (10)	$\ddot{x}_{ai}$ cm/s^2 (11)	x_i cm (12)	$\ddot{x}_{ai}$ cm/s^2 (13)	x_i cm (14)	$\ddot{x}_{ai}$ cm/s^2 (15)
1	1.33	312	0.09	318	0.13	386	0.17	203	0.20	254	0.36	174	0.36	214
2	1.02	473	0.31	162	0.46	234	0.29	129	0.38	200	0.33	217	0.40	231
3	0.59	580	0.20	199	0.25	244	0.18	173	0.24	237	0.26	254	0.30	292

SMC II : $S=100x_1+\dot{x}_1=0$; δ_1=50 N

ST NO (1)	No Control		FSF U=3950N U=13.4%		DOF U=3800N U=12.9%		FSF U=2500N U=8.5%		DOF U=2500N U=8.5%		FSF U=1500N U=5.1%		DOF U=1500N U=5.1%	
	x_i cm (2)	$\ddot{x}_{ai}$ cm/s^2 (3)	x_i cm (4)	$\ddot{x}_{ai}$ cm/s^2 (5)	x_i cm (6)	$\ddot{x}_{ai}$ cm/s^2 (7)	x_i cm (8)	$\ddot{x}_{ai}$ cm/s^2 (9)	x_i cm (10)	$\ddot{x}_{ai}$ cm/s^2 (11)	x_i cm (12)	$\ddot{x}_{ai}$ cm/s^2 (13)	x_i cm (14)	$\ddot{x}_{ai}$ cm/s^2 (15)
1	1.33	312	0.09	318	0.39	466	0.17	203	0.41	353	0.36	174	0.51	279
2	1.02	473	0.31	162	0.37	228	0.29	129	0.38	218	0.33	217	0.42	234
3	0.59	580	0.20	199	0.35	346	0.18	173	0.35	345	0.26	254	0.34	330

and (2.47) are used for the static output feedback where the state vector Z is replaced by the observation vector $\bar{Z}_m$. The parameters appearing in the controllers are : $\alpha_1=1$, $\alpha_1^*=1$, and $\bar{u}_{max}=12.9\%$, 8.5% and 5.1%, respectively. The following gain margins are used: $\delta_1=50$ N·kg·cm/s for the continuous controller, Eq. (2.43), and $\delta_1=50$N for the discontinuous controller, Eq. (2.46). The results for the maximum response quantities are shown in columns (6), (7), (10), (11), (14) and (15) of Table 5-III, denoted by DOF. The results based on the discontinuous controller, Eq. (2.47), are shown in the lower part of Table 5-III, denoted by SMC II. Also shown in columns (4), (5), (8), (9), (12) and (13) are the results for the full-state feedback given in Table 5-I, denoted by FSF. It is observed that the results using the static output feedback are favorable in comparison with that of the full-state feedback. However, cautions should be taken that the performance for the static output feedback depends on the design of the sliding surface as well as the design parameters. For instance, if the sliding surface is considered as $S_1=100x_1+\dot{x}_1=0$ and the same α_1, α_1^*, and δ_1 are used, then the corresponding results are also shown in Table 5-III. A slight degradation for the control performance is observed, because the pole of the sliding surface is not shifted to the left hand side as much as possible.

To show the robustness of the static output feedback control design, we consider the case shown in columns (14)-(15) of Table 5-III for $S_1=1000x_1+\dot{x}_1=0$. With $\pm 30\%$ estimation errors for the stiffness of each story unit, the maximum response quantities are shown in columns (6)-(9) of Table 5-IV. Also shown in columns (4)-(5) are the results from columns (14)-(15) of Table 5-III for comparison. As observed from Table 5-IV, the control designs are very robust.

Case 4: Complete Compensation

When each story unit is equipped with a controller, it has been derived in the previous section that a complete compensation for the earthquake ground acceleration can be achieved using the controllers given by Eqs. (2.34) and (2.36). In other words, the state vector can be reduced to zero. This situation requires a full-state feedback and it will be demonstrated herein. The sliding surface is designed using the LQR method with a diagonal Q matrix $Q_{ii}=[10^4,10^4,10^4,1,1,1]$. The gain margins $\delta_1=\delta_2=\delta_3=50$kN·kg·cm/s for Eq. (2.34) and

Table 5-IV: Maximum Response Quantities of a 3-Story Scaled Building with Stiffness Uncertainty (Static Output Feedback)

CSMC								
STORY NO (1)	No Control		0% U=5.1% (1500N)		+30% U=5.1% (1500N)		-30% U=5.1% (1500N)	
	x_i cm (2)	$\ddot{x}_{ai}$ cm/s^2 (3)	x_i cm (4)	$\ddot{x}_{ai}$ cm/s^2 (5)	x_i cm (6)	$\ddot{x}_{ai}$ cm/s^2 (7)	x_i cm (8)	$\ddot{x}_{ai}$ cm/s^2 (9)
1	1.33	312	0.28	182	0.29	181	0.28	184
2	1.02	473	0.35	243	0.35	244	0.35	243
3	0.59	580	0.23	226	0.23	227	0.23	224
SMC II								
STORY NO (1)	No Control		0% U=5.1 % (1500N)		+30% U=5.1 % (1500N)		-30% U=5.1% (1500N)	
	x_i cm (2)	$\ddot{x}_{ai}$ cm/s^2 (3)	x_i cm (4)	$\ddot{x}_{ai}$ cm/s^2 (5)	x_i cm (6)	$\ddot{x}_{ai}$ cm/s^2 (7)	x_i cm (8)	$\ddot{x}_{ai}$ cm/s^2 (9)
1	1.33	312	0.36	214	0.36	216	0.36	212
2	1.02	473	0.40	231	0.40	231	0.41	230
3	0.59	580	0.30	292	0.30	297	0.29	288

$\delta_1=\delta_2=\delta_3=5$N for Eq. (2.36) are used. In the entire earthquake episode, the maximum response quantities and the maximum control force from each controller are presented in columns (4)-(6) of Table 5-V. As expected, the interstory drifts and relative velocities are all zero, whereas the maximum acceleration of each floor is identical to that of the earthquake excitation 0.112g (109cm/s^2). For the complete compensation of the structural response, a problem of concern is the robustness with respect to system uncertainties. Here we consider $\pm$40% estimate errors for the stiffness of all the story units. The results for the maximum response quantities and the maximum control forces are presented in columns (7)-(12) of Table 5-V. As observed from Table 5-V, the control designs are robust.

Case 5: Parametric Control Using AVS and AVD Systems

Suppose only one active variable stiffness (AVS) system is installed in the first story unit as shown in Fig. 2-1(b). The stiffness of the stand-by bracings is identical to that of the first story unit, i.e., $\bar{k}_{1,1}=980$kN/m. The sliding surface is designed using the LQR method with the diagonal weighting matrix $Q_{ii}=[1000,1,1,1,1,1]$. The resulting sliding surface is: $S_1=22.36\,x_1-23.11\,x_2+16.14\,x_3+1.37\,\dot{x}_1+0.37\,\dot{x}_2-0.015\,\dot{x}_3=0$. The controller given by Eq. (3.7) is used. In thirty seconds of the earthquake episode, the maximum response quantities are presented in columns (4) and (5) of Table 5-VI, denoted by "AVS." It is observed that the installation of an active variable stiffness system in the first story unit is very effective in reducing the building response and the performance of the proposed control method is remarkable. Investigations of static output feedback, robustness and other control algorithms are presented in Yang et al (1993a,1994e).

Instead of an AVS system, we next consider an active variable damper (AVD) installed in the first story unit as shown in Fig. 2-1(c). The maximum damping coefficient is 15.63kN·s/m and the minimum one is zero, i.e., $\xi_{imin}=0$ and $\xi_{imax}=15.63$kN·s/m in Eq. (3.2). The sliding surface is designed using the LQR method with the diagonal weighting matrix $Q_{ii}=(1,1,1,1000,1,1)$. The resulting sliding surface is given by $S_1=0.032x_1-0.306x_2+0.023x_3+\dot{x}_1-0.0005\dot{x}_2-0.00001\dot{x}_3=0$. The simple two-stage controller given by Eq. (3.4) is used. The maximum response quantities are summarized in columns (6) and (7) of Table 5-VI. These numerical results demonstrate that an active variable damper installed in the

Table 5-V : Maximum Response Quantities of a 3-Story Scaled Building with Complete Compensation

CSMC											
STORY NO (1)	No Control		No Uncertainty			+40% K			-40% K		
	x_i cm (2)	$\ddot{x}_{ai}$ cm/s^2 (3)	x_i cm (4)	$\ddot{x}_{ai}$ cm/s^2 (5)	U % (6)	x_i cm (7)	$\ddot{x}_{ai}$ cm/s^2 (8)	U % (9)	x_i cm (10)	$\ddot{x}_{ai}$ cm/s^2 (11)	U % (12)
1	1.33	312	0	109	11.1	0	109	11.1	0	109	11.1
2	1.02	473	0	109	7.43	0	109	7.43	0	109	7.43
3	0.59	580	0	109	3.72	0	109	3.72	0	109	3.72
SMC I											
STORY NO (1)	No Control		No Uncertainty			+40% K			-40% K		
	x_i cm (2)	$\ddot{x}_{ai}$ cm/s^2 (3)	x_i cm (4)	$\ddot{x}_{ai}$ cm/s^2 (5)	U % (6)	x_i cm (7)	$\ddot{x}_{ai}$ cm/s^2 (8)	U % (9)	x_i cm (10)	$\ddot{x}_{ai}$ cm/s^2 (11)	U % (12)
1	1.33	312	0	108	11.1	0	108	11.1	0	110	11.2
2	1.02	473	0	110	7.45	0	110	7.45	0	108	7.41
3	0.59	580	0	109	3.70	0	109	3.70	0	110	3.74

Table 5-VI : Maximum Response Quantities of A 3-Story Scaled Building Equipped with Active Variable Stiffness (AVS) System And Active Variable Damper (AVD) in The First Story Unit

ST NO (1)	No Control		AVS		AVD	
	x_i cm (2)	$\ddot{x}_{ai}$ cm/s^2 (3)	x_i cm (4)	$\ddot{x}_{ai}$ cm/s^2 (5)	x_i cm (6)	$\ddot{x}_{ai}$ cm/s^2 (7)
1	1.33	312	0.25	309	0.62	156
2	1.02	473	0.43	249	0.49	237
3	0.59	580	0.30	298	0.28	274

first story unit is quite effective in reducing the building response. Again, the performance of the proposed control method is remarkable. Investigations of static output feedback for applications to bridge structures are presented in Yang et al (1993b, 1994a).

Example 2: Six-Story Full-Scale Takenaka Building

The six-story full-scale Takenaka Building in Japan is considered. In this test building, an ABS was installed in the first story unit. The mass of each floor is identical, which is equal to 100 metric tons. The fundamental natural frequency is 0.943Hz and the corresponding damping ratio is 1% for all modes. Details of the structural properties, such as stiffness and damping matrices, are given in [Soong et al 1991, Reinhorn et al 1992, 1993a]. The same El Centro earthquake is used as the input excitation except that the maximum acceleration is scaled to 0.3g.

The sliding surface is designed using the LQR method with the diagonal weighting matrix Q. All the diagonal elements of Q are equal to 1.0 except that $Q_{77}=10$. The sliding surface is obtained as P=[15.186, -27.669, 12.865, 2.345, -0.505, 0.311, 1.004, 0.0043, -0.188, 0.0304, 0.0242, 0.0043]. The controllers given by Eq. (2.34) with $\delta_1=10$ N·ton·cm/s and by Eq. (2.36) with $\delta_1=10$N are used. Within 30 seconds of the earthquake episode, the maximum response quantities are presented in columns (6)-(9) of Table 5-VII. Also shown in columns (2) and (3) of Table 5-VII are the maximum response quantities without control. For comparison, the results obtained using the classical LQR method are presented in columns (4) and (5). For the LQR method, the same weighting matrix Q is used but the R matrix, that consists of only one element, is adjusted so that the required maximum control force is 3149kN. It is observed from Table 5-VII that the performance of the sliding mode control method is slightly better than that of the LQR. Finally, the controller given by Eq. (2.37) has been used and the results are identical to those presented in columns (6) and (7) of Table 5-VII.

Table 5-VII : Maximum Response Quantities of a 6-Story Building Equipped with An ABS

STORY NO (1)	No Control		LQR U=3149 kN		CSMC U=3149 kN		SMC I U=3149 kN	
	x_i cm (2)	$\ddot{x}_{ai}$ cm/s^2 (3)	x_i cm (4)	$\ddot{x}_{ai}$ cm/s^2 (5)	x_i cm (6)	$\ddot{x}_{ai}$ cm/s^2 (7)	x_i cm (8)	$\ddot{x}_{ai}$ cm/s^2 (9)
1	1.97	319	1.43	248	1.41	238	1.41	237
2	3.91	628	1.90	193	1.74	177	1.74	176
3	4.34	761	2.06	267	1.83	242	1.83	241
4	4.70	759	1.99	371	1.79	336	1.79	336
5	4.42	891	1.82	337	1.64	297	1.64	297
6	3.04	970	1.41	494	1.27	447	1.27	447

SECTION 6

SLIDING MODE CONTROL OF NONLINEAR AND HYSTERETIC STRUCTURES

6.1 EQUATION OF MOTION OF NONLINEAR STRUCTURES

Consider an n degree-of-freedom nonlinear building structure subjected to a one-dimensional earthquake ground acceleration $\ddot{x}_0(t)$. The vector equation of motion is given by

$$M\ddot{X}(t) + C\dot{X}(t) + F_s[X(t)] = HU(t) + \eta\ddot{x}_0(t) \tag{6.1}$$

in which $X(t)=[x_1,x_2,\ldots,x_n]'$ is an n vector with $x_i(t)$ being the drift of the designated ith story unit; $U(t)=[u_1(t), u_2(t), \ldots, u_r(t)]'$ is a r-vector consisting of r control forces; and η is an n vector denoting the influence of the earthquake excitation. In Eq. (6.1), M and C are (nxn) mass and damping matrices, respectively, where linear viscous damping is assumed for the structure; H is a (nxr) matrix denoting the location of r controllers; and $F_s[X(t)]$ is an n-vector denoting the nonlinear stiffness force that is assumed to be a function of X(t).

The building system considered consists of (n-l) linear elastic elements (or story units) and l nonlinear (or hysteretic) elements. It is assumed that for each nonlinear element (or story unit) there is one controller installed so that the number, r, of controllers is larger than or equal to the number, l, of nonlinear elements, i.e., $r \geq l$. For instance, for a base-isolated building using lead-core rubber bearings, there is, as a minimum, one controller installed to control the base isolation system as shown in Fig. 6-1. If the response of any story unit of the superstructure is nonlinear or inelastic, then there should be one controller installed in that story unit. The restriction that the number of controllers should be larger than or equal to the number of nonlinear elements (story units) is imposed for the convenience in determining the sliding surface. The removal of such a restriction will be discussed later.

Based on the restriction above, the stiffness vector can be separated into two parts:

$$F_s[X(t)] = \tilde{K}X(t) + \tilde{H}f[X(t)] \tag{6.2}$$

in which $\tilde{K}$ is a (nxn) linear elastic stiffness matrix for both the linear story units and the linear elastic parts of the nonlinear or hysteretic story units; and $f=[f_1,f_2,\ldots,f_l]'$ = a l vector representing the nonlinear or hysteretic parts of the restoring forces for nonlinear story units. The nonlinear forces $f_1,f_2,\ldots,f_l$, are numbered to be consistent with those of the controllers.

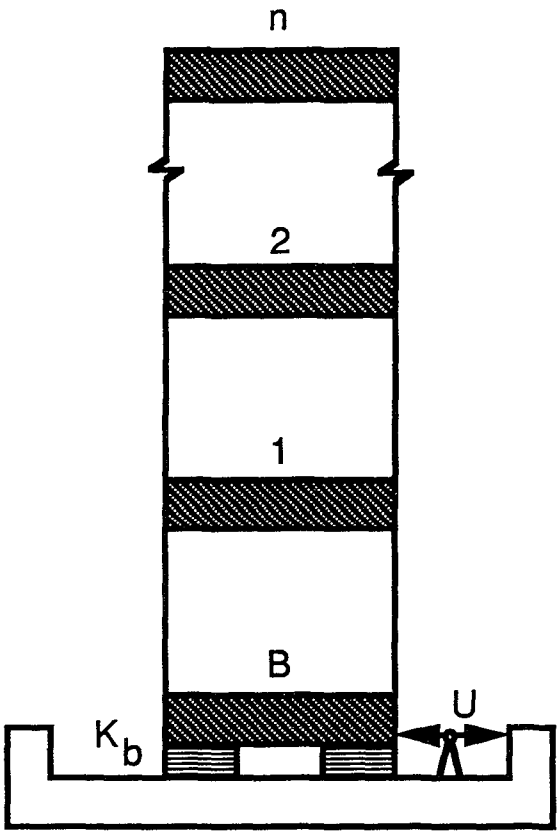

Fig. 6-1 : A Base-Isolated Structural Model

Consequently, the dimension of the location matrix, $\tilde{H}$, for the nonlinear elements (or story units) is (nx$l$) and it can be obtained from the location matrix, H, of the controllers by eliminating r-l columns. In other words, $\tilde{H}$ is a submatrix of H obtained by eliminating the columns of H associated with linear elastic story units.

In the state space, Eqs. (6.1) and (6.2) become

$$\dot{Z}(t) = AZ(t) - \tilde{B}f(Z) + BU(t) + E(t) \tag{6.3}$$

where Z(t) is a 2n state vector; A is a (2nx2n) linear elastic system matrix; B is a (2nxr) matrix; $\tilde{B}$ is a (2nx$l$) matrix; and E(t) is a 2n excitation vector given, respectively, by

$$Z(t) = \begin{bmatrix} X(t) \\ \dot{X}(t) \end{bmatrix}; \; E(t) = \begin{bmatrix} 0 \\ M^{-1}\eta \end{bmatrix} \ddot{X}_0(t); \; A = \begin{bmatrix} 0 & I \\ -M^{-1}\tilde{K} & -M^{-1}C \end{bmatrix}; \; B = \begin{bmatrix} 0 \\ M^{-1}H \end{bmatrix}; \; \tilde{B} = \begin{bmatrix} 0 \\ M^{-1}\tilde{H} \end{bmatrix} \tag{6.4}$$

Note that the $\tilde{B}$ matrix is obtained from B by eliminating r-l columns associated with linear elastic story units.

The state vector Z(t) in Eq. (6.3) consists of the interstory drifts and their derivatives. In some situations, where the use of absolute displacement and velocity variables is more convenient, a transformation of the state vector can be made and the form of the Eq. (6.3) still holds. Without loss of generality, Eq. (6.3) will be used in the following.

6.2 DESIGN OF SLIDING SURFACE

The theory of variable structure system (VSS) or sliding mode control (SMC) is to design controllers to drive the response trajectory into the sliding surface (or switching surface) and maintain it there, whereas the motion on the sliding surface is stable. In the design of the sliding surface, the external excitation E(t) is neglected; however, it is taken into account in the design of controllers. For simplicity, let $S=[S_1,S_2,\ldots,S_r]'=0$ be a r-dimensional sliding surface with r sliding variables, $S_1,S_2,\ldots,S_r$, given by

$$S = PZ = 0 \tag{6.5}$$

in which P is a (rx2n) matrix to be determined such that the motion on the sliding surface is stable. Because of the limitation that each nonlinear story unit is installed with one controller,

i.e., $r \geq l$, the P matrix can be determined in a similar manner described in Section 2 for linear structures. The determination of the P matrix is described briefly in the following. Let

$$Y = DZ \quad or \quad Z = D^{-1} Y \tag{6.6}$$

in which D is a transformation matrix

$$D = \begin{bmatrix} I_{2n-r} & -B_1 B_2^{-1} \\ 0 & I_r \end{bmatrix} \; ; \; D^{-1} = \begin{bmatrix} I_{2n-r} & B_1 B_2^{-1} \\ 0 & I_r \end{bmatrix} ; \; B = \begin{bmatrix} B_1 \\ B_2 \end{bmatrix} \tag{6.7}$$

where I_{2n-r} and I_r are (2n-r) x (2n-r) and (rxr) identity matrices, respectively, and B_1 and B_2 are (2n-r)xr and rxr submatrices obtained from the partition of the B matrix, Eq. (6.4). If the B_2 matrix is singular in the original state equation, then the state equation should be rearranged such that B_2 is nonsingular.

With the transformation matrix D, the state equation, Eq. (6.3), and the sliding surface, Eq. (6.5), become

$$\dot{Y} = \bar{A}\, Y - \tilde{B}^*\, f + \bar{B}\, U \tag{6.8}$$

$$S = \bar{P} Y = 0 \tag{6.9}$$

in which E(t) is neglected and

$$\bar{A} = DAD^{-1} \; ; \; \bar{P} = PD^{-1} \; ; \; \bar{B} = \begin{bmatrix} 0 \\ B_2 \end{bmatrix} ; \; \tilde{B}^* = \begin{bmatrix} 0 \\ \tilde{B}_2 \end{bmatrix} \tag{6.10}$$

where $\tilde{B}_2$ is a (rl) matrix obtained from the B_2 matrix, Eq.(6.7), by eliminating (r-l) columns. As observed from Eq. (6.8), only the last r equations involve the equivalent control force U and the nonlinear force vector f(Z). Thus, the equations of motion on the sliding surface are defined by r linear equations in Eq. (6.9) and 2n-r linear equations in the upper part of Eq. (6.8). Let Y, $\bar{A}$ and $\bar{P}$ be partitioned as follows

$$Y = \begin{bmatrix} Y_1 \\ Y_2 \end{bmatrix} \; ; \; \bar{A} = \begin{bmatrix} \bar{A}_{11} & \bar{A}_{12} \\ \bar{A}_{21} & \bar{A}_{22} \end{bmatrix} \; ; \; \bar{P} = \begin{bmatrix} \bar{P}_1, \bar{P}_2 \end{bmatrix} \tag{6.11}$$

in which Y_1 and Y_2 are 2n-r and r vectors, respectively, and $\bar{A}_{11}$, $\bar{A}_{22}$, $\bar{P}_1$ and $\bar{P}_2$ are (2n-r) x (2n-r), rxr, rx(2n-r) and rxr matrices, respectively. Substituting Eq. (6.11) into Eqs. (6.8) and (6.9), one obtains the linear equations of motion on the sliding surface in the following

$$\dot{Y}_1 = \bar{A}_{11} Y_1 + \bar{A}_{12} Y_2 \tag{6.12}$$

$$S = \bar{P}_1 Y_1 + \bar{P}_2 Y_2 = 0 \tag{6.13}$$

The linear equations of motion on the sliding surface defined by Eqs. (6.12) and (6.13) are identical to that defined by Eqs. (2.16) and (2.17) in Section 2 for linear structures. Consequently, the same procedures for determining the $\bar{P}$ and P matrices described in Section 2 can be used herein. These procedures include the pole assignment method and the LQR method. With the LQR method, the $\bar{P}$ matrix is determined by minimizing

$$J = \int_0^\infty Z'(t)\, Q\, Z(t)\, dt \tag{6.14}$$

in which Q is a (2nx2n) positive definite matrix and a prime indicates the transpose of either a vector or a matrix.

6.3 DESIGN OF CONTROLLERS

Consider a Lyapunov function V as follows

$$V = 0.5\, S'S = 0.5\, Z'P'PZ \tag{6.15}$$

The sufficient condition for the sliding mode S=0 to occur is given by

$$\dot{V} = S'\dot{S} \leq 0 \tag{6.16}$$

Taking the derivative of Eq. (6.15) and using the state equation of motion, Eq. (6.3), one obtains

$$\dot{V} = \lambda(U - G) = \sum_{i=1}^{r} \lambda_i (u_i - G_i) = \sum_{i=1}^{r} \dot{V}_i \tag{6.17}$$

in which λ' and G are r-vectors with the ith elements λ_i and G_i, respectively, and $u_i = u_i(t)$ is the ith control force, where

$$\lambda = S'PB \;\; ; \;\; G = -(PB)^{-1} P(AZ - \tilde{B}f + E) \;\; ; \;\; \dot{V}_i = \lambda_i (u_i - G_i) \tag{6.18}$$

For $\dot{V} \leq 0$, a possible continuous controller is given by

$$u_i(t) = G_i - \delta_i \lambda_i \quad or \quad U = G - \bar{\delta}\lambda' \tag{6.19}$$

in which $\delta_i \geq 0$ is the sliding margin and $\bar{\delta}$ is a (rxr) diagonal matrix with diagonal elements

$\delta_1, \delta_2, \ldots, \delta_r$. Substitution of Eq. (6.19) into Eq. (6.17) leads to $\dot{V} = -\lambda\bar{\delta}\lambda' \leq 0$.

Two possible discontinuous controllers are given by

$$u_i(t) = \begin{cases} G_i - \delta_i H(|\lambda| - \epsilon_0) ; & \text{if } \lambda_i > 0 \\ G_i + \delta_i H(|\lambda| - \epsilon_0) ; & \text{if } \lambda_i < 0 \end{cases} \tag{6.20}$$

and

$$u_i(t) = \begin{cases} G_i - \delta_i H(|\lambda| - \epsilon_0) ; & \text{if } \lambda_i > 0 \text{ , } G_i < 0 \\ G_i + \delta_i H(|\lambda| - \epsilon_0) ; & \text{if } \lambda_i < 0 \text{ , } G_i > 0 \\ 0 ; & \text{otherwise} \end{cases} \tag{6.21}$$

in which $H(|\lambda|-\epsilon_0)$ is the unit step function, i.e. $H(|\lambda|-\epsilon_0)=0$ for $|\lambda| < \epsilon_0$ and $H(\lambda|-\epsilon_0)=1$ for $|\lambda| \geq \epsilon_0$. In the expression above, $|\lambda|$ is any norm of the λ row vector and ϵ_0 is the thickness of the boundary layer of the chattering surface $\lambda=0$ (or the sliding surface $S=0$). The idea of introducing $H(|\lambda|-\epsilon_0)$ is to remove the undesirable chattering effect and ϵ_0 can be designed appropriately to achieve the purpose. It is mentioned that the control force $u_i(t)$ in Eqs. (6.19) - (6.21) is a function of G_i given by Eq. (6.18), which includes the nonlinear characteristics of the structure. Hence, the control force is a nonlinear function of the state vector Z.

6.4 COMPLETE COMPENSATION

When each degree-of-freedom of the structure is implemented with a controller (r=n), e.g., each story unit is equipped with an ABS system, the external earthquake excitation can be compensated completely such that the response state vector approaches to zero. The proof is identical to that for the linear structures given in Section 2. The results given by Eqs. (2.38)-(2.41) of Section 2 hold for nonlinear structures.

6.5 SATURATED CONTROLLERS

Civil engineering structures are designed to be stable without any control system. Let $\dot{V}_{in}$ correspond to $\dot{V}_i$, Eqs. (6.17) and (6.18), when no control action is taken by the ith controller, i.e., $u_i(t)=0$ and

$$\dot{V}_{in} = -\lambda_i G_i \tag{6.22}$$

Then, at every time instant, t, the control action will be taken either to reduce the derivative of the Lyapunov function $\dot{V}_i \leq \dot{V}_{in}$ or to maintain $\dot{V}_i \leq 0$. Based on this premise, the saturated

controller corresponding to the continuous controller in Eq. (6.19) is given in the following

$$u_i(t) = \begin{cases} \alpha_i^* G_i - \delta_i \lambda_i & ; \quad if \quad |\alpha_i^* G_i - \delta_i \lambda_i| \le \bar{u}_{imax} \\ \bar{u}_{imax} sgn[\alpha_i^* G_i - \delta_i \lambda_i] & ; \quad otherwise \end{cases} \tag{6.23}$$

in which $0 \le \alpha^*_i \le 1$ and $\bar{u}_{imax}$ (i=1,2,...,r) represents the upper bound of the ith control force.

The saturated controller corresponding to discontinuous controllers given by Eqs. (6.20) and (6.21) are given as follows

$$u_i^*(t) = \begin{cases} \alpha_i^* G_i - \delta_i H(|\lambda| - \epsilon_0) & ; \quad if \quad \lambda_i > 0 \\ \alpha_i^* G_i + \delta_i H(|\lambda| - \epsilon_0) & ; \quad if \quad \lambda_i < 0 \end{cases} \tag{6.24}$$

$$u_i(t) = \begin{cases} u_i^*(t) & ; \quad if \quad |u_i^*(t)| < \bar{u}_{imax} \\ \bar{u}_{imax} sgn[u_i^*(t)] & ; \quad if \quad |u_i^*(t)| > \bar{u}_{imax} \end{cases} \tag{6.25}$$

and

$$u_i^*(t) = \begin{cases} \alpha_i G_i - \delta_i H(|\lambda| - \epsilon_0) & ; \quad if \quad \lambda_i > 0 \ , \ G_i < 0 \\ \alpha_i G_i + \delta_i H(|\lambda| - \epsilon_0) & ; \quad if \quad \lambda_i < 0 \ , \ G_i > 0 \\ 0 & ; \quad otherwise \end{cases} \tag{6.26}$$

$$u_i(t) = \begin{cases} u_i^*(t) & ; \quad if \quad |u_i^*(t)| < \bar{u}_{imax} \\ \bar{u}_{imax} sgn[u_i^*(t)] & ; \quad if \quad |u_i^*(t)| > \bar{u}_{imax} \end{cases} \tag{6.27}$$

in which $\alpha_i > 0$ (i=1,2,...,r) are design parameters.

The theoretical justification for the controllers above is that at every time instant, either the event $\dot{V} \le 0$ occurs or the event $\dot{V}_i \le \dot{V}_{in}$ occurs. From the condition that $\dot{V}_i \le \dot{V}_{in}$ and the fact that the structure is stable without control, it can be shown that V is bounded, and hence the state vector Z is bounded, i.e., $|Z| < \infty$. Parameters α_i^*, α_i and $\bar{u}_{imax}$ (for i=1,2,...,r) can be used to make a trade-off between the control effort and the structural response. Controllers presented above are referred to as the saturated controllers, since the control effort $u_i(t)$ is saturated (or bounded) at $\bar{u}_{imax}$.

Special controllers that utilize either the full capacity or constant control force of the actuator corresponding to Eqs. (6.24) and (6.26) are bang-bang controllers,

$$u_i(t) = \begin{cases} -\bar{u}_{imax} H(|\lambda| - \epsilon_0) \; ; & \text{if } \lambda_i > 0 \\ \bar{u}_{imax} H(|\lambda| - \epsilon_0) \; ; & \text{if } \lambda_i < 0 \end{cases} \tag{6.28}$$

and

$$u_i(t) = \begin{cases} -\bar{u}_{imax} H(|\lambda| - \epsilon_0) \; ; & \text{if } \lambda_i > 0 \, , \; G_i < 0 \\ \bar{u}_{imax} H(|\lambda| - \epsilon_0) \; ; & \text{if } \lambda_i < 0 \, , \; G_i > 0 \\ 0 \; ; & \text{otherwise} \end{cases} \tag{6.29}$$

The controllers presented above have a nice feature in the sense that if the actual capacity of the actuator used for the control system is exceeded by the demand, a saturation will occur but the controllers still perform well using the maximum capacity.

6.6 ROBUSTNESS OF CONTROLLERS

The theory of variable structure system or sliding mode control was developed for control of uncertain nonlinear systems [e.g., Utkin 1992] and the robustness of such a theory is well documented. The robustness of the controllers presented above with respect to parametric uncertainties of the structure will be demonstrated by simulation results in Section 9.

SECTION 7
STATIC OUTPUT FEEDBACK CONTROL OF NONLINEAR AND HYSTERETIC STRUCTURES

The controllers presented above for nonlinear and hysteretic structures require a full-state feedback either through measurements or an observer. With the requirement of collocated velocity sensors, static output feedback controllers can be derived in a similar manner presented in Section 4 as follows.

Let Z_m be a m-dimensional observation (output) vector consisting of m measured state variables with $m \geq r$, where r is the number of controllers,

$$Z_m = C_m Z \;\; ; \;\; C_m = \begin{bmatrix} \tilde{C} & 0 \\ 0 & I_r \end{bmatrix} \tag{7.1}$$

in which C_m is a (mx2n) observation matrix and I_r is a (rxr) identity matrix, indicating the collocated velocity sensors. Then, the sliding surface P, i.e., $S = P_m Z_m = P_m C_m Z = PZ = 0$ can be designed using the method of pole assignment as described in Section 4.

A possible continuous controller is chosen as

$$U(t) = -(PB)^{-1} P[A(NC_m)Z - \tilde{B}f + E] - \bar{\delta}\lambda' \tag{7.2}$$

in which N is a (2nxm) matrix to be determined such that $\dot{V} \leq 0$. Note that the controller in Eq. (7.2) involves the nonlinear characteristics, f(Z), of the structure. Substituting Eq. (7.2) into Eq. (6.17) and using Eq. (6.18), one obtains

$$\dot{V} = Z'[P'PA(I_{2n} - NC_m) - P'PB\bar{\delta}B'P'P]Z \tag{7.3}$$

Thus, N is chosen such that the matrix Λ in the following is negative semidefinite

$$\Lambda = P'PA(I_{2n} - NC_m) - P'PB\bar{\delta}B'P'P \tag{7.4}$$

where the second matrix $-P'PB\bar{\delta}B'P'P$ is negative semidefinite.

Let $\bar{Z}_m$ be a 2n-dimensional modified observation (output) vector consisting of m measured (output) state variables (i.e., Z_m) and zero elements for those state variables that are not measured. It follows from Eq. (7.1) that

$$\bar{Z}_m = \bar{C}_m Z \tag{7.5}$$

in which $\bar{C}_m$ is a (2nx2n) expanded version of the observation matrix C_m, Eq. (7.1). In other words, C_m is a submatrix of $\bar{C}_m$ and other elements of $\bar{C}_m$ are zero. Then, the sliding surface can be shown to be

$$S = PZ = P\bar{Z}_m = 0 \tag{7.6}$$

A possible choice for the (2nx2n) matrix NC_m in Eq. (7.2) is $\bar{C}_m$, i.e., $NC_m=\bar{C}_m$. With the choice of $NC_m=\bar{C}_m$, the real parts of all eigenvalues of the matrix Λ in Eq. (7.4) are non-positive for $\bar{\delta}=0$, because of the requirement of collocated velocity sensors and the fact that the structure without control is stable. This special controller with $NC_m=\bar{C}_m$ is identical to the continuous controller given by Eq. (6.19) in which Z is replaced by $\bar{Z}_m$ and $S=P\bar{Z}_m$, i.e.,

$$U = G - \bar{\delta}\lambda' \tag{7.7}$$

where

$$\lambda = \bar{Z}_m' P'PB \;\; ; \;\; G = -(PB)^{-1}P(A\bar{Z}_m - \tilde{B}f + E) \tag{7.8}$$

For the discontinuous controller, we choose

$$u_i(t) = \begin{cases} -\left\{(PB)^{-1}P[A(NC_m)Z - \tilde{B}f + E]\right\}_i - \delta_i H(|\lambda| - \epsilon_0) \;;\; if\ \lambda_i > 0 \\ -\left\{(PB)^{-1}P[A(NC_m)Z - \tilde{B}f + E]\right\}_i + \delta_i H(|\lambda| - \epsilon_0) \;;\; if\ \lambda_i < 0 \end{cases} \tag{7.9}$$

in which $\{\ \}_i$ is the ith component of the vector in the bracket and N is a (2nxm) matrix to be determined such that $\dot{V} \le 0$. Again, we can choose $NC_m=\bar{C}_m$ as described in Section 4. This special controller with $NC_m=\bar{C}_m$ in Eq. (7.9) is identical to the controller given by Eq. (6.20) in which Z is replaced by $\bar{Z}_m$ as follows

$$u_i(t) = \begin{cases} G_i - \delta_i H(|\lambda| - \epsilon_0) \;;\; if\ \lambda_i > 0 \\ G_i + \delta_i H(|\lambda| - \epsilon_0) \;;\; if\ \lambda_i < 0 \end{cases} \tag{7.10}$$

where λ_i and G_i are the ith element of λ and G, respectively,

$$\lambda = \bar{Z}_m' P'PB \;\; ; \;\; G = -(PB)^{-1}P(A\bar{Z}_m - \tilde{B}f + E) \tag{7.10}$$

In a similar manner, the three-condition controllers given by Eqs. (6.21) and (6.27) and the bang-bang controllers in Eqs. (6.28) and (6.29) can be used for static output feedback in

which the state vector Z should be replaced by $\bar{Z}_m$. For the three-condition discontinuous controllers above, it is not necessary that $\dot{V} \leq 0$ for all time t unless the sliding margin is large. However, the control action is always taken to reduce $\dot{V}$ such that $\dot{V}_i \leq \dot{V}_{in}$ and hence the response state vector Z can be shown to be bounded. Finally, the saturated continuous controller in Eq. (6.23) and discontinuous controller in Eq. (6.25) can be used for the static output feedback with Z being replaced by $\bar{Z}_m$ and $S = P\bar{Z}_m$; however, the stability condition should be checked by simulation results for each design. Because of the requirement of collocated velocity sensors, the controlled structures are usually stable. The subject of saturation for static output feedback controllers will be reported in the near future.

SECTION 8
CONTROLLED RESPONSE OF HYSTERETIC BUILDINGS

Buildings usually behave hysteretically after yielding occurs. The hysteretic stiffness of a story unit, say the ith story unit, can be modelled as [e.g., Yang et al (1992b)]

$$F_{si} = \alpha_i k_i x_i(t) + (1-\alpha_i) k_i D_{yi} \nu_i \tag{8.1}$$

in which F_{si} is the ith element of the stiffness vector $F_s[X(t)]$, Eq.(6.2), k_i = elastic stiffness, α_i = ratio of the post-yielding to pre-yielding stiffness, D_{yi} = yield deformation, and ν_i = hysteretic variable with $|\nu_i| \leq 1$, where

$$\dot{\nu}_i = D_{y_i}^{-1} \left\{ A_i \dot{x}_i - \beta_i |\dot{x}_i| |\nu_i|^{n_i - 1} \nu_i - \gamma_i \dot{x}_i |\nu_i|^{n_i} \right\} \tag{8.2}$$

In Eq. (8.2), parameters A_i, β_i, γ_i and n_i govern the scale, general shape and smoothness of the hysteresis loop. Note that the ith story unit is linear elastic if $\alpha_i = 1$.

In Eq. (8.1), $\alpha_i k_i x_i(t)$ is the linear elastic stiffness that will appear in the $\tilde{K}$ matrix of Eq. (6.2). The nonlinear or hysteretic stiffnesses f_1, f_2, ..., f_l, appearing in the nonlinear or hysteretic vector, f[X(t)], of Eq. (6.2) is therefore given by

$$f_i = (1-\alpha_i) k_i D_{yi} \nu_i \tag{8.3}$$

With the stiffness vector $F_s[X(t)]$ thus defined in Eq. (6.2) for the hysteretic building, the controlled response of the building can be simulated numerically using Eq. (6.3) for any controller U(t) presented in this report.

SECTION 9
NUMERICAL SIMULATION OF NONLINEAR AND HYSTERETIC STRUCTURES

To demonstrate the applications of the control methods to nonlinear and hysteretic structures, simulation results are presented in this section. Three seismic-excited structures are considered: (1) a single-degree-of-freedom (SDOF) Duffing nonlinear system; (2) an eight-story building equipped with lead-core rubber-bearing isolators and actuators; and (3) a fixed-base eight-story hysteretic building with large ductility. For illustrative purpose, $\epsilon_0=0$ will be used in all the following examples for discontinuous controllers.

Example 1 : A SDOF Duffing Nonlinear System

The same SDOF Duffing nonlinear system presented in Spencer et al (1992) is considered

$$\ddot{x} + 2\,\xi\,\omega\,\dot{x} + \omega^2\,x + \varphi\,\omega^2\,x^3 = U - \ddot{x}_0 \qquad (9.1)$$

where x, $\dot{x}$ and $\ddot{x}$ are displacement, velocity and acceleration, respectively; ω is the natural frequency; ξ is the damping ratio; φ is the nonlinear coefficient; U is the control acceleration; and $\ddot{x}_0$ is the earthquake acceleration. The damping ratio ξ and the natural frequency ω are assumed to be 1% and 1rad/s, respectively. Two different values for φ are used, i.e., $\varphi=10$ and -10. $\varphi=10$ represents a hardening system, whereas $\varphi=-10$ indicates a softening system. The Duffing system is subjected to the El Centro earthquake as shown in Fig. 9-1 but scaled to a maximum ground acceleration of 0.112g. Without any control system, the maximum displacement, x, velocity, $\dot{x}$, and absolute acceleration, $\ddot{x}_a$, in 30 seconds of the earthquake episode are shown in columns (2) and (6) of Table 9-I for the hardening and the softening systems, respectively. As observed from column (6) of Table 9-I, the response of the softening system is unstable.

With the implementation of a control system, the sliding surface is designed as $S_1=80x+\dot{x}=0$. The continuous controller given by Eq. (6.19) with $\delta_1=0.1\text{cm}^2/\text{s}^3$ (CSMC) and the discontinuous controller given by Eq. (6.20) with $\delta_1=0.1\text{cm}/\text{s}^2$ (SMC I) are used. It has been

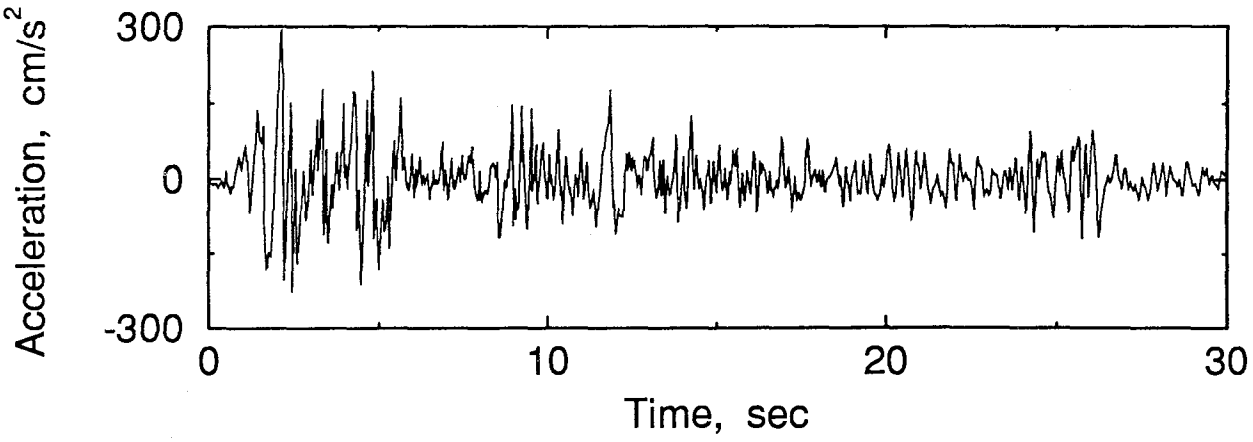

Fig. 9-1: El Centro Earthquake (NS Component).

Table 9-I : Maximum Response Quantities of a Duffing System

CSMC								
CASES	Hardening System				Softening System			
(1)	No Cont. (2)	With Cont. (3)	ω^2 +20% (4)	ω^2 -20% (5)	No Cont. (6)	With Cont. (7)	ω^2 +20% (8)	ω^2 -20% (9)
x (cm)	3.61	0	0	0	unstable	0	0	0
$\dot{x}$ (cm/s)	28.34	0	0	0	unstable	0	0	0
$\ddot{x}_a$ (cm/s^2)	472	110	110	110	unstable	110	110	110
U	--	11.2%	11.2%	11.2%	--	11.2%	11.2%	11.2%
SMC I								
CASES	Hardening System				Softening System			
(1)	No Cont. (2)	With Cont. (3)	ω^2 +20% (4)	ω^2 -20% (5)	No Cont. (6)	With Cont. (7)	ω^2 +20% (8)	ω^2 -20% (9)
x (cm)	3.61	0	0	0	unstable	0	0	0
$\dot{x}$ (cm/s)	28.34	0	0	0	unstable	0	0	0
$\ddot{x}_a$ (cm/s^2)	472	110	110	110	unstable	110	110	110
U	--	11.2%	11.2%	11.2%	--	11.2%	11.2%	11.2%

shown that a complete compensation for the response state vector can be achieved using Eq. (6.19) or (6.20), regardless of a hardening or a softening system. Numerical results for the maximum response quantities are presented in columns (3) and (7) of Table 9-I. The results based on the continuous controller, Eq. (6.19), are presented in the upper portion of Table 9-I, denoted by CSMC. The results based on the two-condition discontinuous controller, Eq. (6.20), are shown in the lower part of Table 9-I denoted by SMC I. In Table 9-I, the maximum control acceleration U is expressed in terms of the percentage of g. Indeed, the response state vector is zero and the structure becomes a rigid body.

To investigate the robustness of the control design with respect to parametric uncertainties, $\pm 20\%$ variations of the frequency (ω^2) from its true value are considered. The same sliding surface given above is used and the design of the controllers is based on $\pm$ 20% variations of the frequency (ω^2) from its actual value. The results for the maximum response quantities are presented in columns (4), (5), (8) and (9) of Table 9-I for the hardening and softening systems, respectively. As demonstrated in Table 9-I the control design is robust.

Consider the autonomous Duffing system subjected to the initial conditions $x(0)=1.0$ cm and $\dot{x}(0)=0$ cm/s as studied in Spencer et al (1992). The continuous sliding mode controller presented in Eq. (6.19) will be used. Substituting the controller given by Eqs. (6.18) and (6.19) into the equation of motion, Eq. (9.1), one obtains

$$\ddot{x} + (p_1 + \delta_1)\dot{x} + p_1\delta_1 x = 0 \tag{9.2}$$

in which the sliding surface is expressed as

$$S_1 = p_1 x + \dot{x} \tag{9.3}$$

The solutions for the response of the controlled structure, Eq. (9.2), are as follows

$$x = \frac{p_1 x(0) + \dot{x}(0)}{p_1 - \delta_1} e^{-\delta_1 t} - \frac{\delta_1 x(0) - \dot{x}(0)}{p_1 - \delta_1} e^{-p_1 t} \tag{9.4}$$

and

$$\dot{x} = -\delta_1 \frac{p_1 x(0) + \dot{x}(0)}{p_1 - \delta_1} e^{-\delta_1 t} + p_1 \frac{\delta_1 x(0) - \dot{x}(0)}{p_1 - \delta_1} e^{-p_1 t} \tag{9.5}$$

As observed from Eqs. (9.2)-(9.5), the responses of the controlled structure are identical for both the hardening system and the softening system. However, the required active control

U is different for these two systems.

For the initial conditions given above, the structural response depends on the design of the sliding surface, p_1, and the sliding margin δ_1. For illustrative purposes, the following three cases are considered: (i) Case 1 with $p_1=2.001$ and $\delta_1=2.0$; (ii) Case 2 with $p_1=3.001$ and $\delta_1=3.0$, and (iii) Case 3 with $p_1=5.001$ and $\delta_1=5.0$. The response time histories, x^2 and $\dot{x}^2$, and the control acceleration U^2 are displayed in Fig. 9-2 for comparison. In Fig. 9-2, the solid curves, dotted curves and dashed curves denote the reesults for Case 1, Case 2 and Case 3, respectively, for the hardening system. The dash-dotted curve shown in Fig. 9-2(c) corresponds to Case 2 for the softening system. As mentioned previously, the responses in Figs. 9-2(a) and 9-2(b) are identical for both the hardening and softening systems. As observed from Fig. 9-2, the displacement x^2 can be reduced more rapidly, at the expense of the velocity response $\dot{x}^2$.

For comparison of the continuous sliding mode control method presented in this report with the polynomial control method presented by Spencer et al (1992), the response quantities for x^2 and $\dot{x}^2$ as well as the required control U^2 are presented in Fig. 9-3. In Fig. 9-3, the solid curves correspond to the results for Case 2 ($p_1=3.001$ and $\delta_1=3.0$) using CSMC and the dotted curves are the results by Spencer et al (1992) using the 5th order polynomial control. Figure 9-3 clearly demonstrates that the performance of continuous sliding mode control is quite remarkable.

Example 2 : An Eight-Story Building Equipped with Rubber-Bearing Isolators and Actuator

An inelastic eight-story building with the following properties is considered : (i) the mass of each floor is identical with $m_i=345.6$ metric tones ($i=1,2,\ldots,8$); (ii) the preyielding stiffness of the eight-story units are k_{i1} ($i=1,2,\ldots,8$) = $3.4\text{x}10^5$, $3.2\text{x}10^5$, $2.85\text{x}10^5$, $2.69\text{x}10^5$, $2.43\text{x}10^5$, $2.07\text{x}10^5$, $1.69\text{x}10^5$, and $1.37\text{x}10^5$ kN/m, respectively, and the postyielding stiffness are $k_{i2}=0.1\ k_{i1}$ for $i=1,2,\ldots,8$, i.e., $\alpha_i=0.1$ and $k_i=k_{i1}$, see Eq. (8.1); and (iii) the viscous damping coefficients for each story unit are $c_i=490$, 467, 410, 386, 349, 298, 243 and 196 kN.sec/m, respectively. The damping coefficients given above result in a damping ratio of 0.38% for the first vibration mode. The fundamental frequency of the unyielded fixed-base building is 5.24 rad./sec. The yielding level for each story unit varies with respect to the stiffness; with the results, $D_{yi}=2.4$, 2.3, 2.2, 2.1, 2.0, 1.9, 1.7 and 1.5 cm, Eq. (8.1). The inelastic parametric

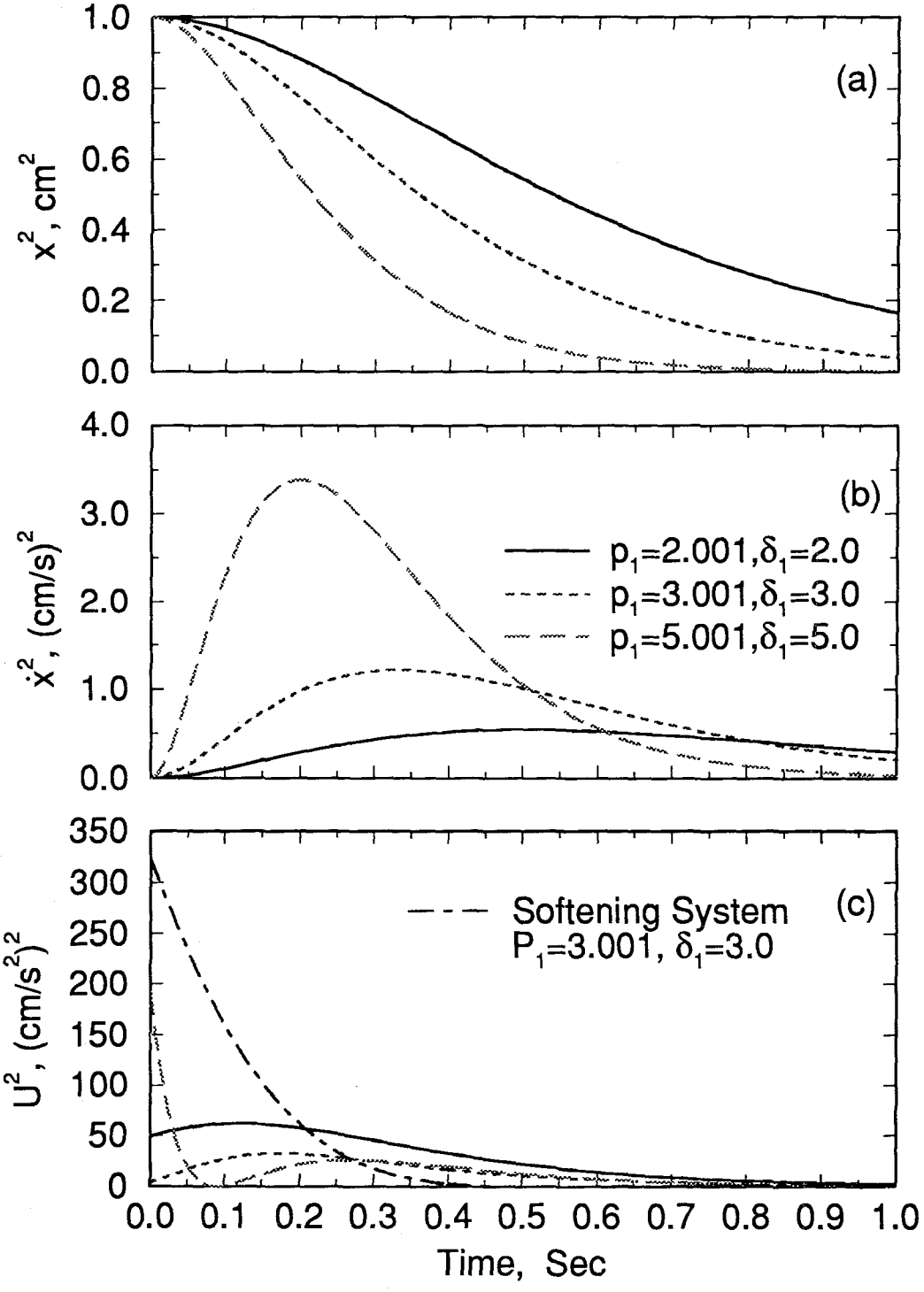

Fig. 9-2 : Response Time Histories of A Duffing Model And Control Acceleration with Initial Condition $x(0)=1.0$ cm And $\dot{x}(0)=0.0$ cm/s

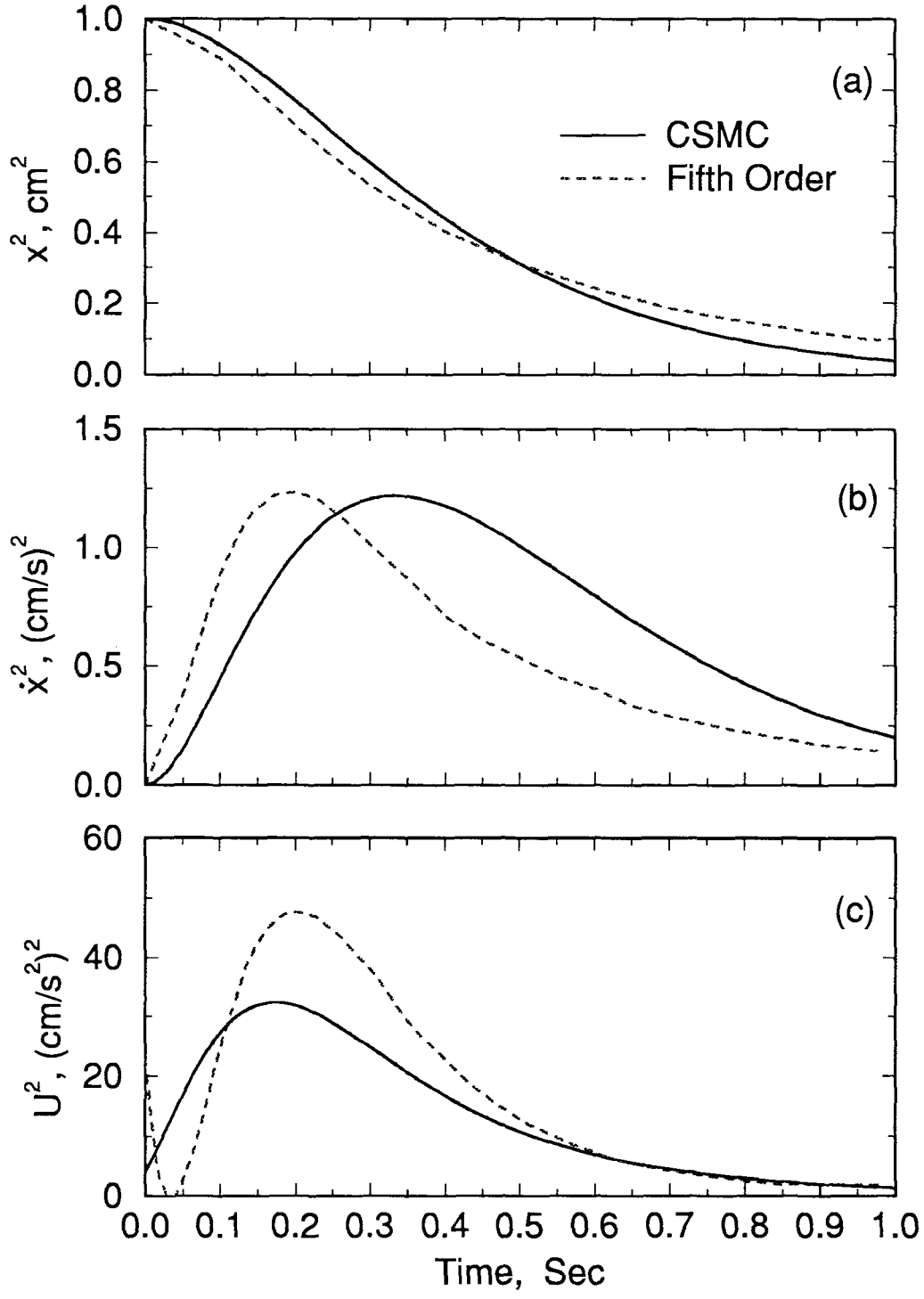

Fig. 9-3 : Comparison of CSMC And Fifth Order Control

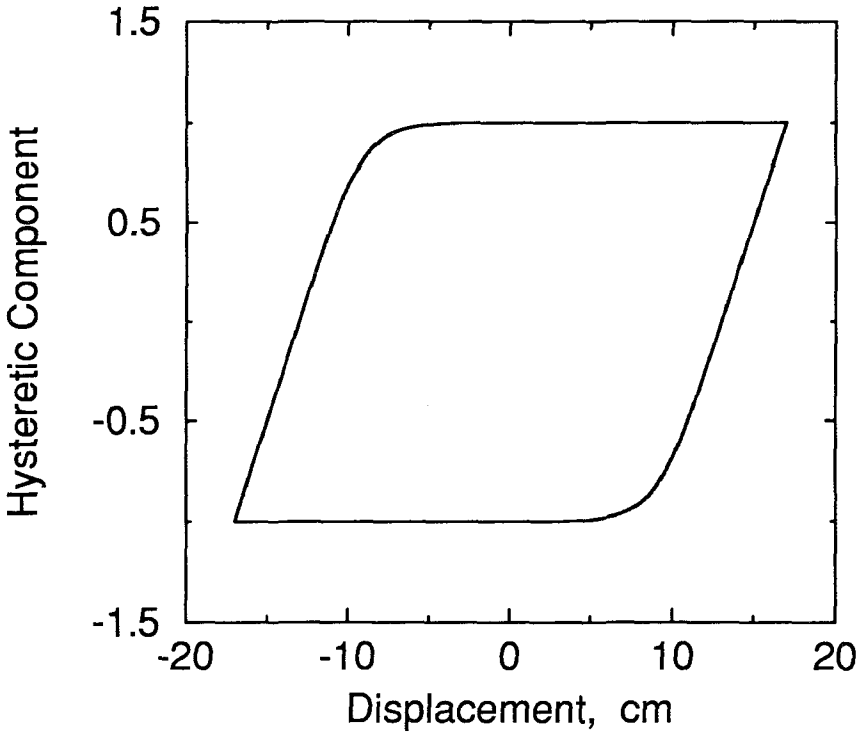

Fig. 9-4 : Hysteresis Loop of Lead-Core Rubber Bearing

values for each story unit are $A_i=1.0$, $\gamma_i=\beta_i=0.5$ and $n_i=95$ for i=1,2,...,8, Eq. (8.2). The building is isolated by lead-core rubber bearings as shown in Fig. 6-1. The mass of the isolation system is $m_b=450$ metric tons and the viscous damping is assumed to be linear with $c_b=26.17$ kN.sec/m. The inelastic parametric values for the isolation system are as follows: $k_b=18050$ kN/m, $\alpha_b=0.6$, $D_{yb}=4$cm, $A_b=1.0$, $\gamma_b=\beta_b=0.5$ and $n_b=3$, Eqs. (8.1)-(8.2). The hysteresis loop for the rubber bearing isolators is shown in Fig. 9-4, in which the hysteretic component v_b is plotted versus the displacement x_b. With the base isolation system, the first natural frequency of the preyielded structure is 2.21 rad/sec and the damping ratio for the first vibration mode is 0.16%.

The El Centro earthquake scaled to a maximum ground acceleration of 0.3g as shown in Fig. 9-1 is used as the input excitation. Within 30 seconds of the earthquake episode, the maximum interstory drift, x_i, and the maximum absolute acceleration, $\ddot{x}_{ai}$, of each floor are presented in columns (3) and (4) of Tables 9-II through 9-IV. In these tables, the yield deformation D_y are shown in column (2) and the first row indicated by "B" is the deformation of rubber-bearings. It is observed from Table 9-II that the response of the building is within the elastic limit; however, the deformation of rubber bearing may be excessive.

To protect the safety and integrity of the rubber bearings, actuators are installed in the base isolation system as shown in Fig. 6-1. The LQR method is used to determine the sliding surface with a diagonal weighting matrix Q; $Q_{11}=10^{-2}$, $Q_{ii}=5000$ for i=2,3,...,9 and $Q_{ii}=1$ for i=10,...,18. The continuous controller given by Eq. (6.19) with the sliding margin $\delta_1=5\text{x}10^5$kN·ton·cm/s is used. The maximum response quantities and the required maximum control force, U, are shown in columns (5) and (6) of Table 9-II. As observed from the table, the deformation of the base isolation system is reduced by more than 50% and the response quantities of the superstructure are also reduced by more than 63%. With the same sliding surface, the discontinuous controllers given by Eqs. (6.20) and (6.21) with $\delta_1=250$kN are used. The results corresponding to the two-condition controller, Eq. (6.20), are shown in columns (5) and (6) of Table 9-III, denoted by SMC I. The results using the three-condition controller, Eq. (6.21), are shown in Table 9-IV, denoted by SMC II.

Next, we consider the static output feedback approach presented in Section 7. Firstly, the responses of the isolation system and the first story units, i.e., x_b, $\dot{x}_b$, x_1 and $\dot{x}_1$, are

Table 9-II : Maximum Response Quantities of An Eight Story Building Equipped with Hybrid Control System Using Continuous Controller (CSMC)

CSMC									
FLOOR NO (1)	D_y cm (2)	With BIS		Full - State U=1484kN		DOF(I) U=1645kN		DOF(II) U=1020kN	
		x_i cm (3)	$\ddot{x}_{ai}$ cm/s^2 (4)	x_i cm (5)	$\ddot{x}_{ai}$ cm/s^2 (6)	x_i cm (7)	$\ddot{x}_{ai}$ cm/s^2 (8)	x_i cm (9)	$\ddot{x}_{ai}$ cm/s^2 (10)
B	4.0	21.4	122	10.7	77	9.72	139	10.4	28
1	2.4	0.62	113	0.14	41	0.24	98	0.21	29
2	2.3	0.59	113	0.14	37	0.22	91	0.20	32
3	2.2	0.65	111	0.16	38	0.30	79	0.21	34
4	2.1	0.63	102	0.15	31	0.34	70	0.20	32
5	2.0	0.63	91	0.14	37	0.41	77	0.19	29
6	1.9	0.64	103	0.18	39	0.51	96	0.18	32
7	1.7	0.60	131	0.20	42	0.57	117	0.16	36
8	1.5	0.41	163	0.15	60	0.42	168	0.11	42

Table 9-III : Maximum Response Quantities of an Eight Story Building Equipped with Hybrid Control System Using Two-Condition Controller (SMC I)

SMC I									
FLOOR NO (1)	D_V cm (2)	With BIS		Full - State U=1846kN		DOF(I) U=2106kN		DOF(II) U=1313kN	
		x_i cm (3)	$\ddot{x}_{ai}$ cm/s^2 (4)	x_i cm (5)	$\ddot{x}_{ai}$ cm/s^2 (6)	x_i cm (7)	$\ddot{x}_{ai}$ cm/s^2 (8)	x_i cm (9)	$\ddot{x}_{ai}$ cm/s^2 (10)
B	4.0	21.4	122	10.6	160	9.74	178	9.72	91
1	2.4	0.62	113	0.14	41	0.24	97	0.22	29
2	2.3	0.59	113	0.14	37	0.22	91	0.21	32
3	2.2	0.65	111	0.16	38	0.30	80	0.22	35
4	2.1	0.63	102	0.15	31	0.34	70	0.21	33
5	2.0	0.63	91	0.14	37	0.41	77	0.20	30
6	1.9	0.64	103	0.18	39	0.51	95	0.18	34
7	1.7	0.60	131	0.20	42	0.57	117	0.16	37
8	1.5	0.41	163	0.15	60	0.42	168	0.11	42

Table 9-IV : Maximum Response Quantities of an Eight Story Building Equipped with Hybrid Control System Using Three-Condition Controller (SMC II)

SMC II									
FLOOR NO (1)	D_y cm (2)	With BIS		Full - State U=1718kN		DOF(I) U=1962kN		DOF(II) U=1177kN	
		x_i cm (3)	$\ddot{x}_{ai}$ cm/s^2 (4)	x_i cm (5)	$\ddot{x}_{ai}$ cm/s^2 (6)	x_i cm (7)	$\ddot{x}_{ai}$ cm/s^2 (8)	x_i cm (9)	$\ddot{x}_{ai}$ cm/s^2 (10)
B	4.0	21.4	122	10.6	308	9.71	351	9.74	213
1	2.4	0.62	113	0.14	42	0.24	98	0.23	31
2	2.3	0.59	113	0.14	37	0.22	92	0.22	34
3	2.2	0.65	111	0.16	38	0.30	79	0.22	38
4	2.1	0.63	102	0.16	31	0.34	70	0.21	36
5	2.0	0.63	91	0.14	37	0.41	77	0.19	34
6	1.9	0.64	103	0.18	40	0.51	95	0.18	33
7	1.7	0.60	131	0.20	42	0.57	116	0.17	37
8	1.5	0.41	163	0.15	60	0.42	168	0.11	45

measured in addition to the ground excitation $\ddot{x}_0$, and the sliding surface is determined by the pole assignment method, Section 4. In this case, three new poles may be assigned and the following three real poles are preassigned: -0.0977, -1.019 and -83.1256. This set of new poles results in the sliding surface: $S_1=0.07071x_b$ -$90.533x_1$ + $0.7954\dot{x}_b$ -$0.2046\dot{x}_1=0$. The static output feedback (continuous) controller given by Eqs. (7.7) and (7.8) with the sliding margin $\delta_1=5x10^5$kN·ton·cm/s is used. Within 30 seconds of the earthquake episode, the maximum response quantities are presented in columns (7) and (8) of Table 9-II, designated as DOF(I). As observed from Table 9-II, the responses quantities of the building are larger than those associated with the full-state feedback controller as expected. However, the control performance is still remarkable as compared with those shown in Yang, et al (1994b). With the same sliding surface and $\delta_1=250$kN, the discontinuous controllers given by Eqs. (6.20) and (6.21) with Z being replaced by $\bar{Z}_m$ are used. The results are presented in columns (7) and (8) of Tables 9-III and 9-IV, denoted by DOF(I).

Secondly, the response quantities of the first 3 story units are measured, i.e., x_b, $\dot{x}_b$, x_1, $\dot{x}_1$, x_2 and $\dot{x}_2$, and five new poles may be preassigned for the determination of the sliding surface. In this example, the following five real poles are preassigned: -1, -2, -3, -5 and -15. This set of new poles results in the following sliding surface: $S_1=-0.01649x_b$ + $40.344x_1$ - $40.7415x_2$ -$0.03508\dot{x}_b$ + $0.9649\dot{x}_1$ + $0.1264\dot{x}_2$. The static output feedback (continuous) controller given by Eq. (7.7) with the same sliding margin $\delta_1=5x10^5$kN·ton·cm/s is used. The corresponding maximum response quantities are presented in columns (9) and (10) of Table 9-II, designated as DOF(II). With the same sliding surface and $\delta_1=250$ kN, the corresponding results using the discontinuous controllers, Eqs. (6.20) and (6.21), with Z being replaced by $\bar{Z}_m$ are presented in columns (9) and (10) of Tables 9-III and 9-IV. It is observed from columns (9) and (10) of Tables 9-II to 9-IV that the control performance improves considerably over the previous case, DOF(I); in particular, the response quantities above the third story unit. As expected, the control performance improves as more state variables are measured. The simulation results presented in Tables 9-II to 9-IV clearly demonstrate that (i) the performance of the proposed control methods is remarkable, and (ii) the control performance using the static output feedback compares favorably with that of the full-state feedback.

To investigate the robustness of the control designs with respect to parametric

Table 9-V : Robustness for Maximum Response Quantities of An Eight Story Building Equipped with Hybrid Control System Using Continuous Controller (CSMC)

CSMC																			
FLOOR NO (1)	D_y cm (2)	Full - State U=1484 kN K_b+0%		Full - State U=1471 kN K_b-10%		Full - State U=1484 kN K_b+10%		DOF(I) U=1645 kN K_b+0%		DOF(I) U=1633 kN K_b-10%		DOF(I) U=1658 kN K_b+10%		DOF(II) U=1020 kN K_b+0%		DOF(II) U=948 kN K_b-10%		DOF(II) U=1074 kN K_b+10%	
		x_i cm (3)	$\ddot{x}_{ai}$ cm/s^2 (4)	x_i cm (5)	$\ddot{x}_{ai}$ cm/s^2 (6)	x_i cm (7)	$\ddot{x}_{ai}$ cm/s^2 (8)	x_i cm (9)	$\ddot{x}_{ai}$ cm/s^2 (10)	x_i cm (11)	$\ddot{x}_{ai}$ cm/s^2 (12)	x_i cm (13)	$\ddot{x}_{ai}$ cm/s^2 (14)	x_i cm (15)	$\ddot{x}_{ai}$ cm/s^2 (16)	x_i cm (17)	$\ddot{x}_{ai}$ cm/s^2 (18)	x_i cm (19)	$\ddot{x}_{ai}$ cm/s^2 (20)
B	4.0	10.7	77	10.6	77	10.8	77	9.72	139	9.71	139	9.72	139	10.4	28	10.3	31	10.2	26
1	2.4	0.14	41	0.14	42	0.14	41	0.24	98	0.24	98	0.24	98	0.21	29	0.24	31	0.20	26
2	2.3	0.14	37	0.14	37	0.14	37	0.22	91	0.22	91	0.22	91	0.20	32	0.22	35	0.20	29
3	2.2	0.16	38	0.16	38	0.16	38	0.30	79	0.30	79	0.30	80	0.21	34	0.22	38	0.20	30
4	2.1	0.15	31	0.16	31	0.15	31	0.34	70	0.34	70	0.34	70	0.20	32	0.20	37	0.19	28
5	2.0	0.14	37	0.14	38	0.14	37	0.41	77	0.41	77	0.41	77	0.19	29	0.19	34	0.18	27
6	1.9	0.18	39	0.18	39	0.18	39	0.51	96	0.51	96	0.51	96	0.18	32	0.18	33	0.17	31
7	1.7	0.20	42	0.20	42	0.20	42	0.57	117	0.57	117	0.57	117	0.16	36	0.17	37	0.15	34
8	1.5	0.15	60	0.15	60	0.15	60	0.42	168	0.43	168	0.42	168	0.11	42	0.11	44	0.10	40

Table 9-VI : Robustness for Maximum Response Quantities of An Eight Story Building Equipped with Hybrid Control System Using Two-condition Discontinuous Controller (SMC I)

SMC I																			
FLOOR NO (1)	D_y cm (2)	Full - State U=1846 kN K_b+0%		Full - State U=1580 kN K_b-10%		Full - State U=1968 kN K_b+10%		DOF(I) U=2106 kN K_b+0%		DOF(I) U=2046 kN K_b-10%		DOF(I) U=2135 kN K_b+10%		DOF(II) U=1313kN K_b+0%		DOF(II) U=1058kN K_b-10%		DOF(II) U=1479kN K_b+10%	
		x_i cm (3)	$\ddot{x}_{ai}$ cm/s^2 (4)	x_i cm (5)	$\ddot{x}_{ai}$ cm/s^2 (6)	x_i cm (7)	$\ddot{x}_{ai}$ cm/s^2 (8)	x_i cm (9)	$\ddot{x}_{ai}$ cm/s^2 (10)	x_i cm (11)	$\ddot{x}_{ai}$ cm/s^2 (12)	x_i cm (13)	$\ddot{x}_{ai}$ cm/s^2 (14)	x_i cm (15)	$\ddot{x}_{ai}$ cm/s^2 (16)	x_i cm (17)	$\ddot{x}_{ai}$ cm/s^2 (18)	x_i cm (19)	$\ddot{x}_{ai}$ cm/s^2 (20)
B	4.0	10.6	160	10.6	159	10.7	179	9.74	178	9.70	199	9.74	174	9.72	91	9.91	211	9.92	111
1	2.4	0.14	41	0.14	42	0.14	42	0.24	97	0.24	98	0.24	98	0.22	29	0.27	32	0.21	27
2	2.3	0.14	37	0.14	37	0.14	37	0.22	91	0.22	91	0.22	91	0.21	32	0.25	37	0.21	31
3	2.2	0.16	38	0.16	38	0.16	38	0.30	80	0.30	79	0.30	79	0.22	35	0.24	40	0.22	33
4	2.1	0.15	31	0.15	31	0.15	31	0.34	70	0.34	69	0.34	67	0.21	33	0.22	40	0.20	31
5	2.0	0.14	37	0.14	38	0.14	37	0.41	77	0.41	80	0.41	77	0.20	30	0.20	37	0.19	29
6	1.9	0.18	39	0.18	39	0.18	39	0.51	95	0.51	93	0.51	95	0.18	34	0.20	36	0.18	33
7	1.7	0.20	42	0.20	42	0.20	42	0.57	117	0.57	117	0.57	117	0.16	37	0.18	40	0.15	36
8	1.5	0.15	60	0.15	60	0.15	60	0.42	168	0.42	168	0.42	167	0.11	42	0.12	47	0.10	41

Table 9-VII : Robustness for Maximum Response Quantities of An Eight Story Building Equipped with Hybrid Control System Using Three-condition Discontinuous Controller (SMC II)

SMC II																			
FLOOR NO (1)	D_y cm (2)	Full - State U=1718kN K_b+0%		Full - State U=1633kN K_b-10%		Full - State U=1799kN K_b+10%		DOF(I) U=1962kN K_b+0%		DOF(I) U=2101kN K_b-10%		DOF(I) U=2021kN K_b+10%		DOF(II) U=1177kN K_b+0%		DOF(II) U=11972kN K_b-10%		DOF(II) U=1452kN K_b+10%	
		x_i cm (3)	$\ddot{x}_{ai}$ cm/s^2 (4)	x_i cm (5)	$\ddot{x}_{ai}$ cm/s^2 (6)	x_i cm (7)	$\ddot{x}_{ai}$ cm/s^2 (8)	x_i cm (9)	$\ddot{x}_{ai}$ cm/s^2 (10)	x_i cm (11)	$\ddot{x}_{ai}$ cm/s^2 (12)	x_i cm (13)	$\ddot{x}_{ai}$ cm/s^2 (14)	x_i cm (15)	$\ddot{x}_{ai}$ cm/s^2 (16)	x_i cm (17)	$\ddot{x}_{ai}$ cm/s^2 (18)	x_i cm (19)	$\ddot{x}_{ai}$ cm/s^2 (20)
B	4.0	10.6	308	10.6	310	10.6	309	9.71	351	9.68	350	9.72	352	9.74	213	10.6	111	9.74	212
1	2.4	0.14	42	0.14	42	0.14	41	0.24	98	0.24	98	0.24	98	0.23	31	0.24	32	0.21	29
2	2.3	0.14	37	0.14	37	0.14	37	0.22	92	0.23	92	0.22	92	0.22	34	0.22	35	0.21	32
3	2.2	0.16	38	0.16	38	0.16	38	0.30	79	0.30	80	0.30	78	0.22	38	0.21	38	0.21	35
4	2.1	0.16	31	0.16	31	0.16	31	0.34	70	0.34	68	0.34	69	0.21	36	0.20	36	0.20	33
5	2.0	0.14	37	0.14	37	0.14	38	0.41	77	0.41	80	0.41	77	0.19	34	0.19	33	0.19	32
6	1.9	0.18	40	0.18	40	0.18	40	0.51	95	0.51	93	0.51	95	0.18	33	0.18	33	0.17	31
7	1.7	0.20	42	0.20	42	0.20	42	0.57	116	0.57	116	0.57	116	0.17	37	0.16	37	0.16	36
8	1.5	0.15	60	0.15	60	0.15	60	0.42	168	0.42	168	0.42	167	0.11	45	0.11	44	0.11	42

uncertainties for both full state feedback and static output feedback controllers, $\pm 10\%$ variations for the stiffness of the base isolation system, K_b, are considered. The designs of both the sliding surface and the controllers are based on $\pm 10\%$ variations of K_b from its actual value. The results for the maximum response quantities are presented in Tables 9-V to 9-VII. In these tables, the results in the columns corresponding to K_b $+0\%$ are identical to those presented in Tables 9-II to 9-IV, indicating no uncertainty in K_b. As observed from these tables, the control designs are robust.

Example 3 : A Fixed-Base Eight-Story Building with Large Ductility

The same eight-story inelastic building described in the previous example is considered except that it is a fixed-base building without the base isolation system. The same El Centro earthquake scaled to a maximum ground acceleration of 1g is used as the input excitation. In 30 seconds of the earthquake episode, the maximum interstory drift, x_i, and the maximum absolute floor acceleration, $\ddot{x}_{ai}$, are presented in columns (3) and (4) of Tables 9-VIII and 9-IX. As observed from these tables, yielding occurs in every story unit with a large ductility and the building would have failed without any control system. Under the excitation of 1g strong earthquake, it is necessary to install controllers on each floor as demonstrated in Yang et al (1992a) due to the fact that the postyielding stiffness $\alpha_i k_i$ of each story unit is quite small, i.e., $\alpha_i = 0.1$. Consequently, an active bracing system is installed on every floor.

With an active bracing system installed on every floor of the building, it has been shown analytically that a complete compensation for the building response can be achieved. For the design of the sliding surface using the LQR method, a diagonal weighting matrix Q with diagonal elements $Q_{ii} = [10^6, 10^6, 10^6, 10^6, 10^6, 10^6, 10^6, 10^6, 1, 1, 1, 1, 1, 1, 1, 1]$ is considered. The continuous controller given by Eq. (6.19) with $\delta_i = 1\text{kN}\cdot\text{ton}\cdot\text{cm/s}$ for $i = 1,2,3,\ldots,8$ is used. The maximum response quantities and the maximum required horizontal control forces, u_i, are presented in columns (5)-(7) of Table 9-VIII. As expected, the response of the building is completely compensated and the controlled building behaves like a rigid body. Similar results are shown in Table 9-IX, when the discontinuous controller, Eq. (6.20), is used with the same sliding surface and $\delta_i = 1\text{kN}$; $i = 1,2,\ldots,8$.

Suppose the maximum horizontal force for each actuator is restricted to $\bar{u}_{max} = 21{,}589\text{kN}$ (Case 1) and the continuous saturated controller given by Eq. (6.23) with $\alpha_i^* = 1.0$ for

$i=1,2,\ldots,8$ is considered. The same sliding surface and the following sliding margins are used: $\delta_1=10^3$kN·ton·cm/s and $\delta_i=10^5$kN·ton·cm/s for $i=2,3,\ldots 8$. The maximum response quantities and the required horizontal control forces, u_i, are shown in columns (8)-(10) of Table 9-VIII, designated as Case 1. Similarly, the discontinuous saturated controller in Eq. (6.27) with the sliding margins $\delta_i=1$kN for $i=1,2,\ldots,8$, is used. The sliding surface is designed using the LQR method with the following diagonal Q matrix: $Q_{ii}=10^4$ for $i=1,2,\ldots,8$ and $Q_{ii}=1$ for $i=9,10,\ldots,16$. The maximum response quantities are shown in columns (8)-(10) of Table 9-IX, designated as Case 1.

We next consider Case 2 in which the maximum control force for each controller is restricted to $\bar{u}_{max}=11{,}600$kN. For the continuous saturated controller given by Eq. (6.23) with $\alpha^*_i=1.0$ for $i=1, 2,\ldots,8$, the same sliding surface in Case 1 is used and the following sliding margins are chosen: $\delta_1=\delta_2=1$ kN·ton·cm/s and $\delta_i=10^6$kN·ton·cm/s for $i=3, 4,\ldots,8$. The maximum response quantities are presented in columns (11) to (13) of Table 9-VIII, designated as Case 2. For the discontinuous saturated controller in Eq. (6.27) with the sliding margin $\delta_i=100$kN for $i=1, 2,\ldots,8$, the sliding surface is designed using the following diagonal Q matrix: $Q_{ii}=100$ for $i=1,2,\ldots,8$ and $Q_{ii}=1$ for $i=9,10,\ldots,16$. The corresponding results are shown in columns (11)-(13) of Table 9-IX, designated as Case 2. It is observed from Tables 9-VIII and 9-IX that the performance of the control methods for either the full compensation or the saturated controllers is remarkable.

Finally, the robustness with respect to the uncertainties of structural parameters for the case of full compensation shown in columns (5)-(7) of Table 9-VIII and 9-IX is investigated. $\pm 20\%$ variations of the stiffness, k_i, and yielding displacements, D_{yi}, for all story units, from their true values are considered. The designs for both the sliding surface and the controllers (both continuous and discontinuous) are based on $\pm 20\%$ variations from their actual values. The numerical results for the maximum response quantities as well as the maximum control forces are presented in columns (6)-(17) of Tables 9-X and 9-XI. For comparison, the corresponding response quantities without uncertainty taken from columns (5)- (7) of Tables 9-VIII and 9-IX are also shown in columns (3)-(5) of Tables 9-X and 9-XI, respectively. Numerical results clearly demonstrate that the control designs are robust with respect to parametric uncertainties.

Table 9-VIII : Maximum Response Quantities of A Fixed-Base 8-Story Building Using Continuous Controller (CSMC)

CSMC												
FLOOR NO (1)	Dy cm (2)	Without Control		Complete Compensation			Case 1 Umax=21589kN			Case 2 Umax=11600kN		
		x_i cm (3)	$\ddot{x}_{ai}$ cm/s^2 (4)	x_i cm (5)	ui kN (6)	$\ddot{x}_{ai}$ cm/s^2 (7)	x_i cm (8)	ui kN (9)	$\ddot{x}_{ai}$ cm/s^2 (10)	x_i cm (11)	ui kN (12)	$\ddot{x}_{ai}$ cm/s^2 (13)
1	2.4	5.03	1031	0	27097	980	0.84	21589	2676	1.97	11600	6150
2	2.3	4.19	1155	0	23710	980	0.25	20929	2061	1.40	11600	7584
3	2.2	5.37	1078	0	20323	980	0.27	19187	1053	1.09	11600	7246
4	2.1	5.50	1169	0	16936	980	0.33	16714	847	0.92	11600	6977
5	2.0	6.84	1213	0	13548	980	0.29	13731	910	0.75	11600	6913
6	1.9	8.49	1000	0	10161	980	0.24	10451	978	0.70	11600	6879
7	1.7	10.5	817	0	6774	980	0.19	7021	1011	0.56	11600	6874
8	1.5	4.56	720	0	3387	980	0.10	3523	1021	0.31	11600	3483

Table 9-IX : Maximum Response Quantities of a Fixed-Base 8-Story Building Using Discontinuous Controller

FLOOR NO (1)	Dy cm (2)	Without Control		SMCI			SMCII					
				Complete Compensation			Case 1 Umax=21589kN			Case 2 Umax=11600kN		
		x_i cm (3)	$\ddot{x}_{ai}$ cm/s^2 (4)	x_i cm (5)	uj kN (6)	$\ddot{x}_{ai}$ cm/s^2 (7)	x_i cm (8)	uj kN (9)	$\ddot{x}_{ai}$ cm/s^2 (10)	x_i cm (11)	uj kN (12)	$\ddot{x}_{ai}$ cm/s^2 (13)
1	2.4	5.03	1031	0	27095	979	0.65	21589	6307	1.85	11600	3600
2	2.3	4.19	1155	0	23711	981	0.63	21589	6375	1.84	11600	3672
3	2.2	5.37	1078	0	20321	979	0.60	21589	6354	1.83	11600	3652
4	2.1	5.50	1169	0	16937	980	0.53	21589	6375	1.79	11600	3578
5	2.0	6.84	1213	0	13550	981	0.46	21589	6373	1.69	11600	3569
6	1.9	8.49	1000	0	10160	980	0.37	21589	6337	1.52	11600	3537
7	1.7	10.5	817	0	6773	979	0.26	21589	6290	1.12	11600	3243
8	1.5	4.56	720	0	3389	981	0.13	16450	4759	0.57	6822	1820

Table 9-X : Maximum Response Quantities of a Fixed-Base 8-Story Building with System Uncertainties; Continuous Sliding Mode Control (CSMC)

CSMC																
FLOOR NO (1)	YIELD DIS (2)	0% Variation			Dy-20%			Dy+20%			K-20%			K+20%		
		x_i cm (3)	U kN (4)	$\ddot{x}_{ai}$ cm/s^2 (5)	x_i cm (6)	U kN (7)	$\ddot{x}_{ai}$ cm/s^2 (8)	x_i cm (9)	U kN (10)	$\ddot{x}_{ai}$ cm/s^2 (11)	x_i cm (12)	U kN (13)	$\ddot{x}_{ai}$ cm/s^2 (14)	x_i cm (15)	U kN (16)	$\ddot{x}_{ai}$ cm/s^2 (17)
1	2.4	0	27097	980	0	27097	980	0	27097	980	0	27097	980	0	27097	980
2	2.3	0	23710	980	0	23710	980	0	23710	980	0	23710	980	0	23710	980
3	2.2	0	20323	980	0	20323	980	0	20323	980	0	20323	980	0	20323	980
4	2.1	0	16936	980	0	16936	980	0	16936	980	0	16936	980	0	16936	980
5	2.0	0	13548	980	0	13548	980	0	13548	980	0	13548	980	0	13548	980
6	1.9	0	10161	980	0	10161	980	0	10161	980	0	10161	980	0	10161	980
7	1.7	0	6774	980	0	6774	980	0	6774	980	0	6774	980	0	6774	980
8	1.5	0	3387	980	0	3387	980	0	3387	980	0	3387	980	0	3387	980

Table 9-XI : Maximum Response Quantities of a Fixed-Base 8-Story Building with System Uncertainties; Two-Condition Discontinuous Sliding Mode Control (SMC I)

SMC I																	
FLOOR NO (1)	YIELD DIS (2)	0% Variation			Dy-20%			Dy+20%			K-20%			K+20%			
		x_i cm (3)	U kN (4)	$\ddot{x}_{ai}$ cm/s^2 (5)	x_i cm (6)	U kN (7)	$\ddot{x}_{ai}$ cm/s^2 (8)	x_i cm (9)	U kN (10)	$\ddot{x}_{ai}$ cm/s^2 (11)	x_i cm (12)	U kN (13)	$\ddot{x}_{ai}$ cm/s^2 (14)	x_i cm (15)	U kN (16)	$\ddot{x}_{ai}$ cm/s^2 (17)
1	2.4	0	27095	979	0	27095	979	0	27095	979	0	27095	979	0	27095	979
2	2.3	0	23711	981	0	23711	981	0	23711	981	0	23711	981	0	23711	981
3	2.2	0	20321	979	0	20321	979	0	20321	979	0	20321	979	0	20321	979
4	2.1	0	16937	980	0	16937	980	0	16937	980	0	16937	980	0	16937	980
5	2.0	0	13550	981	0	13550	981	0	13550	981	0	13550	981	0	13550	981
6	1.9	0	10160	980	0	10160	980	0	10160	980	0	10160	980	0	10160	980
7	1.7	0	6773	979	0	6773	979	0	6773	979	0	6773	979	0	6773	979
8	1.5	0	3389	981	0	3389	981	0	3389	981	0	3389	981	0	3389	981

SECTION 10
CONCLUSIONS AND DISCUSSION

10.1 LINEAR STRUCTURES

Control methods based on the theory of variable structure system (VSS) or sliding mode control (SMC) have been presented for control of seismic-excited linear structures. Emphasis is placed on continuous sliding mode control methods that do not have undesirable chattering effect and the control forces are continuous. This is the first systematic investigation of the possible applications of sliding mode control to civil engineering structures. For the controllers presented, there is no adverse effect on the control performance should the actuator be saturated due to unexpected extreme earthquakes. Saturated controllers have been proposed, which reduce to the bang-bang controllers in the extreme case in which the full capacity of the actuator is utilized. It is demonstrated through simulation results that, (i) the controllers presented are robust with respect to parametric uncertainties of the structure, and (ii) the control performance is remarkable.

One reason for the good performance of the control methods presented is that the earthquake ground excitation (or feedforward compensation) is taken into account in the design of the controller. In fact, when each story unit is equipped with a controller, it has been shown, both theoretically and numerically, that a complete compensation for the earthquake excitation can be achieved, i.e., the response state vector approaches zero. Numerical results further demonstrate that with appropriate design the controller for a complete compensation is robust with respect to system uncertainties. Such a complete compensation for the response state vector can not be achieved using other control methods, such as LQR, pole assignment, etc.

Practical implementations of active/hybrid control systems to civil engineering structures indicate that it is not practical to install all sensors to measure the full state vector, whereas the use of an observer increases the on-line computational efforts and a system time delay. In this report, static output feedback controllers using only the measured information from a few sensors installed at strategic locations have been presented. The performance of the static output feedback controllers is shown to be quite reasonable.

The sliding mode controllers presented have been modified for applications to parametric

control. In particular, controllers are presented for applications to active variable stiffness (AVS) systems and active variable dampers (AVD). Simulation results demonstrate that the performance of these parametric controllers is remarkable.

Both continuous and discontinuous sliding mode controllers have been presented. The continuous controllers can be implemented for practical applications without difficulty, because there is no chattering effect and the control forces are continuous. The undesirable chattering effect has been removed for discontinuous controllers by introducing a boundary layer along the chattering surface in which the sliding margins are zero. With actuators as control devices, however, the actuator may not be able to follow the discontinuous control force. In this connection, compensators should be used in conjunction with discontinuous controllers for practical implementations [e.g., Yang, et al 1994h]. Using compensators, the discontinuous controllers become electrical command signals, that can be switched discontinuously. This subject will be reported in the near future.

Shaking table experimental tests have been conducted at SUNY, Buffalo to verify the continuous sliding mode control methods. The test structure used was the linear three-story 1/4-scaled building model, equipped with an active tendon control system, which was used extensively at SUNY, Buffalo [e.g., Soong 1990, Dyke, et al 1994]. Different earthquake records were used as the input excitations, including the El Centro, Pacoima, Hachinoke and Taft. Experimental data correlate satisfactorily with simulation results. Extensive experimental results demonstrate that the continuous sliding mode control, in particular the static output feedback controller using only the measured information from a few sensors, are very promising for practical implementations of active control systems on seismic-excited linear structures. The experimental results were described in detail in Yang, et al (1994f).

10.2 NONLINEAR AND HYSTERETIC STRUCTURES

Sliding mode control (SMC) methods have been presented for control of nonlinear or hysteretic civil engineering structures subjected to strong earthquakes. Again, emphasis has been placed on continuous sliding mode controllers for practical implementations. Static output feedback controllers using only a few sensors are also presented. This type of controllers is very useful for practical applications to complex civil engineering structures. Since the feedforward

compensation is accounted for in the design of controllers, a complete compensation for the response of the building can be achieved as demonstrated analytically and by simulation results. Numerical simulation results demonstrate that the performance of the sliding mode control methods is remarkable for nonlinear and hysteretic structures.

Extensive simulation results indicate that robustness of the control methods depends on the design of the sliding surface. The control design is more robust if the poles of the closed-loop system for the sliding surface are shifted more to the left hand side in the complex plane. This situation is similar to the classical control method based on the pole assignment.

At the beginning of Section 6, it is expediently assumed that, as a minimum, one controller should be installed in each nonlinear or inelastic story unit (or element). This is true for buildings and bridges equipped with aseismic hybrid protective systems [Yang et al 1992b, 1993d]. Because of this restriction, the sliding surface is a linear combination of the state vector, and general methods for determining the sliding surface are available. The restriction can be removed and the sliding surface becomes a nonlinear function of the state vector. In this case, however, the method for determining the nonlinear sliding surface is more involved and it should be considered for each specific problem as described in Utkin (1992). One possible approximation is to linearize the nonlinear story units in which controllers are not installed for the determination of the linear sliding surface. In the design of the controller, however, such linearization is not necessary.

Finally, we have conducted shaking table tests for sliding mode control methods using a three-story 1/4 scaled building model equipped with frictional-type sliding bearings and an actuator at SUNY Buffalo. Experimental results for control of such a highly nonlinear system demonstrated that the control methods presented are very promising. Details of the experimental results and their correlations with simulation results were reported in Yang, et al (1993d).

SECTION 11
REFERENCES

1. Calise, A.J., Sweriduk, G.D., Hsu, C.C., Craig, J.H. and Goodno, B.J. (1993), "Active/ Passive Damping of Building Structures Using Robust Control and Architectural Cladding", Proc. 9th VPI&SU Symp. on Dynamics and Control of Structures, pp. 191-206, edited by L. Meirovitch, May, Blacksburg, VA.
2. Dyke, S.J., Spencer, B.F., Quest, P., Sain, M.K. and Kaspari, D.C. (1994), "Experimental Verifications of Acceleration Feedback Control Strategies for MDOF Structures", 2nd Int'l. Conf. on Computationl Stochastic Mechanics, Greece.
3. Feng, Q., Fujii, S., and Shinozuka, M. (1990), "Use of a Variable Damper for Hybrid Control of Bridge Response Under Earthquake", Proc. U.S. National Workshop on Structural Control, USC, CA, pp. 107-111.
4. Feng, Q., Shinozuka, M. and Fujii, S. (1991), "Hybrid Isolation System Using Friction-Controllable Sliding Bearings", Dynamics and Control of Large Structures, edited by L. Meirovitch, VPI&SU Press, Blacksburg, VA, pp. 207-218.
5. Inaudi, J.A. and Kelly, J.M. (1993), "Hybrid Isolation Systems for Equipment Protection", J. of Earthquake Engineering and Structural Dynamics, Vol. 22, No. 4, pp. 297-313.
6. Kawashima, K., Unjoh, S. and Shimizu (1992a), "Seismic Response of Highway Bridges by Variable Damper", Proc. 24th Joint Meeting, US-Japan Panel on Wind and Seismic Effects, UJNR, Maryland.
7. Kawashima, K., Unjoh, S., Iida, H. and Mukai, H. (1992b), "Effectiveness of the Variable Damper for Reducing Seismic Response of Highway Bridges", Proc. 2nd US-Japan Workshop on Earthquake Protective System for Bridges, pp. 479-494, Tsukuba, Japan.
8. Kobori, T. and Kamagata, S. (1992a), "Dynamic Intelligent Buildings - Active Seismic Response Control", in Intelligent Structures - 2, edited by Y. K. Wen, pp. 279-282.

9. Kobori, T. and Kamagata, S. (1992b), "Active Variable Stiffness System - Active Seismic Response Control", Proc. US-Italy-Japan Workshop/Symposium on Structural Control and Intelligent Systems, pp. 140-153 (edited by G.W. Housner, S.F. Masri, F. Casciati and H. Kameda).

10. Lai, M.L. and Soong, T.T. (1992), "Seismic Design Considerations of Secondary Structural Systems", J. of Structural Engineering, ASCE, Vol. 117, No. 2, pp. 459-472.

11. Nagarajaiah, S., Riley, M.A. and Reinhorn, A.M. (1993), "Hybrid Control of Sliding Isolated Bridges", J. of Engineering Mechanics, ASCE, Vol. 119, No. 11, pp. 2317-2332.

12. Reinhorn, A.M., Soong, T.T. and Yen, C.Y. (1987), "Base Isolated Structures With Active Control", Recent Advances in Design, Analysis, Testing and Qualification Methods, ASME, PVP-Vol. 127, pp. 413-419.

13. Reinhorn, A.M. and Soong, T.T., et al (1992), "Active Bracing Systems: A Full-Scale Implementation of Active Control", Report No. NCEER-92-0020, National Center for Earthquake Engineering Research, Buffalo, New York.

14. Reinhorn, A.M., Soong, T.T., Riley, M.A., Lin, R.C., Aizawa, S. and Higashino, M. (1993a), "Full-Scale Implementation of Active Control, Part II: Installation and Performance", J. of Structural Engineering, ASCE, Vol. 118, No. 6.

15. Reinhorn, A.M., Nagarajaiah, S., Riley, M.A. and Subramaniam, R. (1993b), "Hybrid Control of Sliding Isolated Structures", Proc. ASCE Structures Congress '93, Irvine, CA, pp. 766-771.

16. Reinhorn, A.M., Nagarajaiah, S., Subramanian, R. and Riley, M. (1993c), "Study of Hybrid Systems for Structural and Nonstructural Systems", Proc. Int'l. Workshop on Structural Control and Intelligent Systems, pp. 405-416, edited by G.W. Housner and S.F. Masri, Honolulu, HI.

17. Riley, M.A., Subramaniam, R., Nagarajaiah, S. and Reinhorn, A.M. (1993), "Hybrid Control of Sliding Base-Isolated Structures", Proc. ATC-17-1 Seminar on Seismic Isolation, Passive Energy Dissipation and Active Control, San Francisco, CA, pp. 799-810.

18. Schmitendorf, W.E., Jabbari, F. and Yang, J.N. (1994), "Robust Control Techniques for Buildings under Earthquake Excitation", J. of Earthquake Engineering and Structural Dynamics, Vol. 23, No. 5, pp. 539-552.

19. Slotine, J.J.E. and Li, W. (1991), Applied Nonlinear Control, Prentice Hall, NJ.

20. Soong, T.T. (1990), Active Structural Control: Theory and Application, New York: Longman Scientific and Technical, New York.

21. Soong, T.T., Reinhorn, A.M., Wang, W.P. and Lin, R.C. (1991), "Full Scale Implementation of Active Control, Part I: Design and Simulations", J. of Structural Engineering, ASCE, Vol. 117, No. 11, pp. 3516-3535.

22. Spencer, B.F., Suhardjo, J. and Sain, M.K. (1991), "Frequency Domain Control Algorithms for Civil Engineering Applications", Proc. Intn'l. Workshop on Technology for Hong Kong's Infrastructure Development, Hong Kong, pp. 169-178.

23. Spencer, B.F., Suhardjo, J. and Sain, M.K. (1992), "Nonlinear Optimal Control of a Duffing System", Int'l. J. of Nonlinear Mechanics, Vol. 27, No. 2, pp. 157-172.

24. Suhardjo, J., Spencer, B.F., Sain, M.K. and Tomasula, D. (1992), "Nonlinear Control of a Tension Leg Platform", in Innovative Long Span Structures, Vol., pp. 416-474, IASS-CSCE Congress, Toronto, Canada.

25. Spencer, B.F., Sain, M.K., et al (1993), "Reliability-Based Design of Active Control Strategies", Proc. ATC-17-1, Seminar on Seismic Isolation, Passive Energy Dissipation, and Active Control, Vol. 2, pp. 761-772, San Francisco.

26. Utkin, V.I. (1992), Sliding Modes in Control Optimization, Springer-Verlag, New York.

27. Yang, J.N. and Akbarpour,A., (1991), "Effect of System Uncertainty on Control of Seismic-Excited Buildings," J. Eng. Mechanics, ASCE, Vol.116, No.2, pp.462-478.

28. Yang, J.N., Li, Z. and Vongchavalitkul, S. (1992a), "A Generalization of Optimal Control Theory: Linear and Nonlinear Control", National Center for Earthquake Engineering Research Technical Report, NCEER-92-0026.

29. Yang, J.N., Li, Z. and Liu, S.C. (1992b), "Stable Controllers for Instantaneous Optimal Control", J. of Engineering Mechanics, ASCE, Vol. 118, No. 8, pp. 1612-1630.

30. Yang, J.N. and Li, Z. (1993a), "Active Stiffness Control of Seismic-Excited Buildings", Proc. 3rd Pan American Congress of Applied Mechanics-PACAM III, Sao Paulo, Brazil, January 4-8, pp. 568-571.

31. Yang, J.N., Li, Z. and Vongchavalitkul, S. (1993b), "Hybrid Control of Seismic-Excited Bridge Structure Using Variable Dampers", in Structural Engineering in Natural Hazards Mitigation, Vol. 1, pp. 778-783, ASCE, 1993 ASCE Structures Congress, Irvine, CA.

32. Yang, J.N., Li, Z., Wu, J.C. and Young, K.D. (1993c), "A Discontinuous Control Method for Civil Engineering Structures", in Dynamics and Control of Large Structures, edited by L. Meirovitch, pp. 167-180, Proc. 9th VPI&SU Symp. on Dynamics and Control of Large Structures, Blacksburg, VA.

33. Yang, J.N., Li, Z. and Wu, J.C. (1993d), "Discontinuous Nonlinear Control of Base-Isolated Buildings", Proc. International Workshop on Structural Control, pp. 551-563, edited by G.W. Housner and S.F. Masri, December, Honolulu, HI.

34. Yang, J.N., Li, Z., Wu, J.C., Kawashima, K. and Unjoh, S. (1994a), "Hybrid Protective Systems for Seismic-Excited Bridges", Proc. 3rd US-Japan Workshop on Protective Systems for Bridges, pp. 3-65 to 3-79, Berkeley, CA.

35. Yang, J.N., Li, Z. and Vongchavalitkul, S. (1994b),"A Generalization of Optimal Control Theory: Linear and Nonlinear Control", J. of Engineering Mechanics, ASCE, Vol. 120, No. 2, February, 1994, pp. 266-283.

36. Yang, J.N., Li, Z., Wu, J.C. and Hsu, I.R. (1994c),"Dynamic Linearization for Sliding Isolated Buildings", Journal of Engineering Structures, April 1994.

37. Yang, J.N., Li, Z. and Wu, J.C. (1994d), "Discontinuous Control of Seismic-Excited Nonlinear and Hysteretic Structures", in Proc. ASCE Structures Congress XII, pp. 393-398, Atlanta, GA.

38. Yang, J.N., Li, Z. and Wu, J.C. (1994e), "Control of Seismic-Excited Buildings Using Active Variable Stiffness Systems", Proc. 1994 American Control Conference, pp. 1083-1088, June 29-July 1, Baltimore, MD.

39. Yang, J.N., Wu, J.C., Reinhorn, A.M., Riley, M., Schmitendorf, W.E. and Jabbari, F. (1994f), "Experimental Verifications of H_∞ and Sliding Mode Control for Seismic-Excited Buildings", paper to appear in Proc. First World Conference on Structural Control, Pasadena, CA.

40. Yang, J.N., Wu, J.C. and Hsu, S.Y. (1994g), "Parametric Control of Seismic-Excited Structures", paper to appear in Proc. First World Conference on Structural Control, Pasadena, CA.

41. Yang, J.N., Agrawal, A.K. and Wu, J.C. (1994h), "Sliding Mode Control of Structures Subjected to Seismic Loads", paper to appear in Proc. First World Conference on Structural Control, Pasadena, CA.

42. Young, K.D. (editor) (1993), Variable Structure Control for Robotics and Aerospace Applications, Elsevier, New York.

43. Zhou, F. and Fisher, D.G., (1992) "Continuous Sliding Mode Control," International Journal of Control, Vol. 55, No. 2, pp. 313-327.

NATIONAL CENTER FOR EARTHQUAKE ENGINEERING RESEARCH
LIST OF TECHNICAL REPORTS

The National Center for Earthquake Engineering Research (NCEER) publishes technical reports on a variety of subjects related to earthquake engineering written by authors funded through NCEER. These reports are available from both NCEER's Publications Department and the National Technical Information Service (NTIS). Requests for reports should be directed to the Publications Department, National Center for Earthquake Engineering Research, State University of New York at Buffalo, Red Jacket Quadrangle, Buffalo, New York 14261. Reports can also be requested through NTIS, 5285 Port Royal Road, Springfield, Virginia 22161. NTIS accession numbers are shown in parenthesis, if available.

NCEER-87-0001 "First-Year Program in Research, Education and Technology Transfer," 3/5/87, (PB88-134275).

NCEER-87-0002 "Experimental Evaluation of Instantaneous Optimal Algorithms for Structural Control," by R.C. Lin, T.T. Soong and A.M. Reinhorn, 4/20/87, (PB88-134341).

NCEER-87-0003 "Experimentation Using the Earthquake Simulation Facilities at University at Buffalo," by A.M. Reinhorn and R.L. Ketter, to be published.

NCEER-87-0004 "The System Characteristics and Performance of a Shaking Table," by J.S. Hwang, K.C. Chang and G.C. Lee, 6/1/87, (PB88-134259). This report is available only through NTIS (see address given above).

NCEER-87-0005 "A Finite Element Formulation for Nonlinear Viscoplastic Material Using a Q Model," by O. Gyebi and G. Dasgupta, 11/2/87, (PB88-213764).

NCEER-87-0006 "Symbolic Manipulation Program (SMP) - Algebraic Codes for Two and Three Dimensional Finite Element Formulations," by X. Lee and G. Dasgupta, 11/9/87, (PB88-218522).

NCEER-87-0007 "Instantaneous Optimal Control Laws for Tall Buildings Under Seismic Excitations," by J.N. Yang, A. Akbarpour and P. Ghaemmaghami, 6/10/87, (PB88-134333). This report is only available through NTIS (see address given above).

NCEER-87-0008 "IDARC: Inelastic Damage Analysis of Reinforced Concrete Frame - Shear-Wall Structures," by Y.J. Park, A.M. Reinhorn and S.K. Kunnath, 7/20/87, (PB88-134325).

NCEER-87-0009 "Liquefaction Potential for New York State: A Preliminary Report on Sites in Manhattan and Buffalo," by M. Budhu, V. Vijayakumar, R.F. Giese and L. Baumgras, 8/31/87, (PB88-163704). This report is available only through NTIS (see address given above).

NCEER-87-0010 "Vertical and Torsional Vibration of Foundations in Inhomogeneous Media," by A.S. Veletsos and K.W. Dotson, 6/1/87, (PB88-134291).

NCEER-87-0011 "Seismic Probabilistic Risk Assessment and Seismic Margins Studies for Nuclear Power Plants," by Howard H.M. Hwang, 6/15/87, (PB88-134267).

NCEER-87-0012 "Parametric Studies of Frequency Response of Secondary Systems Under Ground-Acceleration Excitations," by Y. Yong and Y.K. Lin, 6/10/87, (PB88-134309).

NCEER-87-0013 "Frequency Response of Secondary Systems Under Seismic Excitation," by J.A. HoLung, J. Cai and Y.K. Lin, 7/31/87, (PB88-134317).

NCEER-87-0014 "Modelling Earthquake Ground Motions in Seismically Active Regions Using Parametric Time Series Methods," by G.W. Ellis and A.S. Cakmak, 8/25/87, (PB88-134283).

NCEER-87-0015 "Detection and Assessment of Seismic Structural Damage," by E. DiPasquale and A.S. Cakmak, 8/25/87, (PB88-163712).

NCEER-87-0016 "Pipeline Experiment at Parkfield, California," by J. Isenberg and E. Richardson, 9/15/87, (PB88-163720). This report is available only through NTIS (see address given above).

NCEER-87-0017 "Digital Simulation of Seismic Ground Motion," by M. Shinozuka, G. Deodatis and T. Harada, 8/31/87, (PB88-155197). This report is available only through NTIS (see address given above).

NCEER-87-0018 "Practical Considerations for Structural Control: System Uncertainty, System Time Delay and Truncation of Small Control Forces," J.N. Yang and A. Akbarpour, 8/10/87, (PB88-163738).

NCEER-87-0019 "Modal Analysis of Nonclassically Damped Structural Systems Using Canonical Transformation," by J.N. Yang, S. Sarkani and F.X. Long, 9/27/87, (PB88-187851).

NCEER-87-0020 "A Nonstationary Solution in Random Vibration Theory," by J.R. Red-Horse and P.D. Spanos, 11/3/87, (PB88-163746).

NCEER-87-0021 "Horizontal Impedances for Radially Inhomogeneous Viscoelastic Soil Layers," by A.S. Veletsos and K.W. Dotson, 10/15/87, (PB88-150859).

NCEER-87-0022 "Seismic Damage Assessment of Reinforced Concrete Members," by Y.S. Chung, C. Meyer and M. Shinozuka, 10/9/87, (PB88-150867). This report is available only through NTIS (see address given above).

NCEER-87-0023 "Active Structural Control in Civil Engineering," by T.T. Soong, 11/11/87, (PB88-187778).

NCEER-87-0024 "Vertical and Torsional Impedances for Radially Inhomogeneous Viscoelastic Soil Layers," by K.W. Dotson and A.S. Veletsos, 12/87, (PB88-187786).

NCEER-87-0025 "Proceedings from the Symposium on Seismic Hazards, Ground Motions, Soil-Liquefaction and Engineering Practice in Eastern North America," October 20-22, 1987, edited by K.H. Jacob, 12/87, (PB88-188115).

NCEER-87-0026 "Report on the Whittier-Narrows, California, Earthquake of October 1, 1987," by J. Pantelic and A. Reinhorn, 11/87, (PB88-187752). This report is available only through NTIS (see address given above).

NCEER-87-0027 "Design of a Modular Program for Transient Nonlinear Analysis of Large 3-D Building Structures," by S. Srivastav and J.F. Abel, 12/30/87, (PB88-187950).

NCEER-87-0028 "Second-Year Program in Research, Education and Technology Transfer," 3/8/88, (PB88-219480).

NCEER-88-0001 "Workshop on Seismic Computer Analysis and Design of Buildings With Interactive Graphics," by W. McGuire, J.F. Abel and C.H. Conley, 1/18/88, (PB88-187760).

NCEER-88-0002 "Optimal Control of Nonlinear Flexible Structures," by J.N. Yang, F.X. Long and D. Wong, 1/22/88, (PB88-213772).

NCEER-88-0003 "Substructuring Techniques in the Time Domain for Primary-Secondary Structural Systems," by G.D. Manolis and G. Juhn, 2/10/88, (PB88-213780).

NCEER-88-0004 "Iterative Seismic Analysis of Primary-Secondary Systems," by A. Singhal, L.D. Lutes and P.D. Spanos, 2/23/88, (PB88-213798).

NCEER-88-0005 "Stochastic Finite Element Expansion for Random Media," by P.D. Spanos and R. Ghanem, 3/14/88, (PB88-213806).

NCEER-88-0006 "Combining Structural Optimization and Structural Control," by F.Y. Cheng and C.P. Pantelides, 1/10/88, (PB88-213814).

NCEER-88-0007 "Seismic Performance Assessment of Code-Designed Structures," by H.H-M. Hwang, J-W. Jaw and H-J. Shau, 3/20/88, (PB88-219423).

NCEER-88-0008 "Reliability Analysis of Code-Designed Structures Under Natural Hazards," by H.H-M. Hwang, H. Ushiba and M. Shinozuka, 2/29/88, (PB88-229471).

NCEER-88-0009 "Seismic Fragility Analysis of Shear Wall Structures," by J-W Jaw and H.H-M. Hwang, 4/30/88, (PB89-102867).

NCEER-88-0010 "Base Isolation of a Multi-Story Building Under a Harmonic Ground Motion - A Comparison of Performances of Various Systems," by F-G Fan, G. Ahmadi and I.G. Tadjbakhsh, 5/18/88, (PB89-122238).

NCEER-88-0011 "Seismic Floor Response Spectra for a Combined System by Green's Functions," by F.M. Lavelle, L.A. Bergman and P.D. Spanos, 5/1/88, (PB89-102875).

NCEER-88-0012 "A New Solution Technique for Randomly Excited Hysteretic Structures," by G.Q. Cai and Y.K. Lin, 5/16/88, (PB89-102883).

NCEER-88-0013 "A Study of Radiation Damping and Soil-Structure Interaction Effects in the Centrifuge," by K. Weissman, supervised by J.H. Prevost, 5/24/88, (PB89-144703).

NCEER-88-0014 "Parameter Identification and Implementation of a Kinematic Plasticity Model for Frictional Soils," by J.H. Prevost and D.V. Griffiths, to be published.

NCEER-88-0015 "Two- and Three- Dimensional Dynamic Finite Element Analyses of the Long Valley Dam," by D.V. Griffiths and J.H. Prevost, 6/17/88, (PB89-144711).

NCEER-88-0016 "Damage Assessment of Reinforced Concrete Structures in Eastern United States," by A.M. Reinhorn, M.J. Seidel, S.K. Kunnath and Y.J. Park, 6/15/88, (PB89-122220).

NCEER-88-0017 "Dynamic Compliance of Vertically Loaded Strip Foundations in Multilayered Viscoelastic Soils," by S. Ahmad and A.S.M. Israil, 6/17/88, (PB89-102891).

NCEER-88-0018 "An Experimental Study of Seismic Structural Response With Added Viscoelastic Dampers," by R.C. Lin, Z. Liang, T.T. Soong and R.H. Zhang, 6/30/88, (PB89-122212). This report is available only through NTIS (see address given above).

NCEER-88-0019 "Experimental Investigation of Primary - Secondary System Interaction," by G.D. Manolis, G. Juhn and A.M. Reinhorn, 5/27/88, (PB89-122204).

NCEER-88-0020 "A Response Spectrum Approach For Analysis of Nonclassically Damped Structures," by J.N. Yang, S. Sarkani and F.X. Long, 4/22/88, (PB89-102909).

NCEER-88-0021 "Seismic Interaction of Structures and Soils: Stochastic Approach," by A.S. Veletsos and A.M. Prasad, 7/21/88, (PB89-122196).

NCEER-88-0022 "Identification of the Serviceability Limit State and Detection of Seismic Structural Damage," by E. DiPasquale and A.S. Cakmak, 6/15/88, (PB89-122188). This report is available only through NTIS (see address given above).

NCEER-88-0023 "Multi-Hazard Risk Analysis: Case of a Simple Offshore Structure," by B.K. Bhartia and E.H. Vanmarcke, 7/21/88, (PB89-145213).

NCEER-88-0024 "Automated Seismic Design of Reinforced Concrete Buildings," by Y.S. Chung, C. Meyer and M. Shinozuka, 7/5/88, (PB89-122170). This report is available only through NTIS (see address given above).

NCEER-88-0025 "Experimental Study of Active Control of MDOF Structures Under Seismic Excitations," by L.L. Chung, R.C. Lin, T.T. Soong and A.M. Reinhorn, 7/10/88, (PB89-122600).

NCEER-88-0026 "Earthquake Simulation Tests of a Low-Rise Metal Structure," by J.S. Hwang, K.C. Chang, G.C. Lee and R.L. Ketter, 8/1/88, (PB89-102917).

NCEER-88-0027 "Systems Study of Urban Response and Reconstruction Due to Catastrophic Earthquakes," by F. Kozin and H.K. Zhou, 9/22/88, (PB90-162348).

NCEER-88-0028 "Seismic Fragility Analysis of Plane Frame Structures," by H.H-M. Hwang and Y.K. Low, 7/31/88, (PB89-131445).

NCEER-88-0029 "Response Analysis of Stochastic Structures," by A. Kardara, C. Bucher and M. Shinozuka, 9/22/88, (PB89-174429).

NCEER-88-0030 "Nonnormal Accelerations Due to Yielding in a Primary Structure," by D.C.K. Chen and L.D. Lutes, 9/19/88, (PB89-131437).

NCEER-88-0031 "Design Approaches for Soil-Structure Interaction," by A.S. Veletsos, A.M. Prasad and Y. Tang, 12/30/88, (PB89-174437). This report is available only through NTIS (see address given above).

NCEER-88-0032 "A Re-evaluation of Design Spectra for Seismic Damage Control," by C.J. Turkstra and A.G. Tallin, 11/7/88, (PB89-145221).

NCEER-88-0033 "The Behavior and Design of Noncontact Lap Splices Subjected to Repeated Inelastic Tensile Loading," by V.E. Sagan, P. Gergely and R.N. White, 12/8/88, (PB89-163737).

NCEER-88-0034 "Seismic Response of Pile Foundations," by S.M. Mamoon, P.K. Banerjee and S. Ahmad, 11/1/88, (PB89-145239).

NCEER-88-0035 "Modeling of R/C Building Structures With Flexible Floor Diaphragms (IDARC2)," by A.M. Reinhorn, S.K. Kunnath and N. Panahshahi, 9/7/88, (PB89-207153).

NCEER-88-0036 "Solution of the Dam-Reservoir Interaction Problem Using a Combination of FEM, BEM with Particular Integrals, Modal Analysis, and Substructuring," by C-S. Tsai, G.C. Lee and R.L. Ketter, 12/31/88, (PB89-207146).

NCEER-88-0037 "Optimal Placement of Actuators for Structural Control," by F.Y. Cheng and C.P. Pantelides, 8/15/88, (PB89-162846).

NCEER-88-0038 "Teflon Bearings in Aseismic Base Isolation: Experimental Studies and Mathematical Modeling," by A. Mokha, M.C. Constantinou and A.M. Reinhorn, 12/5/88, (PB89-218457). This report is available only through NTIS (see address given above).

NCEER-88-0039 "Seismic Behavior of Flat Slab High-Rise Buildings in the New York City Area," by P. Weidlinger and M. Ettouney, 10/15/88, (PB90-145681).

NCEER-88-0040 "Evaluation of the Earthquake Resistance of Existing Buildings in New York City," by P. Weidlinger and M. Ettouney, 10/15/88, to be published.

NCEER-88-0041 "Small-Scale Modeling Techniques for Reinforced Concrete Structures Subjected to Seismic Loads," by W. Kim, A. El-Attar and R.N. White, 11/22/88, (PB89-189625).

NCEER-88-0042 "Modeling Strong Ground Motion from Multiple Event Earthquakes," by G.W. Ellis and A.S. Cakmak, 10/15/88, (PB89-174445).

NCEER-88-0043 "Nonstationary Models of Seismic Ground Acceleration," by M. Grigoriu, S.E. Ruiz and E. Rosenblueth, 7/15/88, (PB89-189617).

NCEER-88-0044 "SARCF User's Guide: Seismic Analysis of Reinforced Concrete Frames," by Y.S. Chung, C. Meyer and M. Shinozuka, 11/9/88, (PB89-174452).

NCEER-88-0045 "First Expert Panel Meeting on Disaster Research and Planning," edited by J. Pantelic and J. Stoyle, 9/15/88, (PB89-174460).

NCEER-88-0046 "Preliminary Studies of the Effect of Degrading Infill Walls on the Nonlinear Seismic Response of Steel Frames," by C.Z. Chrysostomou, P. Gergely and J.F. Abel, 12/19/88, (PB89-208383).

NCEER-88-0047 "Reinforced Concrete Frame Component Testing Facility - Design, Construction, Instrumentation and Operation," by S.P. Pessiki, C. Conley, T. Bond, P. Gergely and R.N. White, 12/16/88, (PB89-174478).

NCEER-89-0001 "Effects of Protective Cushion and Soil Compliancy on the Response of Equipment Within a Seismically Excited Building," by J.A. HoLung, 2/16/89, (PB89-207179).

NCEER-89-0002 "Statistical Evaluation of Response Modification Factors for Reinforced Concrete Structures," by H.H-M. Hwang and J-W. Jaw, 2/17/89, (PB89-207187).

NCEER-89-0003 "Hysteretic Columns Under Random Excitation," by G-Q. Cai and Y.K. Lin, 1/9/89, (PB89-196513).

NCEER-89-0004 "Experimental Study of `Elephant Foot Bulge' Instability of Thin-Walled Metal Tanks," by Z-H. Jia and R.L. Ketter, 2/22/89, (PB89-207195).

NCEER-89-0005 "Experiment on Performance of Buried Pipelines Across San Andreas Fault," by J. Isenberg, E. Richardson and T.D. O'Rourke, 3/10/89, (PB89-218440). This report is available only through NTIS (see address given above).

NCEER-89-0006 "A Knowledge-Based Approach to Structural Design of Earthquake-Resistant Buildings," by M. Subramani, P. Gergely, C.H. Conley, J.F. Abel and A.H. Zaghw, 1/15/89, (PB89-218465).

NCEER-89-0007 "Liquefaction Hazards and Their Effects on Buried Pipelines," by T.D. O'Rourke and P.A. Lane, 2/1/89, (PB89-218481).

NCEER-89-0008 "Fundamentals of System Identification in Structural Dynamics," by H. Imai, C-B. Yun, O. Maruyama and M. Shinozuka, 1/26/89, (PB89-207211).

NCEER-89-0009 "Effects of the 1985 Michoacan Earthquake on Water Systems and Other Buried Lifelines in Mexico," by A.G. Ayala and M.J. O'Rourke, 3/8/89, (PB89-207229).

NCEER-89-R010 "NCEER Bibliography of Earthquake Education Materials," by K.E.K. Ross, Second Revision, 9/1/89, (PB90-125352).

NCEER-89-0011 "Inelastic Three-Dimensional Response Analysis of Reinforced Concrete Building Structures (IDARC-3D), Part I - Modeling," by S.K. Kunnath and A.M. Reinhorn, 4/17/89, (PB90-114612).

NCEER-89-0012 "Recommended Modifications to ATC-14," by C.D. Poland and J.O. Malley, 4/12/89, (PB90-108648).

NCEER-89-0013 "Repair and Strengthening of Beam-to-Column Connections Subjected to Earthquake Loading," by M. Corazao and A.J. Durrani, 2/28/89, (PB90-109885).

NCEER-89-0014 "Program EXKAL2 for Identification of Structural Dynamic Systems," by O. Maruyama, C-B. Yun, M. Hoshiya and M. Shinozuka, 5/19/89, (PB90-109877).

NCEER-89-0015 "Response of Frames With Bolted Semi-Rigid Connections, Part I - Experimental Study and Analytical Predictions," by P.J. DiCorso, A.M. Reinhorn, J.R. Dickerson, J.B. Radziminski and W.L. Harper, 6/1/89, to be published.

NCEER-89-0016 "ARMA Monte Carlo Simulation in Probabilistic Structural Analysis," by P.D. Spanos and M.P. Mignolet, 7/10/89, (PB90-109893).

NCEER-89-P017 "Preliminary Proceedings from the Conference on Disaster Preparedness - The Place of Earthquake Education in Our Schools," Edited by K.E.K. Ross, 6/23/89, (PB90-108606).

NCEER-89-0017 "Proceedings from the Conference on Disaster Preparedness - The Place of Earthquake Education in Our Schools," Edited by K.E.K. Ross, 12/31/89, (PB90-207895). This report is available only through NTIS (see address given above).

NCEER-89-0018 "Multidimensional Models of Hysteretic Material Behavior for Vibration Analysis of Shape Memory Energy Absorbing Devices, by E.J. Graesser and F.A. Cozzarelli, 6/7/89, (PB90-164146).

NCEER-89-0019 "Nonlinear Dynamic Analysis of Three-Dimensional Base Isolated Structures (3D-BASIS)," by S. Nagarajaiah, A.M. Reinhorn and M.C. Constantinou, 8/3/89, (PB90-161936). This report is available only through NTIS (see address given above).

NCEER-89-0020 "Structural Control Considering Time-Rate of Control Forces and Control Rate Constraints," by F.Y. Cheng and C.P. Pantelides, 8/3/89, (PB90-120445).

NCEER-89-0021 "Subsurface Conditions of Memphis and Shelby County," by K.W. Ng, T-S. Chang and H-H.M. Hwang, 7/26/89, (PB90-120437).

NCEER-89-0022 "Seismic Wave Propagation Effects on Straight Jointed Buried Pipelines," by K. Elhmadi and M.J. O'Rourke, 8/24/89, (PB90-162322).

NCEER-89-0023 "Workshop on Serviceability Analysis of Water Delivery Systems," edited by M. Grigoriu, 3/6/89, (PB90-127424).

NCEER-89-0024 "Shaking Table Study of a 1/5 Scale Steel Frame Composed of Tapered Members," by K.C. Chang, J.S. Hwang and G.C. Lee, 9/18/89, (PB90-160169).

NCEER-89-0025 "DYNA1D: A Computer Program for Nonlinear Seismic Site Response Analysis - Technical Documentation," by Jean H. Prevost, 9/14/89, (PB90-161944). This report is available only through NTIS (see address given above).

NCEER-89-0026 "1:4 Scale Model Studies of Active Tendon Systems and Active Mass Dampers for Aseismic Protection," by A.M. Reinhorn, T.T. Soong, R.C. Lin, Y.P. Yang, Y. Fukao, H. Abe and M. Nakai, 9/15/89, (PB90-173246).

NCEER-89-0027 "Scattering of Waves by Inclusions in a Nonhomogeneous Elastic Half Space Solved by Boundary Element Methods," by P.K. Hadley, A. Askar and A.S. Cakmak, 6/15/89, (PB90-145699).

NCEER-89-0028 "Statistical Evaluation of Deflection Amplification Factors for Reinforced Concrete Structures," by H.H.M. Hwang, J-W. Jaw and A.L. Ch'ng, 8/31/89, (PB90-164633).

NCEER-89-0029 "Bedrock Accelerations in Memphis Area Due to Large New Madrid Earthquakes," by H.H.M. Hwang, C.H.S. Chen and G. Yu, 11/7/89, (PB90-162330).

NCEER-89-0030 "Seismic Behavior and Response Sensitivity of Secondary Structural Systems," by Y.Q. Chen and T.T. Soong, 10/23/89, (PB90-164658).

NCEER-89-0031 "Random Vibration and Reliability Analysis of Primary-Secondary Structural Systems," by Y. Ibrahim, M. Grigoriu and T.T. Soong, 11/10/89, (PB90-161951).

NCEER-89-0032 "Proceedings from the Second U.S. - Japan Workshop on Liquefaction, Large Ground Deformation and Their Effects on Lifelines, September 26-29, 1989," Edited by T.D. O'Rourke and M. Hamada, 12/1/89, (PB90-209388).

NCEER-89-0033 "Deterministic Model for Seismic Damage Evaluation of Reinforced Concrete Structures," by J.M. Bracci, A.M. Reinhorn, J.B. Mander and S.K. Kunnath, 9/27/89.

NCEER-89-0034 "On the Relation Between Local and Global Damage Indices," by E. DiPasquale and A.S. Cakmak, 8/15/89, (PB90-173865).

NCEER-89-0035 "Cyclic Undrained Behavior of Nonplastic and Low Plasticity Silts," by A.J. Walker and H.E. Stewart, 7/26/89, (PB90-183518).

NCEER-89-0036 "Liquefaction Potential of Surficial Deposits in the City of Buffalo, New York," by M. Budhu, R. Giese and L. Baumgrass, 1/17/89, (PB90-208455).

NCEER-89-0037 "A Deterministic Assessment of Effects of Ground Motion Incoherence," by A.S. Veletsos and Y. Tang, 7/15/89, (PB90-164294).

NCEER-89-0038 "Workshop on Ground Motion Parameters for Seismic Hazard Mapping," July 17-18, 1989, edited by R.V. Whitman, 12/1/89, (PB90-173923).

NCEER-89-0039 "Seismic Effects on Elevated Transit Lines of the New York City Transit Authority," by C.J. Costantino, C.A. Miller and E. Heymsfield, 12/26/89, (PB90-207887).

NCEER-89-0040 "Centrifugal Modeling of Dynamic Soil-Structure Interaction," by K. Weissman, Supervised by J.H. Prevost, 5/10/89, (PB90-207879).

NCEER-89-0041 "Linearized Identification of Buildings With Cores for Seismic Vulnerability Assessment," by I-K. Ho and A.E. Aktan, 11/1/89, (PB90-251943).

NCEER-90-0001 "Geotechnical and Lifeline Aspects of the October 17, 1989 Loma Prieta Earthquake in San Francisco," by T.D. O'Rourke, H.E. Stewart, F.T. Blackburn and T.S. Dickerman, 1/90, (PB90-208596).

NCEER-90-0002 "Nonnormal Secondary Response Due to Yielding in a Primary Structure," by D.C.K. Chen and L.D. Lutes, 2/28/90, (PB90-251976).

NCEER-90-0003 "Earthquake Education Materials for Grades K-12," by K.E.K. Ross, 4/16/90, (PB91-251984).

NCEER-90-0004 "Catalog of Strong Motion Stations in Eastern North America," by R.W. Busby, 4/3/90, (PB90-251984).

NCEER-90-0005 "NCEER Strong-Motion Data Base: A User Manual for the GeoBase Release (Version 1.0 for the Sun3)," by P. Friberg and K. Jacob, 3/31/90 (PB90-258062).

NCEER-90-0006 "Seismic Hazard Along a Crude Oil Pipeline in the Event of an 1811-1812 Type New Madrid Earthquake," by H.H.M. Hwang and C-H.S. Chen, 4/16/90(PB90-258054).

NCEER-90-0007 "Site-Specific Response Spectra for Memphis Sheahan Pumping Station," by H.H.M. Hwang and C.S. Lee, 5/15/90, (PB91-108811).

NCEER-90-0008 "Pilot Study on Seismic Vulnerability of Crude Oil Transmission Systems," by T. Ariman, R. Dobry, M. Grigoriu, F. Kozin, M. O'Rourke, T. O'Rourke and M. Shinozuka, 5/25/90, (PB91-108837).

NCEER-90-0009 "A Program to Generate Site Dependent Time Histories: EQGEN," by G.W. Ellis, M. Srinivasan and A.S. Cakmak, 1/30/90, (PB91-108829).

NCEER-90-0010 "Active Isolation for Seismic Protection of Operating Rooms," by M.E. Talbott, Supervised by M. Shinozuka, 6/8/9, (PB91-110205).

NCEER-90-0011 "Program LINEARID for Identification of Linear Structural Dynamic Systems," by C-B. Yun and M. Shinozuka, 6/25/90, (PB91-110312).

NCEER-90-0012 "Two-Dimensional Two-Phase Elasto-Plastic Seismic Response of Earth Dams," by A.N. Yiagos, Supervised by J.H. Prevost, 6/20/90, (PB91-110197).

NCEER-90-0013 "Secondary Systems in Base-Isolated Structures: Experimental Investigation, Stochastic Response and Stochastic Sensitivity," by G.D. Manolis, G. Juhn, M.C. Constantinou and A.M. Reinhorn, 7/1/90, (PB91-110320).

NCEER-90-0014 "Seismic Behavior of Lightly-Reinforced Concrete Column and Beam-Column Joint Details," by S.P. Pessiki, C.H. Conley, P. Gergely and R.N. White, 8/22/90, (PB91-108795).

NCEER-90-0015 "Two Hybrid Control Systems for Building Structures Under Strong Earthquakes," by J.N. Yang and A. Danielians, 6/29/90, (PB91-125393).

NCEER-90-0016 "Instantaneous Optimal Control with Acceleration and Velocity Feedback," by J.N. Yang and Z. Li, 6/29/90, (PB91-125401).

NCEER-90-0017 "Reconnaissance Report on the Northern Iran Earthquake of June 21, 1990," by M. Mehrain, 10/4/90, (PB91-125377).

NCEER-90-0018 "Evaluation of Liquefaction Potential in Memphis and Shelby County," by T.S. Chang, P.S. Tang, C.S. Lee and H. Hwang, 8/10/90, (PB91-125427).

NCEER-90-0019 "Experimental and Analytical Study of a Combined Sliding Disc Bearing and Helical Steel Spring Isolation System," by M.C. Constantinou, A.S. Mokha and A.M. Reinhorn, 10/4/90, (PB91-125385).

NCEER-90-0020 "Experimental Study and Analytical Prediction of Earthquake Response of a Sliding Isolation System with a Spherical Surface," by A.S. Mokha, M.C. Constantinou and A.M. Reinhorn, 10/11/90, (PB91-125419).

NCEER-90-0021 "Dynamic Interaction Factors for Floating Pile Groups," by G. Gazetas, K. Fan, A. Kaynia and E. Kausel, 9/10/90, (PB91-170381).

NCEER-90-0022 "Evaluation of Seismic Damage Indices for Reinforced Concrete Structures," by S. Rodriguez-Gomez and A.S. Cakmak, 9/30/90, PB91-171322).

NCEER-90-0023 "Study of Site Response at a Selected Memphis Site," by H. Desai, S. Ahmad, E.S. Gazetas and M.R. Oh, 10/11/90, (PB91-196857).

NCEER-90-0024 "A User's Guide to Strongmo: Version 1.0 of NCEER's Strong-Motion Data Access Tool for PCs and Terminals," by P.A. Friberg and C.A.T. Susch, 11/15/90, (PB91-171272).

NCEER-90-0025 "A Three-Dimensional Analytical Study of Spatial Variability of Seismic Ground Motions," by L-L. Hong and A.H.-S. Ang, 10/30/90, (PB91-170399).

NCEER-90-0026 "MUMOID User's Guide - A Program for the Identification of Modal Parameters," by S. Rodriguez-Gomez and E. DiPasquale, 9/30/90, (PB91-171298).

NCEER-90-0027 "SARCF-II User's Guide - Seismic Analysis of Reinforced Concrete Frames," by S. Rodriguez-Gomez, Y.S. Chung and C. Meyer, 9/30/90, (PB91-171280).

NCEER-90-0028 "Viscous Dampers: Testing, Modeling and Application in Vibration and Seismic Isolation," by N. Makris and M.C. Constantinou, 12/20/90 (PB91-190561).

NCEER-90-0029 "Soil Effects on Earthquake Ground Motions in the Memphis Area," by H. Hwang, C.S. Lee, K.W. Ng and T.S. Chang, 8/2/90, (PB91-190751).

NCEER-91-0001 "Proceedings from the Third Japan-U.S. Workshop on Earthquake Resistant Design of Lifeline Facilities and Countermeasures for Soil Liquefaction, December 17-19, 1990," edited by T.D. O'Rourke and M. Hamada, 2/1/91, (PB91-179259).

NCEER-91-0002 "Physical Space Solutions of Non-Proportionally Damped Systems," by M. Tong, Z. Liang and G.C. Lee, 1/15/91, (PB91-179242).

NCEER-91-0003 "Seismic Response of Single Piles and Pile Groups," by K. Fan and G. Gazetas, 1/10/91, (PB92-174994).

NCEER-91-0004 "Damping of Structures: Part 1 - Theory of Complex Damping," by Z. Liang and G. Lee, 10/10/91, (PB92-197235).

NCEER-91-0005 "3D-BASIS - Nonlinear Dynamic Analysis of Three Dimensional Base Isolated Structures: Part II," by S. Nagarajaiah, A.M. Reinhorn and M.C. Constantinou, 2/28/91, (PB91-190553).

NCEER-91-0006 "A Multidimensional Hysteretic Model for Plasticity Deforming Metals in Energy Absorbing Devices," by E.J. Graesser and F.A. Cozzarelli, 4/9/91, (PB92-108364).

NCEER-91-0007 "A Framework for Customizable Knowledge-Based Expert Systems with an Application to a KBES for Evaluating the Seismic Resistance of Existing Buildings," by E.G. Ibarra-Anaya and S.J. Fenves, 4/9/91, (PB91-210930).

NCEER-91-0008 "Nonlinear Analysis of Steel Frames with Semi-Rigid Connections Using the Capacity Spectrum Method," by G.G. Deierlein, S-H. Hsieh, Y-J. Shen and J.F. Abel, 7/2/91, (PB92-113828).

NCEER-91-0009 "Earthquake Education Materials for Grades K-12," by K.E.K. Ross, 4/30/91, (PB91-212142).

NCEER-91-0010 "Phase Wave Velocities and Displacement Phase Differences in a Harmonically Oscillating Pile," by N. Makris and G. Gazetas, 7/8/91, (PB92-108356).

NCEER-91-0011 "Dynamic Characteristics of a Full-Size Five-Story Steel Structure and a 2/5 Scale Model," by K.C. Chang, G.C. Yao, G.C. Lee, D.S. Hao and Y.C. Yeh," 7/2/91, (PB93-116648).

NCEER-91-0012 "Seismic Response of a 2/5 Scale Steel Structure with Added Viscoelastic Dampers," by K.C. Chang, T.T. Soong, S-T. Oh and M.L. Lai, 5/17/91, (PB92-110816).

NCEER-91-0013 "Earthquake Response of Retaining Walls; Full-Scale Testing and Computational Modeling," by S. Alampalli and A-W.M. Elgamal, 6/20/91, to be published.

NCEER-91-0014 "3D-BASIS-M: Nonlinear Dynamic Analysis of Multiple Building Base Isolated Structures," by P.C. Tsopelas, S. Nagarajaiah, M.C. Constantinou and A.M. Reinhorn, 5/28/91, (PB92-113885).

NCEER-91-0015 "Evaluation of SEAOC Design Requirements for Sliding Isolated Structures," by D. Theodossiou and M.C. Constantinou, 6/10/91, (PB92-114602).

NCEER-91-0016 "Closed-Loop Modal Testing of a 27-Story Reinforced Concrete Flat Plate-Core Building," by H.R. Somaprasad, T. Toksoy, H. Yoshiyuki and A.E. Aktan, 7/15/91, (PB92-129980).

NCEER-91-0017 "Shake Table Test of a 1/6 Scale Two-Story Lightly Reinforced Concrete Building," by A.G. El-Attar, R.N. White and P. Gergely, 2/28/91, (PB92-222447).

NCEER-91-0018 "Shake Table Test of a 1/8 Scale Three-Story Lightly Reinforced Concrete Building," by A.G. El-Attar, R.N. White and P. Gergely, 2/28/91, (PB93-116630).

NCEER-91-0019 "Transfer Functions for Rigid Rectangular Foundations," by A.S. Veletsos, A.M. Prasad and W.H. Wu, 7/31/91.

NCEER-91-0020 "Hybrid Control of Seismic-Excited Nonlinear and Inelastic Structural Systems," by J.N. Yang, Z. Li and A. Danielians, 8/1/91, (PB92-143171).

NCEER-91-0021 "The NCEER-91 Earthquake Catalog: Improved Intensity-Based Magnitudes and Recurrence Relations for U.S. Earthquakes East of New Madrid," by L. Seeber and J.G. Armbruster, 8/28/91, (PB92-176742).

NCEER-91-0022 "Proceedings from the Implementation of Earthquake Planning and Education in Schools: The Need for Change - The Roles of the Changemakers," by K.E.K. Ross and F. Winslow, 7/23/91, (PB92-129998).

NCEER-91-0023 "A Study of Reliability-Based Criteria for Seismic Design of Reinforced Concrete Frame Buildings," by H.H.M. Hwang and H-M. Hsu, 8/10/91, (PB92-140235).

NCEER-91-0024 "Experimental Verification of a Number of Structural System Identification Algorithms," by R.G. Ghanem, H. Gavin and M. Shinozuka, 9/18/91, (PB92-176577).

NCEER-91-0025 "Probabilistic Evaluation of Liquefaction Potential," by H.H.M. Hwang and C.S. Lee," 11/25/91, (PB92-143429).

NCEER-91-0026 "Instantaneous Optimal Control for Linear, Nonlinear and Hysteretic Structures - Stable Controllers," by J.N. Yang and Z. Li, 11/15/91, (PB92-163807).

NCEER-91-0027 "Experimental and Theoretical Study of a Sliding Isolation System for Bridges," by M.C. Constantinou, A. Kartoum, A.M. Reinhorn and P. Bradford, 11/15/91, (PB92-176973).

NCEER-92-0001 "Case Studies of Liquefaction and Lifeline Performance During Past Earthquakes, Volume 1: Japanese Case Studies," Edited by M. Hamada and T. O'Rourke, 2/17/92, (PB92-197243).

NCEER-92-0002 "Case Studies of Liquefaction and Lifeline Performance During Past Earthquakes, Volume 2: United States Case Studies," Edited by T. O'Rourke and M. Hamada, 2/17/92, (PB92-197250).

NCEER-92-0003 "Issues in Earthquake Education," Edited by K. Ross, 2/3/92, (PB92-222389).

NCEER-92-0004 "Proceedings from the First U.S. - Japan Workshop on Earthquake Protective Systems for Bridges," Edited by I.G. Buckle, 2/4/92, (PB94-142239, A99, MF-A06).

NCEER-92-0005 "Seismic Ground Motion from a Haskell-Type Source in a Multiple-Layered Half-Space," A.P. Theoharis, G. Deodatis and M. Shinozuka, 1/2/92, to be published.

NCEER-92-0006 "Proceedings from the Site Effects Workshop," Edited by R. Whitman, 2/29/92, (PB92-197201).

NCEER-92-0007 "Engineering Evaluation of Permanent Ground Deformations Due to Seismically-Induced Liquefaction," by M.H. Baziar, R. Dobry and A-W.M. Elgamal, 3/24/92, (PB92-222421).

NCEER-92-0008 "A Procedure for the Seismic Evaluation of Buildings in the Central and Eastern United States," by C.D. Poland and J.O. Malley, 4/2/92, (PB92-222439).

NCEER-92-0009 "Experimental and Analytical Study of a Hybrid Isolation System Using Friction Controllable Sliding Bearings," by M.Q. Feng, S. Fujii and M. Shinozuka, 5/15/92, (PB93-150282).

NCEER-92-0010 "Seismic Resistance of Slab-Column Connections in Existing Non-Ductile Flat-Plate Buildings," by A.J. Durrani and Y. Du, 5/18/92.

NCEER-92-0011 "The Hysteretic and Dynamic Behavior of Brick Masonry Walls Upgraded by Ferrocement Coatings Under Cyclic Loading and Strong Simulated Ground Motion," by H. Lee and S.P. Prawel, 5/11/92, to be published.

NCEER-92-0012 "Study of Wire Rope Systems for Seismic Protection of Equipment in Buildings," by G.F. Demetriades, M.C. Constantinou and A.M. Reinhorn, 5/20/92.

NCEER-92-0013 "Shape Memory Structural Dampers: Material Properties, Design and Seismic Testing," by P.R. Witting and F.A. Cozzarelli, 5/26/92.

NCEER-92-0014 "Longitudinal Permanent Ground Deformation Effects on Buried Continuous Pipelines," by M.J. O'Rourke, and C. Nordberg, 6/15/92.

NCEER-92-0015 "A Simulation Method for Stationary Gaussian Random Functions Based on the Sampling Theorem," by M. Grigoriu and S. Balopoulou, 6/11/92, (PB93-127496).

NCEER-92-0016 "Gravity-Load-Designed Reinforced Concrete Buildings: Seismic Evaluation of Existing Construction and Detailing Strategies for Improved Seismic Resistance," by G.W. Hoffmann, S.K. Kunnath, A.M. Reinhorn and J.B. Mander, 7/15/92, (PB94-142007, A08, MF-A02).

NCEER-92-0017 "Observations on Water System and Pipeline Performance in the Limón Area of Costa Rica Due to the April 22, 1991 Earthquake," by M. O'Rourke and D. Ballantyne, 6/30/92, (PB93-126811).

NCEER-92-0018 "Fourth Edition of Earthquake Education Materials for Grades K-12," Edited by K.E.K. Ross, 8/10/92.

NCEER-92-0019 "Proceedings from the Fourth Japan-U.S. Workshop on Earthquake Resistant Design of Lifeline Facilities and Countermeasures for Soil Liquefaction," Edited by M. Hamada and T.D. O'Rourke, 8/12/92, (PB93-163939).

NCEER-92-0020 "Active Bracing System: A Full Scale Implementation of Active Control," by A.M. Reinhorn, T.T. Soong, R.C. Lin, M.A. Riley, Y.P. Wang, S. Aizawa and M. Higashino, 8/14/92, (PB93-127512).

NCEER-92-0021 "Empirical Analysis of Horizontal Ground Displacement Generated by Liquefaction-Induced Lateral Spreads," by S.F. Bartlett and T.L. Youd, 8/17/92, (PB93-188241).

NCEER-92-0022 "IDARC Version 3.0: Inelastic Damage Analysis of Reinforced Concrete Structures," by S.K. Kunnath, A.M. Reinhorn and R.F. Lobo, 8/31/92, (PB93-227502, A07, MF-A02).

NCEER-92-0023 "A Semi-Empirical Analysis of Strong-Motion Peaks in Terms of Seismic Source, Propagation Path and Local Site Conditions, by M. Kamiyama, M.J. O'Rourke and R. Flores-Berrones, 9/9/92, (PB93-150266).

NCEER-92-0024 "Seismic Behavior of Reinforced Concrete Frame Structures with Nonductile Details, Part I: Summary of Experimental Findings of Full Scale Beam-Column Joint Tests," by A. Beres, R.N. White and P. Gergely, 9/30/92, (PB93-227783, A05, MF-A01).

NCEER-92-0025 "Experimental Results of Repaired and Retrofitted Beam-Column Joint Tests in Lightly Reinforced Concrete Frame Buildings," by A. Beres, S. El-Borgi, R.N. White and P. Gergely, 10/29/92, (PB93-227791, A05, MF-A01).

NCEER-92-0026 "A Generalization of Optimal Control Theory: Linear and Nonlinear Structures," by J.N. Yang, Z. Li and S. Vongchavalitkul, 11/2/92, (PB93-188621).

NCEER-92-0027 "Seismic Resistance of Reinforced Concrete Frame Structures Designed Only for Gravity Loads: Part I - Design and Properties of a One-Third Scale Model Structure," by J.M. Bracci, A.M. Reinhorn and J.B. Mander, 12/1/92, (PB94-104502, A08, MF-A02).

NCEER-92-0028 "Seismic Resistance of Reinforced Concrete Frame Structures Designed Only for Gravity Loads: Part II - Experimental Performance of Subassemblages," by L.E. Aycardi, J.B. Mander and A.M. Reinhorn, 12/1/92, (PB94-104510, A08, MF-A02).

NCEER-92-0029 "Seismic Resistance of Reinforced Concrete Frame Structures Designed Only for Gravity Loads: Part III - Experimental Performance and Analytical Study of a Structural Model," by J.M. Bracci, A.M. Reinhorn and J.B. Mander, 12/1/92, (PB93-227528, A09, MF-A01).

NCEER-92-0030 "Evaluation of Seismic Retrofit of Reinforced Concrete Frame Structures: Part I - Experimental Performance of Retrofitted Subassemblages," by D. Choudhuri, J.B. Mander and A.M. Reinhorn, 12/8/92, (PB93-198307, A07, MF-A02).

NCEER-92-0031 "Evaluation of Seismic Retrofit of Reinforced Concrete Frame Structures: Part II - Experimental Performance and Analytical Study of a Retrofitted Structural Model," by J.M. Bracci, A.M. Reinhorn and J.B. Mander, 12/8/92, (PB93-198315, A09, MF-A03).

NCEER-92-0032 "Experimental and Analytical Investigation of Seismic Response of Structures with Supplemental Fluid Viscous Dampers," by M.C. Constantinou and M.D. Symans, 12/21/92, (PB93-191435).

NCEER-92-0033 "Reconnaissance Report on the Cairo, Egypt Earthquake of October 12, 1992," by M. Khater, 12/23/92, (PB93-188621).

NCEER-92-0034 "Low-Level Dynamic Characteristics of Four Tall Flat-Plate Buildings in New York City," by H. Gavin, S. Yuan, J. Grossman, E. Pekelis and K. Jacob, 12/28/92, (PB93-188217).

NCEER-93-0001 "An Experimental Study on the Seismic Performance of Brick-Infilled Steel Frames With and Without Retrofit," by J.B. Mander, B. Nair, K. Wojtkowski and J. Ma, 1/29/93, (PB93-227510, A07, MF-A02).

NCEER-93-0002 "Social Accounting for Disaster Preparedness and Recovery Planning," by S. Cole, E. Pantoja and V. Razak, 2/22/93, (PB94-142114, A12, MF-A03).

NCEER-93-0003 "Assessment of 1991 NEHRP Provisions for Nonstructural Components and Recommended Revisions," by T.T. Soong, G. Chen, Z. Wu, R-H. Zhang and M. Grigoriu, 3/1/93, (PB93-188639).

NCEER-93-0004 "Evaluation of Static and Response Spectrum Analysis Procedures of SEAOC/UBC for Seismic Isolated Structures," by C.W. Winters and M.C. Constantinou, 3/23/93, (PB93-198299).

NCEER-93-0005 "Earthquakes in the Northeast - Are We Ignoring the Hazard? A Workshop on Earthquake Science and Safety for Educators," edited by K.E.K. Ross, 4/2/93, (PB94-103066, A09, MF-A02).

NCEER-93-0006 "Inelastic Response of Reinforced Concrete Structures with Viscoelastic Braces," by R.F. Lobo, J.M. Bracci, K.L. Shen, A.M. Reinhorn and T.T. Soong, 4/5/93, (PB93-227486, A05, MF-A02).

NCEER-93-0007 "Seismic Testing of Installation Methods for Computers and Data Processing Equipment," by K. Kosar, T.T. Soong, K.L. Shen, J.A. HoLung and Y.K. Lin, 4/12/93, (PB93-198299).

NCEER-93-0008 "Retrofit of Reinforced Concrete Frames Using Added Dampers," by A. Reinhorn, M. Constantinou and C. Li, to be published.

NCEER-93-0009 "Seismic Behavior and Design Guidelines for Steel Frame Structures with Added Viscoelastic Dampers," by K.C. Chang, M.L. Lai, T.T. Soong, D.S. Hao and Y.C. Yeh, 5/1/93, (PB94-141959, A07, MF-A02).

NCEER-93-0010 "Seismic Performance of Shear-Critical Reinforced Concrete Bridge Piers," by J.B. Mander, S.M. Waheed, M.T.A. Chaudhary and S.S. Chen, 5/12/93, (PB93-227494, A08, MF-A02).

NCEER-93-0011 "3D-BASIS-TABS: Computer Program for Nonlinear Dynamic Analysis of Three Dimensional Base Isolated Structures," by S. Nagarajaiah, C. Li, A.M. Reinhorn and M.C. Constantinou, 8/2/93, (PB94-141819, A09, MF-A02).

NCEER-93-0012 "Effects of Hydrocarbon Spills from an Oil Pipeline Break on Ground Water," by O.J. Helweg and H.H.M. Hwang, 8/3/93, (PB94-141942, A06, MF-A02).

NCEER-93-0013 "Simplified Procedures for Seismic Design of Nonstructural Components and Assessment of Current Code Provisions," by M.P. Singh, L.E. Suarez, E.E. Matheu and G.O. Maldonado, 8/4/93, (PB94-141827, A09, MF-A02).

NCEER-93-0014 "An Energy Approach to Seismic Analysis and Design of Secondary Systems," by G. Chen and T.T. Soong, 8/6/93, (PB94-142767, A11, MF-A03).

NCEER-93-0015 "Proceedings from School Sites: Becoming Prepared for Earthquakes - Commemorating the Third Anniversary of the Loma Prieta Earthquake," Edited by F.E. Winslow and K.E.K. Ross, 8/16/93.

NCEER-93-0016 "Reconnaissance Report of Damage to Historic Monuments in Cairo, Egypt Following the October 12, 1992 Dahshur Earthquake," by D. Sykora, D. Look, G. Croci, E. Karaesmen and E. Karaesmen, 8/19/93, (PB94-142221, A08, MF-A02).

NCEER-93-0017 "The Island of Guam Earthquake of August 8, 1993," by S.W. Swan and S.K. Harris, 9/30/93, (PB94-141843, A04, MF-A01).

NCEER-93-0018 "Engineering Aspects of the October 12, 1992 Egyptian Earthquake," by A.W. Elgamal, M. Amer, K. Adalier and A. Abul-Fadl, 10/7/93, (PB94-141983, A05, MF-A01).

NCEER-93-0019 "Development of an Earthquake Motion Simulator and its Application in Dynamic Centrifuge Testing," by I. Krstelj, Supervised by J.H. Prevost, 10/23/93, (PB94-181773, A-10, MF-A03).

NCEER-93-0020 "NCEER-Taisei Corporation Research Program on Sliding Seismic Isolation Systems for Bridges: Experimental and Analytical Study of a Friction Pendulum System (FPS)," by M.C. Constantinou, P. Tsopelas, Y-S. Kim and S. Okamoto, 11/1/93, (PB94-142775, A08, MF-A02).

NCEER-93-0021 "Finite Element Modeling of Elastomeric Seismic Isolation Bearings," by L.J. Billings, Supervised by R. Shepherd, 11/8/93, to be published.

NCEER-93-0022 "Seismic Vulnerability of Equipment in Critical Facilities: Life-Safety and Operational Consequences," by K. Porter, G.S. Johnson, M.M. Zadeh, C. Scawthorn and S. Eder, 11/24/93, (PB94-181765, A16, MF-A03).

NCEER-93-0023 "Hokkaido Nansei-oki, Japan Earthquake of July 12, 1993, by P.I. Yanev and C.R. Scawthorn, 12/23/93, (PB94-181500, A07, MF-A01).

NCEER-94-0001 "An Evaluation of Seismic Serviceability of Water Supply Networks with Application to the San Francisco Auxiliary Water Supply System," by I. Markov, Supervised by M. Grigoriu and T. O'Rourke, 1/21/94.

NCEER-94-0002 "NCEER-Taisei Corporation Research Program on Sliding Seismic Isolation Systems for Bridges: Experimental and Analytical Study of Systems Consisting of Sliding Bearings, Rubber Restoring Force Devices and Fluid Dampers," Volumes I and II, by P. Tsopelas, S. Okamoto, M.C. Constantinou, D. Ozaki and S. Fujii, 2/4/94, (PB94-181740, A09, MF-A02 and PB94-181757, A12, MF-A03).

NCEER-94-0003 "A Markov Model for Local and Global Damage Indices in Seismic Analysis," by S. Rahman and M. Grigoriu, 2/18/94.

NCEER-94-0004 "Proceedings from the NCEER Workshop on Seismic Response of Masonry Infills," edited by D.P. Abrams, 3/1/94, (PB94-180783, A07, MF-A02).

NCEER-94-0005 "The Northridge, California Earthquake of January 17, 1994: General Reconnaissance Report," edited by J.D. Goltz, 3/11/94, (PB193943, A10, MF-A03).

NCEER-94-0006 "Seismic Energy Based Fatigue Damage Analysis of Bridge Columns: Part I - Evaluation of Seismic Capacity," by G.A. Chang and J.B. Mander, 3/14/94.

NCEER-94-0007 "Seismic Isolation of Multi-Story Frame Structures Using Spherical Sliding Isolation Systems," by T.M. Al-Hussaini, V.A. Zayas and M.C. Constantinou, 3/17/94, (PB193745, A09, MF-A02).

NCEER-94-0008 "The Northridge, California Earthquake of January 17, 1994: Performance of Highway Bridges," edited by I.G. Buckle, 3/24/94, (PB94-193851, A06, MF-A02).

NCEER-94-0009 "Proceedings of the Third U.S.-Japan Workshop on Earthquake Protective Systems for Bridges," edited by I.G. Buckle and I. Friedland, 3/31/94, (PB94-195815, A99, MF-MF).

NCEER-94-0010 "3D-BASIS-ME: Computer Program for Nonlinear Dynamic Analysis of Seismically Isolated Single and Multiple Structures and Liquid Storage Tanks," by P.C. Tsopelas, M.C. Constantinou and A.M. Reinhorn, 4/12/94.

NCEER-94-0011 "The Northridge, California Earthquake of January 17, 1994: Performance of Gas Transmission Pipelines," by T.D. O'Rourke and M.C. Palmer, 5/16/94.

NCEER-94-0012 "Feasibility Study of Replacement Procedures and Earthquake Performance Related to Gas Transmission Pipelines," by T.D. O'Rourke and M.C. Palmer, 5/25/94.

NCEER-94-0013 "Seismic Energy Based Fatigue Damage Analysis of Bridge Columns: Part II - Evaluation of Seismic Demand," by G.A. Chang and J.B. Mander, 6/1/94, to be published.

NCEER-94-0014 "NCEER-Taisei Corporation Research Program on Sliding Seismic Isolation Systems for Bridges: Experimental and Analytical Study of a System Consisting of Sliding Bearings and Fluid Restoring Force/Damping Devices," by P. Tsopelas and M.C. Constantinou, 6/13/94.

NCEER-94-0015 "Generation of Hazard-Consistent Fragility Curves for Seismic Loss Estimation Studies," by H. Hwang and J-R. Huo, 6/14/94.

NCEER-94-0016 "Seismic Study of Building Frames with Added Energy-Absorbing Devices," by W.S. Pong, C.S. Tsai and G.C. Lee, 6/20/94.

NCEER-94-0017 "Sliding Mode Control for Seismic-Excited Linear and Nonlinear Civil Engineering Structures," by J. Yang, J. Wu, A. Agrawal and Z. Li, 6/21/94.